



**Silesian University of Technology**

Sara Sarraj, MSc Eng.

*Modification of Selected Bioactive and Mechanical  
Properties of Polydimethylsiloxane for External  
Medical Applications*

PhD dissertation

Supervisor:

Małgorzata Szymiczek, PhD, DSc Eng.

Gliwice 2024

## ***Acknowledgment***

*First and foremost, I would like to express my sincere gratitude to my supervisor, prof. dr hab. inż. Małgorzata Szymiczek. Thank you for your guidance, support, knowledge, and patience when I had crazy ideas. Thank you for always believing I could achieve more and pushing me forward to reach higher goals.*

*I would also like to thank all my colleagues who have shown me big support and help throughout this incredible journey, whether in the form of laboratory assistance or a smile to brighten sometimes grayer days.*

*A word of thanks is also directed to my friends, who always believed I could go harder instead of going home. Thank you for your words of encouragement, shared laughter over more or less scientifically related topics, and support.*

*I would also like to thank my partner, my backbone, for supporting me and bravely handling my ever-changing moods during the final phases of this crazy journey. Thank you for being there whenever I felt lost and for guiding me back to solid ground.*

*Last but certainly not least, I would like to express my deepest gratitude to my parents and family. You have been my lifelong supporters through all my ups and downs, always there whenever I needed extra comfort. A special thanks to my mom, my best friend, my role model, my secret keeper, and my dance partner. Words cannot express how dear you are to me, and if it weren't for you, I would have missed out on this amazing journey. Thank you for making me strive for more. A special thanks to my dad, my laughter companion, my role model, and now a fellow scientist. Thank you for having faith in me and supporting me.*

## Abstract

Advancements in materials engineering, particularly in polymeric materials, alongside the increasing demands of the medical industry, drive the search for new alternative solutions, often based on biomaterials and/or biofillers. The selection of polymeric materials and the modifications applied, including fillers, is conditioned by the application area and the associated requirements. Such materials must exhibit biocompatibility and often possess additional properties relevant to their application, such as antibacterial, antifungal, or anti-allergic characteristics.

Various solutions utilizing inorganic and organic fillers are known, often employing mechanisms of synergistic interaction that simultaneously influence the biological and physicochemical properties required for potential applications. A thorough literature review clearly indicates that it is possible to modify polymeric materials with organic fillers for medical applications. Polymers are used in many areas, including as components of medical equipment, implants, hygiene products, and dressings, which determine their operational characteristics. Despite a range of different solutions, there is a justified need to develop new materials that could serve as alternatives to currently used dressings, particularly for long-term use on wounds while maintaining the required antibacterial properties, which are crucial for the healing process. A promising response to these defined needs could be biocomposites based on elastomeric materials modified for antibacterial properties.

The research problem addressed in this work involved the development of an elastomeric dressing material that combines both antibacterial activity and the required physicochemical properties. The research focused on developing new materials with bioactive properties based on polydimethylsiloxane (PDMS) modified with various forms of plant-derived fillers. Polydimethylsiloxane is a synthetic elastomer from the siloxane group. Its biocompatibility, high gas permeability, chemical inertness, and thermal stability make PDMS highly desirable in applications requiring both flexibility and durability. In the medical sector, PDMS is used in implants, contact lenses, scaffolds, patches, and wound dressings, which serve to protect wounds from infection and facilitate the healing process. Various types of dressings modified with inorganic additives are known, but they involve time-consuming production processes, increased costs, and the

need to use various chemical substances. In this study, the developed materials address these challenges by utilizing widely available organic additives. The preparation process is characterized by reduced time and financial investment, as well as limited use of chemical substances.

To improve the bioactive properties, herbal fillers were introduced into the matrix selected based on criteria such as polyphenol content, availability, antimicrobial activity, and health benefits. These included thyme, sage, and rosemary, which are rich in polyphenols and exhibit antioxidant, anti-inflammatory, and antibacterial properties. The study developed a technology for modifying the fillers and producing biocomposites based on polydimethylsiloxane with herb content of 2.5%, 5%, 7.5%, and 10% by weight.

The obtained biocomposites were subjected to a series of tests to evaluate the impact of the fillers, varied in form and material, on the physicochemical properties (density, contact angle, absorbance, crystallinity degree), mechanical properties (rebound resilience, hardness, abrasion, static tensile testing), and biological properties (antibacterial activity, cell viability), as well as aging studies in an artificial plasma environment. Based on FTIR spectra analysis, the influence of modification and aging on structural changes in the material was determined.

The results indicate that introducing modified thyme, sage, and rosemary into polydimethylsiloxane alters the antibacterial activity level depending on the filler's type and content. The highest antibacterial activity was obtained for PDMS modified with sage; however, it is noteworthy that all biocomposites exhibit bacteriostatic properties. Considering the overall results, the best solution is the introduction of modified thyme at a weight ratio of 2.5%.

Moreover, some materials exhibited high cell viability during fibroblast tests, suggesting they promote cell proliferation. Although the functional properties of the materials were altered, in many cases, these changes did not disqualify the materials from external applications, such as wound dressings. The developed materials represent a significant advancement in the field of medicine, particularly in wound dressing applications. Furthermore, these composites, based on naturally derived additives, are environmentally friendly and pose no threat during production, use, or disposal, in accordance with the principles of sustainable development.

## Streszczenie

Postęp w inżynierii materiałowej, szczególnie w materiałach polimerowych, oraz coraz wyższe wymagania stawiane przez przemysł medyczny, determinuje poszukiwanie nowych alternatywnych rozwiązań, często opartych na biomateriałach i/lub bionapełniaczach. Dobór materiałów polimerowych, a także stosowanych modyfikacji, w tym napełniaczy, jest uwarunkowany obszarem aplikacji i związanymi z nim wymogami. Tego typu materiały muszą wykazywać biokompatybilność, a często również inne własności wynikające obszaru stosowania np. antybakteryjne, antygrzybiczne, antyalergiczne itd.

Znane są różne rozwiązania wykorzystujące napełniacze nieorganiczne i organiczne często wykorzystujące mechanizmy synergicznego oddziaływania, wpływające jednocześnie na własności biologiczne i fizykochemiczne wymagane przez potencjalną aplikację.

Przeprowadzona analiza literaturowa jednoznacznie wskazuje, że możliwa jest modyfikacja materiałów polimerowych napełniaczami organicznymi w aplikacjach medycznych. Materiały polimerowe są stosowane w wielu obszarach m.in. jako elementy sprzętu medycznego, implanty, środki higieny, opatrunki, co determinuje ich charakterystyki eksploatacyjne. Pomimo szeregu różnych rozwiązań, pojawia się uzasadniona potrzeba opracowania nowych materiałów, które mogłyby stanowić alternatywę dla obecnie stosowanych opatrunków szczególnie w aspekcie długotrwałego stosowania na rany przy zachowaniu wymaganej antybakteryjności, co ma istotny wpływ na proces gojenia. Odpowiedzią na tak zdefiniowane potrzeby, mogą stanowić biokompozyty na bazie materiałów elastomerowych modyfikowane pod kątem własności antybakteryjnych.

Podjęty w pracy problem badawczy dotyczył opracowania elastomerowego materiału opatrunkowego, który łączył w sobie zarówno aktywność antybakteryjną jak i wymagane własności fizykochemiczne. W ramach pracy, prowadzono badania dotyczące opracowania nowych materiałów o własnościach bioaktywnych na osnowie polidimetylosiloksanu (PDMS) modyfikowanych różną postacią napełniaczy pochodzenia roślinnego. Polidimetylosiloksan jest syntetycznym elastomerem z grupy siloksanów. Jego biokompatybilność, wysoka przepuszczalność gazów, chemiczna

obojętność oraz stabilność termiczna sprawiają, że PDMS jest niezwykle pożądanym w aplikacjach wymagających zarówno elastyczności, jak i trwałości. W sektorze medycznym PDMS jest wykorzystywany w implantach, soczewkach kontaktowych, rusztowaniach, plastrach oraz opatrunkach na rany, które służą do zabezpieczenia ran przed zakażeniem i ułatwiają proces gojenia. Znane są różne rodzaje opatrunków modyfikowanych dodatkami nieorganicznymi jednak wiąże się z koniecznością przeprowadzenia czasochłonnych procesów produkcyjnych, zwiększonymi kosztami oraz potrzebą użycia różnorodnych substancji chemicznych. W ramach niniejszej pracy opracowano materiały, które stanowią odpowiedź na powyższe wyzwania poprzez zastosowanie szeroko dostępnych dodatków organicznych. Proces ich przygotowania charakteryzuje się mniejszym nakładem czasowym i finansowym oraz ograniczonym stosowaniem substancji chemicznych.

Celem poprawy własności bioaktywnych wprowadzono napełniacze ziołowe wyselekcjonowane na podstawie przyjętych kryteriów tj. zawartości związków polifenolowych, dostępności, aktywności przeciwdrobnoustrojowa, a także korzyści zdrowotnych. Były to tymianek, szalwia oraz rozmaryn, które są bogate w polifenole oraz wykazują właściwości przeciwutleniające, przeciwzapalne i przeciwbakteryjne. W ramach pracy opracowano technologię modyfikacji napełniaczy i wytwarzania biokompozytów na osnowie polidimetylosiloksanu o zawartości 2,5; 5; 7,5; i 10% wag. ziół.

Uzyskane biokompozyty poddano serii testów mających na celu ocenę wpływu zastosowanych, zróżnicowanych pod kątem postaci i materiału, napełniaczy na właściwości fizykochemiczne (gęstość, kąt zwilżania, chłonność, stopień krystaliczności), mechaniczne (odbojność, twardość, ścieralność, statyczna próba rozciągania) i biologiczne (aktywność antybakteryjna, żywotność komórek), a także badaniom starzeniowym w środowisku sztucznego osocza. Na podstawie analizy widm FTIR określono wpływ modyfikacji i starzenia na zmiany strukturalne zachodzące w materiale.

Wyniki wskazują, że wprowadzenie modyfikowanego tymianku, szalwii i rozmarynu do polidimetylosiloksanu zmienia poziom aktywności antybakteryjnej w zależności od rodzaju i zawartości napełniacza. Najwyższą aktywność antybakteryjną uzyskano dla PDMS modyfikowanego szalwią, lecz warto zaznaczyć, że wszystkie biokompozyty wykazują właściwości bakteriostatyczne. Biorąc pod uwagę całokształt

wyników można stwierdzić, że najlepszym rozwiązaniem jest wprowadzenie modyfikowanego tymianku w stosunku wagowym 2.5%.

Ponadto niektóre materiały wykazywały wysoką żywotność komórek podczas testów na fibroblastach, co sugeruje, że sprzyjają one proliferacji komórek. Choć właściwości funkcjonalne materiałów uległy zmianie, w wielu przypadkach zmiany te nie dyskwalifikowały materiałów z zastosowań zewnętrznych, takich jak opatrunki na rany. Opracowane materiały stanowią znaczący postęp w dziedzinie medycyny, zwłaszcza w zastosowaniach opatrunków na rany. Co więcej, te kompozyty, bazujące na dodatkach pochodzenia naturalnego, są przyjazne dla środowiska. Ponadto nie stwarzają zagrożenia w trakcie produkcji, użytkowania ani utylizacji, zgodnie z zasadami zrównoważonego rozwoju.

## Table of Contents

<b>Abstract .....</b>	<b>3</b>
<b>Streszczenie.....</b>	<b>5</b>
<b>List of abbreviations .....</b>	<b>10</b>
<b>1. Introduction.....</b>	<b>13</b>
<b>2. Literature review .....</b>	<b>16</b>
<b>2.1. Elastomers in medicine .....</b>	<b>16</b>
<b>2.2. Polydimethylsiloxane as a biomaterial .....</b>	<b>21</b>
2.2.1. Characterization and properties.....	21
2.2.2. Applications in medicine.....	23
2.2.3. Wound dressings and microbes adherence.....	26
<b>2.3. Natural bioactive fillers – conventional and potentially novel.....</b>	<b>30</b>
2.3.1. Animal-derived additives .....	30
2.3.2. Plant-derived additives .....	33
<b>2.4. Materials testing methods of polymers used in the medical industry .....</b>	<b>43</b>
<b>2.5. Organic fillers-enriched composites with enhanced antimicrobial properties ...</b>	<b>45</b>
2.5.1. Materials modified with essential oils.....	45
2.5.2. Materials modified with polyphenolic extracts.....	48
2.5.3. Materials modified with powdered plants .....	51
<b>3. Literature review conclusions.....</b>	<b>55</b>
<b>4. PhD thesis and aims.....</b>	<b>57</b>
<b>5. Methodology .....</b>	<b>58</b>
<b>5.1. Materials .....</b>	<b>59</b>
5.1.1. Biocomposites' matrix.....	59
5.1.2. Fillers' preparation .....	60
5.1.3. Fillers' characterization .....	63
5.1.4. Making of biocomposites .....	71
<b>5.2. Biocomposites testing methods.....</b>	<b>75</b>
5.2.1. Density.....	75
5.2.2. Contact angle.....	76
5.2.3. In vitro absorption .....	76
5.2.4. Rebound resilience .....	77
5.2.5. Hardness measurements .....	78
5.2.6. Abrasion resistance.....	78
5.2.7. Tensile testing.....	79
5.2.8. Accelerated degradation .....	81
5.2.9. Fourier transform infrared spectroscopy .....	82
5.2.10. Differential scanning calorimetry.....	82
5.2.11. Microscopic observations.....	82
5.2.12. Antibacterial activity assessment .....	83
5.2.13. Cell viability assay .....	85



<b>6.</b>	<b>Results .....</b>	<b>87</b>
6.1.	Density measurements .....	87
6.2.	Static tensile testing .....	88
6.3.	Hardness measurements .....	93
6.4.	Water contact angle measurements .....	95
6.5.	Antibacterial activity assessment .....	96
6.6.	Biocomposites assessment – I analysis .....	99
6.7.	In vitro absorption .....	101
6.8.	Rebound resilience .....	102
6.9.	Abrasion resistance .....	104
6.10.	FTIR analysis .....	105
6.11.	DSC analysis .....	106
6.12.	Accelerated degradation .....	108
6.13.	Microscopic topography analysis .....	116
6.14.	Biocomposites assessment – II analysis .....	122
6.15.	Cell viability assay .....	124
<b>7.</b>	<b>Summary and conclusions .....</b>	<b>125</b>
7.1.	Summary .....	125
7.2.	Conclusions .....	130
7.3.	Future research directions .....	133
<b>8.</b>	<b>References .....</b>	<b>134</b>
<b>9.</b>	<b>Standards references .....</b>	<b>160</b>
	<b>List of figures .....</b>	<b>162</b>
	<b>List of tables .....</b>	<b>164</b>

## List of abbreviations

<b>A</b>	Absorption
<b>ANOVA</b>	Analysis of Variance
<b>ATCC</b>	American Type Culture Collection
<b>ATR</b>	Attenuated Total Reflection
<b>BG</b>	Bioactive Glass
<b>CAD</b>	Corona-Charged Aerosol Detector
<b>CCL-1</b>	CC Chemokine Ligand 1
<b>CFU</b>	Colony-Forming Unit
<b>D</b>	Difunctional Monomer
<b>D<sub>10</sub></b>	10 <sup>th</sup> Percentile
<b>D<sub>50</sub></b>	50 <sup>th</sup> Percentile
<b>D<sub>90</sub></b>	90 <sup>th</sup> Percentile
<b>DMSO</b>	Dimethyl Sulfoxide
<b>DSC</b>	Differential Scanning Calorimetry
<b>DW</b>	Dry Weight
<b>EDS</b>	Energy Dispersive Spectrometry
<b>EMEM</b>	Eagle's Minimum Essential Medium
<b>ER</b>	Rosemary Extract
<b>ES</b>	Sage Extract
<b>ET</b>	Thyme Extract
<b>EUR</b>	Eucommia Ulmoides Rubber
<b>FBS</b>	Fetal Bovine Serum
<b>FTIR</b>	Fourier Transform Infrared Spectroscopy

<b>GAE</b>	Gallic Acid Equivalents
<b>HA</b>	Hyaluronic Acid
<b>IR</b>	Infrared
<b>LC-MS</b>	Liquid Chromatography-Mass Spectrometry
<b>LD</b>	Laser Diffraction
<b>M</b>	Monofunctional Monomer
<b>MEMS</b>	Microelectromechanical Systems
<b>MR</b>	Modified Rosemary
<b>MS</b>	Modified Sage
<b>MS</b>	Mass Spectrometer
<b>MT</b>	Modified Thyme
<b>MTT</b>	3-[4,5-Dimethylthiazol-2-Yl]-2,5 Diphenyl Tetrazolium Bromide
<b>NRL</b>	Natural Rubber Latex
<b>PBS</b>	Phosphate-Buffered Saline
<b>PCL</b>	Polycaprolactone
<b>PDMS</b>	Polydimethylsiloxane
<b>PVC</b>	Polyvinyl Chloride
<b>Q</b>	Tetrafunctional Monomer
<b>Q-TOF</b>	Quadrupole-Time of Flight
<b>R</b>	Logarithmic Reduction
<b>RPMI 1640</b>	Cell Culture Medium Developed at Roswell Park Memorial Institute (RPMI)
<b>RTV</b>	Room-Temperature Vulcanized

<b>SCDLP</b>	Soybean Casein Digest Broth with Lecithin and Polyoxyethylene Sorbitan Monooleate
<b>SEM</b>	Scanning Electron Microscope
<b>SHE</b>	Self-Healing Elastomer
<b>SIBS</b>	Poly(Styrene-Block-Isobutylene-Block-Styrene)
<b>T</b>	Tetrafunctional Monomer
<b>T<sub>g</sub></b>	Glass Transition Temperature
<b>TEO</b>	Thyme Essential Oil
<b>TPC</b>	Total Phenolic Content
<b>TPE</b>	Thermoplastic Elastomers
<b>TPO</b>	Polyolefin
<b>TPU</b>	Polyurethane
<b>TSE</b>	Thermoset Elastomers
<b>UR</b>	Unmodified Rosemary
<b>US</b>	Unmodified Sage
<b>UT</b>	Unmodified Thyme
<b>UV</b>	Ultraviolet
<b>WCA</b>	Water Contact Angle
<b>WPU</b>	Waterborne Polyurethane
<b>ΔV</b>	Volume Loss
<b>ε<sub>B</sub></b>	Strain at Break
<b>ρ</b>	Density
<b>σ<sub>B</sub></b>	Stress at Break

# 1. Introduction

The development of biomaterials began in the early 20<sup>th</sup> century with pioneering experiments conducted by figures such as Alexis Carrel, a renowned surgeon, yet significant breakthroughs were achieved only in the latter half of the century [1]. The ever-evolving demands of the medical field necessitate ongoing research and development of novel material solutions that address the complex challenges of creating biocompatible, durable, and functional materials for use within the human body. This collaborative effort and interdisciplinary exchange of ideas have laid the foundation for the modern field of biomaterials. Over the past 40 years, substantial attention has been directed towards polymers, metals, and ceramics, resulting in major advancements in medical science [2].

Polymeric materials are relatively facile to shape and modify, and their ability to be controlled and designed with specific characteristics renders them an interesting alternative to traditional materials. In medicine, a wide variety of polymers is applied, from thermoplastics (e.g., polyethylene, polypropylene, polycarbonate) and thermosets (e.g., epoxy and acrylic resins) to elastomers (e.g., natural rubber, silicone).

Due to their advantageous properties, elastomers are increasingly utilized across various industrial sectors, including the medical industry. The application of polymeric materials in these contexts opens up new possibilities but may also introduce several adverse effects, such as allergies and intense immune responses. Furthermore, ensuring the stability of these materials is crucial for their effective use in medical applications.

Elastomers are a class of polymeric materials known for their elasticity and durability, which play a crucial role in medical applications. A statistical report from 2021 indicated that the global market demand for elastomeric materials surpassed 2,900 kilotons [3]. This demand is projected to continue increasing, as illustrated in Figure 1.1.

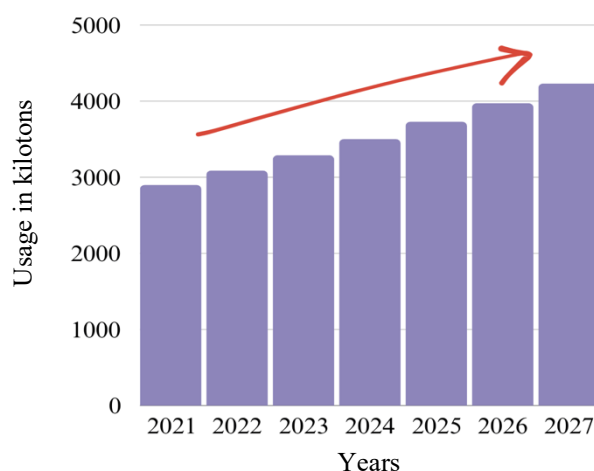


Figure 1.1. The compounded annual growth rate of medical elastomers

These viscoelastic polymers generally have long chains held together by weak intermolecular forces, giving them high flexibility when stress is applied. Owing to their low cross-linking degree, they can return to their original shape upon lifting the applied stress [4]. Moreover, these materials are characterized by low glass transition temperatures, hydrophobicity, and good adhesion. Depending on their origin, elastomers can be categorized into two groups: natural materials derived from plants and synthetic ones obtained from petroleum. Each group has distinct medical applications, determined by the specific field and the required properties.

In terms of external applications such as wound dressings, polydimethylsiloxane (PDMS) stands out as the most renowned. However, its resistance to microbes poses a limitation in such applications. Current strategies involving inorganic additive incorporation often necessitate chemical inputs during production, leading to by-product waste and significant time and financial expenses. As a result of the advancements in materials engineering, there is an increasing emphasis on organic-based fillers to enhance specific properties, particularly antimicrobial efficacy and health-promoting attributes. Nevertheless, the availability of works regarding organically modified polydimethylsiloxane remains somewhat restricted, impeding the exploitation of its full range of tailored properties for specific medical uses. While plant-derived additives, such as essential oils and extracts, have been extensively studied, the direct incorporation of plants in powder form remains underexplored.

This work aims to explore novel modifications of polydimethylsiloxane to enhance its suitability for external medical applications. Specifically, the research seeks to improve properties such as antimicrobial activity while preserving operational characteristics. Through systematic experimentation and analysis, the work endeavors to develop advanced materials that fulfill the exacting demands of modern medical applications.

The findings from this research could lead to the development of next-generation medical materials with enhanced performance and broader application potential. By advancing the understanding of how specific modifications influence the properties of polydimethylsiloxane, this work will contribute to the design of more effective and versatile medical devices, ultimately improving patient outcomes and advancing the field of medical science.

The structure of this dissertation is organized into two main sections. The first section comprises a literature review on the use of elastomers in medicine, with a particular focus on current studies concerning polydimethylsiloxane and potential strategies for enhancing the bioactivity of these materials (Chapters 2 and 3). The conclusions drawn from the literature review form the basis for developing the thesis and objectives of the research presented in Chapter 4. The second section encompasses the experimental work (Chapters 5 and 6), which includes the characterization of materials and fillers, the fabrication of composites, and the evaluation of their physicochemical, mechanical, and biological properties. Finally, Chapters 7 provide a summary of the key findings, discuss their implications, and offer recommendations for future research directions.

## 2. Literature review

### 2.1. Elastomers in medicine

A diverse range of elastomers has been utilized in the medical field for both internal and external applications, owing to their unique properties and adaptability. Depending on the specific application, required properties, and operating conditions, different materials are employed, including thermoplastics, thermosets, rubbers, and silicones that are vulcanized either chemically or thermally. This chapter will analyze some of the most prevalent elastomers used in medical applications and their typical uses.

Natural rubber latex (NRL) is a biopolymer obtained mainly from *Hevea brasiliensis*, native to the Amazon rubber tree, and it is found to be used in various medical applications. Most common applications include gloves, tubes, pacifiers, and the broad area of tissue engineering as membranes or wound dressings [5]. These particular applications, besides biocompatibility, require excellent functional properties, such as high tensile strength and elasticity, all of which NRL possesses [6]. In recent years, researchers have been focusing on natural rubber derived from *Eucommia ulmoides* as an alternative source due to the high demand for NRL. The flexible nature of *Eucommia ulmoides* rubber (EUR) is attributed to its linear molecular chain, and its excellent mechanical properties are ensured by its high molecular weight [7]. These properties, among others, have enabled its use as root canal fillings and scaffolds.

Synthetic elastomers comprise thermoplastic (TPEs) and thermoset elastomers (TSEs). Although these two subgroups share many properties, they differ in structure and behavior under specific working conditions. The classification of polymers as thermoplastic or thermoset is determined by their glass transition temperature ( $T_g$ ). For thermoset elastomers, heating the material above  $T_g$  results in irreversible solidification. Conversely, thermoplastic elastomers, when heated above the glass transition temperature, transform into a viscous liquid state, and upon cooling, they form semicrystalline or glassy solids [8]. Thermoplastic elastomers are long-chained polymers, and their structure contains soft segments that induce the elastomeric features and hard segments, mainly glassy or semicrystalline domains [9]. Moreover, they exhibit high stretchability due to the absence of crosslink junctions; however, they possess limited chemical resistance and



low stability at high temperatures. In contrast, TPEs, characterized by their three-dimensional structure, can revert to their original shape after deformation. Additionally, thermoset elastomers maintain their mechanical properties and stability under elevated temperatures and in chemically aggressive environments [10],[11].

Polyesters are thermoplastic polymers extensively used in medicine. This group of polymers comprises monomers bound together by ester bonds, which can be broken down by hydrolysis, leading to the material's biodegradation [12]. This trait is essential from a tissue engineering perspective as the functions shift from the degrading material to the newly formed tissue. Numerous studies reported in the literature focus on tailoring the properties of polyesters to adapt them for specific applications. One study reported the favorable elasticity, biocompatibility, and biodegradability properties of poly(lactide)-co-poly( $\beta$ -methyl- $\delta$ -valerolactone)-co-poly(lactide). The study demonstrated that these properties were maintained regardless of the environment (dry or aqueous), with the strain at break reaching almost 1000% and the material recovering to its initial state after the load was removed. Furthermore, cytotoxicity tests confirmed the non-cytotoxic nature of this material, indicating significant potential in the fields of tissue engineering and cell cultivation [13]. Moreover, polyesters can be applied for wireless skin hydration monitoring sensors, where the polyester-based material presents high mechanical strength and reduced water vapor transmission, or as sutures to facilitate collagen formation for ligament repair [14],[15]. Additionally, studies have explored the potential of 3D printing polyester-based thermoplastic elastomers (TPEs) for drug-delivery applications. In one study, researchers successfully created progesterone-filled 3D-printed polyester-based implants and inserts, which is an important step toward personalized medicine [16].

Polyurethanes (TPU) are commonly used because of their excellent biocompatibility and hemocompatibility. Their application in medicine dates back to the latter half of the 20th century when they were used to develop heart valve leaflets exhibiting good durability [17]. Innovative waterborne polyurethanes (WPU) were developed to provide eco-friendly alternatives to traditional solvent-based systems by utilizing water as a dispersing solvent and minimizing the use of toxic solvents [18]. Recent advancements in creating polyurethane urea thermoplastic elastomers aim to produce materials with controlled physical network density to enable the design of adaptable materials with shape memory. Researchers can adjust these elastomers'

morphology and mechanical properties by modifying the ratio and type of crystallizable blocks, thereby improving their suitability for various medical devices [19]. Other studies involved self-healing elastomers (SHEs) designed for *in vivo* use in different biomedical applications, such as repairing tissues in aortic aneurysms, nerve coaptation, and bone immobilization [20]. In another work, research has also concentrated on developing durable, recyclable, and degradable elastomers. For instance, a polyurethane elastomer based on polycaprolactone (PCL) has displayed high toughness and can be recycled at least three times without compromising its mechanical integrity. This elastomer can biologically degrade within a short period and has effectively promoted wound healing in biomedical applications [21].

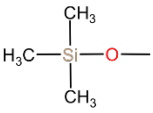
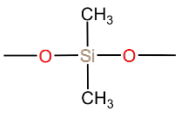
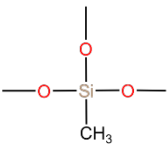

In addition to the materials discussed earlier, polyvinyl chloride (PVC) or poly(styrene-block-isobutylene-block-styrene) (SIBS) are employed in the biomedical field. PVC is mainly used to fabricate single-use gloves for patients with rubber allergies. A test proved that allergens known to cause dermatitis were present in the PVC gloves, and their level was very low [22]. SIBS was investigated for its potential application in the production of heart valves. Comparative tests with the commercially used polytetrafluoroethylene proved that SIBS exhibits reduced calcification levels while demonstrating comparable hemocompatibility [23].

The second group of synthetic elastomers is thermoset elastomers. These polymers possess chemically bonded crosslinks, forming a network-like structure that imparts characteristic elastomeric recoverability. Additionally, these materials are typically characterized by low glass transition and melting temperatures [24].

Polysiloxanes are among the most common semi-inorganic polymers used in the medical field. They consist of a silicon-oxygen (Si–O) backbone with two monovalent organic radicals attached to each silicon atom ( $-\text{R}_2\text{Si}-\text{O}-$ ) [25]–[27]. These materials possess unique properties due to their hybrid structure, which includes a polar inorganic backbone and nonpolar organic functional groups. Due to their dual-nature backbones, they are frequently termed polyorganosiloxanes. This combination establishes a strong link between the polymer's molecular structure and its physicochemical properties. Polysiloxanes can adopt five principal structures: linear (present in volatile and nonvolatile fluids), cyclic ring polymer (volatile fluids), branched (resins and adhesives – often used as crosslinkers), and cross-linked structure that can transform into a three-

dimensional network (resins, rubbers, and elastomers). These structures utilize four types of monomers: monofunctional (M), difunctional (D), trifunctional (T), and tetrafunctional (Q) [28],[29] presented in Table 2.1 [30].

Table 2.1. Polysiloxane units [30]

Monomer	Monofunctional	Difunctional	Trifunctional	Tetrafunctional
Structure				
Occurrence	At the end of chains	In linear polymers, silicone fluids or greases	In cross-linked polymers (soft or rigid resins)	In cross-linked polymers (rigid resins)

Due to their wide variety, polysiloxanes have found numerous applications in different fields of medicine, e.g., contact lenses [28], drug delivery systems [31], prostheses [32],[33], artificial skin and organs [34], patches and wound dressings [35]. Moreover, an extensive study has been conducted on polysiloxane membranes modified with various ratios of N-acetyl-l-cysteine cochlear implants to resist bacterial adherence and biofilm formation. These membranes were tested for microbial adherence against *Streptococcus pneumoniae* and implanted in rats for four weeks to assess in vivo performance. Physical characterization confirmed the stability and integrity of the membranes before and after exposure to microbial environments [36]. Furthermore, the cytocompatibility of polysiloxane/bioactive glass (BG) composite films was evaluated for use in biomedical coatings. These films demonstrated excellent homogeneity and biocompatibility with osteoblast-like cells. The coatings showed no toxicity and promoted cell growth, suggesting their potential for medical implant applications [37]. In other studies, a newly developed siloxane poly(urethane-urea) was assessed for its suitability in synthetic heart valve leaflets. The material exhibited desirable mechanical properties and excellent biostability. Comprehensive biocompatibility testing proved no observed cytotoxicity and systemic tissue response, with no adverse effects noted. The material could be a promising candidate for flexible leaflets in synthetic heart valve replacements [38].

In the context of external medical applications, particularly wound dressings, polydimethylsiloxane (PDMS) is the most commonly utilized elastomer. This is attributed to several key factors. Firstly, PDMS is relatively easy to produce, thus reducing manufacturing costs. This advantage makes it an attractive material for large-scale medical applications. Moreover, the ease with which modifiers can be incorporated into the polymeric matrix further enhances its appeal for applications requiring material-specific properties. Additionally, PDMS possesses the necessary biocompatibility. This is a crucial requirement for any material used in medical applications, particularly those involving direct contact with wounds or skin.

The following chapters will provide a comprehensive exploration of PDMS. This includes an in-depth literature analysis of its properties, contributing to its suitability for medical applications. Moreover, the chapters will discuss the various ways PDMS is currently employed within the medical field, with a particular focus on its role in wound dressings. Finally, potential methods for enhancing the properties of PDMS will be investigated. These enhancements aim to optimize PDMS for specific applications, thereby broadening its utility and effectiveness in medical treatments.

## 2.2. Polydimethylsiloxane as a biomaterial

### 2.2.1. Characterization and properties

Polydimethylsiloxane is considered the most common polysiloxane used in medical applications. As the name suggests, this material, apart from the typical siloxane (Si-O) bond for polysiloxanes, contains two methyl substituents (CH<sub>3</sub>) attached to the silicon atom as a repetitive unit in the chemical structure, as illustrated in Figure 2.1. These units define the molecular weight and the viscoelasticity of the material as well as provide chemical and thermal stability [39]. Moreover, the methyl groups are prevalent in PDMS's chemical structure, imparting hydrophobic characteristics with a surface tension of around 20.4 mN/m. Furthermore, crosslinking reactions involving groups such as phenyl and vinyl can induce substantial modifications in the properties of PDMS for various specialized applications [40].

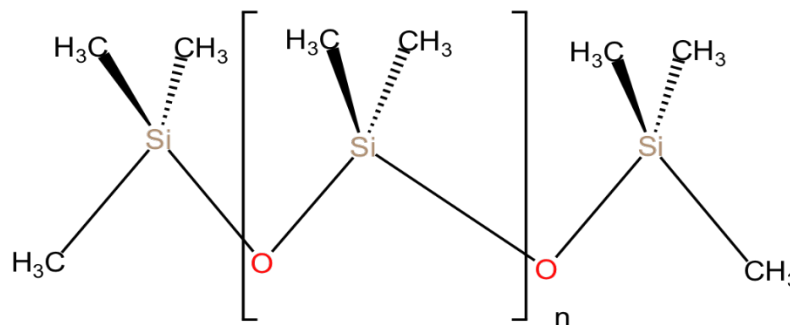


Figure 2.1. PDMS chemical structure formula

Polydimethylsiloxane forms elastomers through cross-linking reactions like condensation (moisture cure), addition (hydrosilylation), or radical reactions conducted at higher temperatures. Condensation cross-linking is used in applications that utilize environmental moisture to cure inward from the exterior surface. There are 1- and 2-part systems, which share common features, e.g., the release of by-products and a shrinkage of up to 1%. Addition cross-linking, such as hydrosilylation, eliminates shrinkage problems associated with condensation systems and involves vinyl end-blocked polymers reacting with SiH groups, though it requires careful handling of catalysts and intermediates. Moreover, this type of cross-linking does not involve the release of by-products, which is desirable for medical applications [26],[41].

Polydimethylsiloxane exhibits numerous properties that render it an attractive polymer across various fields. One notable characteristic is its exceptional flexibility, attributed to the highly dynamic flexibility of its molecular chains. This flexibility significantly influences the polymer's glass transition temperature, resulting in notably low values. The glass transition temperature is particularly low for PDMS, recorded at approximately  $-125\text{ }^{\circ}\text{C}$  [42],[43]. Other main properties include transparency, chemical and thermal stability, and gas permeability [44],[45].

Polydimethylsiloxane is highly valued in biomedical applications due to its biocompatibility and biostability, meaning it does not cause adverse effects upon contact with biological tissues. Although the exact mechanisms for biocompatibility are not fully understood, interactions with water in proteins and physicochemical characteristics such as surface free energy, stiffness, surface charge, and wettability are crucial factors. Structural biocompatibility is also important, as a mismatch in mechanical properties between an implant and surrounding tissues can cause inflammation or inadequate support. However, PDMS does not possess inherent antibacterial properties, which makes it susceptible to biofilm formation and bacterial infections [46].

Mechanically, pure PDMS typically exhibits an elastic modulus between 1.32 and 2.97 MPa and a tensile strength from 3.51 to 5.13 MPa, varying with the curing agent ratio and temperature [47]. Tensile strength increases with temperature up to  $125\text{ }^{\circ}\text{C}$ , beyond which it decreases, while Young's modulus continues to increase linearly with temperature. An increase in the curing agent ratio reduces PDMS's flexibility and consequently decreases Young's modulus. Moreover, the hardness, in most cases, is proportional to the material's Young's modulus [48].

Several key properties are essential for polydimethylsiloxane intended for external medical applications on the skin, such as wound dressings, patches, and transdermal delivery systems. These include biocompatibility, non-toxicity, high gas permeability, UV radiation resistance, flexibility, low reactivity, durability against atmospheric conditions, hydrophilic or hydrophobic characteristics tailored to specific applications, adhesive or anti-adhesive properties as required, transparency, and resilience to stretching and deformation [49].

### 2.2.2. Applications in medicine

As stated in Section 2.2.1, polydimethylsiloxane finds wide applications in the medical field owing to its unique properties. These applications can be classified into three main groups: non-body-contacting, body-contacting, and implantable devices.

In the field of medical devices that do not involve direct body contact, PDMS has been applied in blood-contacting devices. For such applications, polydimethylsiloxane exhibits favorable properties, such as gas permeability, nontoxicity, and stability against oxidative stress. One study explored the fabrication of PDMS-based polyurethane-urea incorporating zwitterion sulfobetaine for conduits and microfluidic devices. The results indicated that the obtained composites exhibit higher mechanical properties (tensile strength – 8.7 MPa, strain at break – 330%) than the PDMS control samples (2.0 MPa and 130%, respectively). Moreover, the deposition of fibrinogen (one of the coagulation factors) was less for the composites, indicating the anti-fouling properties [50]. In another research conducted by Dabaghi et al. [51], polydimethylsiloxane was utilized in the creation of a microfluidic multilayer extracorporeal gas exchange device. The results presented the potential of such structures as an alternative to hollow fiber membranes due to their high gas transfer efficiency on a small scale,

For body-contacting medical devices, applications such as contact lenses, patches, and wound dressings are among the most prevalent. Contact lenses were initially manufactured using poly(methyl methacrylate) in the early 1930s. It was not until the 1980s that silicone lenses began to emerge [52]. Since their introduction, researchers have continuously experimented with improving these lenses to enhance patient comfort. Roostaei et al. [53] explored the fabrication of PDMS lenses designed for color blindness correction, demonstrating the potential effectiveness of these lenses in addressing color vision deficiencies (Figure 2.2). The stability of the fabricated plasmonic contact lenses was examined in phosphate-buffered saline solution, demonstrating excellent stability in this environment, all while correcting deuteranomaly color blindness.

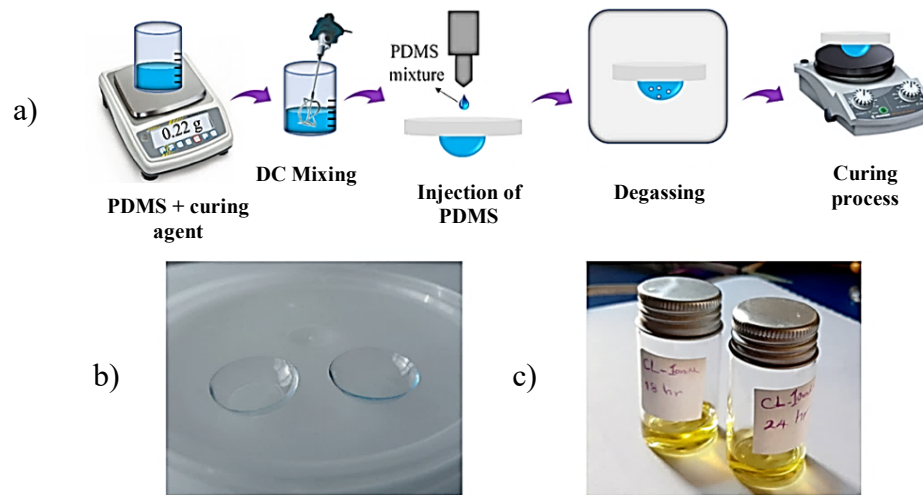


Figure 2.2. PDMS-based contact lens: fabrication process – a), the obtained PDMS lenses – b), and incubation of lenses in gold solution – c) [53]

Another study of research on contact lenses has focused on the development of smart contact lenses capable of monitoring intraocular pressure. This approach involves fabricating a multilayer lens equipped with an ocular tonometer to continuously monitor the pressure inside the eye. The results from these studies indicate that the developed lenses positively impact glaucoma care, do not initiate cellular damage, and maintain the required gas permeability level offering a non-invasive method for managing this condition [54].

Polydimethylsiloxane is frequently utilized in body-contacting devices, particularly in patches and dressings, due to its notable flexibility and durability. As wound dressings will be specifically addressed in Section 2.2.3, the examples provided here will focus solely on patch-related applications. PDMS-based patches are employed in various applications, such as glucose monitoring [55], ultrasensitive flexible chemical sensors [56], controlled drug release [57], body temperature regulation [58], and flexible sensors integrated with microelectromechanical systems (MEMS) [59], tailored to the intended application.

In the field of implantology, polydimethylsiloxane has been employed in heart valve prostheses. The initial application of this material dates back to the early 1960s with the development of the Starr-Edwards heart valve by Dr. Albert Starr and Lowell Edwards. This innovative valve featured a cage-like design constructed from stainless steel, a Teflon sewing ring, and a silicone ball, as depicted in Figure 2.3. Over 175,000 of these



valves were implanted until production ceased in the early 2000s. Notably, these prostheses demonstrated remarkable durability, with some lasting over 40 years post-implantation. Subsequent modifications to the valve design involved adjustments in shape and size to reduce thrombogenicity, enhancing the overall performance and safety of the heart valve prostheses [60],[61].



Figure 2.3. Starr-Edwards heart valve [60]

Recent advancements in manufacturing synthetic heart valves have led researchers to focus on bioinspired prostheses entirely made from silicone using additive manufacturing technology, as presented in Figure 2.4. This innovative approach allows customizing heart valves to fit the patient's anatomical structure. Additionally, the use of 3D printing technology significantly broadens the application scope, as it not only accelerates the production process but also facilitates the individualization of each prosthetic solution. This approach represents a significant step forward in enhancing the adaptability and effectiveness of synthetic heart valves [62].



Figure 2.4. Bioinspired 3D-printed heart valve [62]

### 2.2.3. Wound dressings and microbes adherence

The skin, as the largest organ by surface area, serves as the primary barrier of the human body, safeguarding it against external environmental factors such as extreme temperatures, mechanical damage to internal organs and tissues, ultraviolet radiation, and microbial infections. These protective functions render the skin susceptible to injuries, particularly wounds, which can be defined as disruptions of the epidermis—the outer layer of the skin. Such disruptions can subsequently result in damage to muscles and even organs [63]. Depending on the healing duration, they are classified as either acute or chronic wounds. The wound healing process is categorized into four overlapping phases: hemostasis, which occurs within several hours post-injury; inflammation, lasting up to three days; proliferation, spanning from four to twenty-one days; and remodeling, which can extend up to a year [64].

During hemostasis, muscle contractions and elevated calcium levels quickly close arterial vessels, forming a blood clot that serves as a scaffold for cell infiltration [65]. Inflammation follows, marked by neutrophils and monocytes migrating to the injury site to remove pathogens and debris while producing cytokines to amplify the response [66]. Macrophages arrive to secrete growth factors, transitioning the wound to the proliferative phase, where new tissue forms through cell proliferation and migration, including fibroblasts synthesizing fibrillar components and endothelial cells driving neo-angiogenesis [67]. The remodeling phase, starting around three weeks post-injury and lasting over a year, replaces type III collagen with type I collagen, enhancing tensile strength. The wound becomes rich in collagen and extracellular matrix proteins, achieving an avascular and acellular environment, with the healed skin attaining about 80% of its original tensile strength despite the non-regeneration of hair follicles and sweat glands [68],[69].

Impaired healing often results from microbial contamination in chronic wounds, which compromises the granulation tissue collagen. Approximately 40% of wound infections are attributed to the Gram-positive bacterium *Staphylococcus aureus*, while *Escherichia coli*, a Gram-negative bacterium, is responsible for more than 30% of cases [70]. Other pathogens such as *Pseudomonas aeruginosa*, *Proteus mirabilis*, *Enterococcus spp.*, and *Acinetobacter baumannii* are also recognized for their propensity

to infect wounds, thereby hindering the healing process [71],[72]. Untreated infected wounds can lead to severe health problems or even, in some cases, patient mortality.

The wound infection continuum comprises three phases: contamination, colonization, and infection. Contamination involves the presence of bacteria from the surrounding environment, with their minimal presence in the wound not significantly impacting the inflammatory response during the healing process. The second phase, colonization, begins when proliferating bacteria are present without eliciting a noticeable response from the host. In this phase, the presence of bacteria can influence the healing process in two ways: it can either enhance healing by increasing wound bed perfusion through local inflammation or impede it, depending on the bacterial load. The effect of bacterial colonization varies among individuals and is influenced by their specific physiological conditions. Wound infection occurs when microbial proliferation penetrates deep into the wound bed, triggering a local or systemic immune reaction and causing host tissue injury [73],[74].

Dressings are utilized to protect wounds from contamination and to reduce the risk of infection. Wound dressings can be classified into three categories: passive dressings that require frequent changes, skin substitutes that replace damaged skin, and bioactive dressings, as illustrated in Figure 2.5 [75],[76]. These dressings may contain agents that promote healing [77],[78] or antimicrobial agents that inhibit bacterial cell proliferation and biofilm formation, thereby preventing infection. The literature documents numerous dressings incorporated with active compounds such as drugs [79] or antimicrobial/antiseptic compounds [80],[81] to protect wounds from potential infections or to treat existing ones.

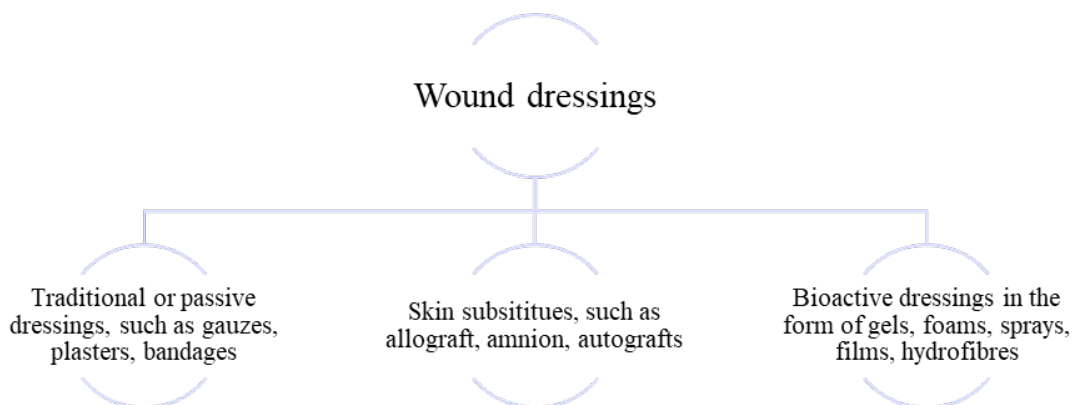


Figure 2.5. Wound dressings classification [75]

In two similar studies, researchers successfully incorporated reduced graphene oxide into polydimethylsiloxane PDMS, resulting in a composite material with significant antibacterial activity. This composite not only effectively inhibited bacterial growth but also promoted wound healing by enhancing re-epithelialization and granulation tissue formation. The presence of reduced graphene oxide improved the overall performance of PDMS in wound care applications, demonstrating its potential as an advanced wound dressing material [82],[83].

Another innovative approach involved the creation of a sandwich structure comprising three distinct layers: a superlyophobic PDMS layer, a superlyophilic gauze layer, and another lyophobic PDMS layer. This configuration was designed to optimize the wound dressing's performance by strategically combining the hydrophobic and hydrophilic properties. The superlyophobic PDMS layer repels liquids due to low surface energy, preventing external contamination, while the superlyophilic gauze layer ensures optimal moisture management and adherence to the wound bed. The lyophobic PDMS layer further protects the wound from external agents. This multilayered structure significantly reduced wound infection rates, highlighting its effectiveness in wound care [84].

Additionally, studies have explored the development of multifunctional PDMS-based aerogel wound dressings incorporated with silver nanoparticles. These aerogels demonstrated exceptional antibacterial properties, attributed to the well-known antimicrobial effects of silver nanoparticles. The incorporation of silver nanoparticles not only provided high antibacterial activity but also maintained the biocompatibility of the aerogel, ensuring that it is safe for use on wounds. This multifunctional wound dressing showed promise in both preventing infection and promoting healing, making it a valuable addition to advanced wound care solutions [85].

The results presented in the literature indicate the favorable impact of inorganic additives on materials' ability to combat microbes and promote wound healing. These additives, such as metal oxides and nanoparticles, have shown significant potential in enhancing the antimicrobial properties of wound dressings. However, the practical application of these inorganic additives faces considerable challenges. The production and incorporation of such compounds are often not financially efficient, involving high costs and complex, time-consuming synthesis processes. Moreover, while the inorganic

additives themselves are generally not harmful to the environment, the chemicals and processes involved in their production can pose environmental risks.

As a result, scientific research is increasingly turning towards naturally derived compounds as alternatives. These natural compounds, such as plant extracts, essential oils, and biopolymers, offer several advantages. They can exhibit similar or even superior antimicrobial activity compared to inorganic additives, often through mechanisms such as disrupting bacterial cell walls or inhibiting enzyme activity. Additionally, naturally derived compounds tend to be more biocompatible and less likely to cause adverse patient reactions. Furthermore, the production of natural antimicrobial agents is typically more environmentally friendly. These compounds can be extracted from renewable resources using more sustainable methods that minimize the use of harmful chemicals and reduce waste.

## **2.3. Natural bioactive fillers – conventional and potentially novel**

In recent years, there has been a significant increase in interest in naturally-derived compounds, driven by consumer demand for healthier and more sustainable products. These additives are sourced from natural origins and can be classified as either animal- or plant-derived. In addition to their availability and renewability, these additives are perceived as safer alternatives to synthetic inorganic fillers. However, despite their advantages, several factors may limit their use. For instance, some of these additives may trigger allergic reactions in specific individuals. Other limiting factors include variability in quality, lack of uniformity due to variations in source materials, and limited shelf life due to degradation. Furthermore, there are ethical issues related to animal welfare and sourcing practices for animal-derived additives.

Overall, these compounds vary not only in their sources but also in their functions and potential applications. This chapter explores selected types of natural additives (animal- and plant-derived) and their applications in health and medicine, with a detailed analysis of plant-based fillers.

### **2.3.1. Animal-derived additives**

Animal-derived fillers have a substantial historical background and have played essential roles in medical and cosmetic fields. Their significance arises from their biocompatibility, efficacy, and the numerous advantages they present over synthetic alternatives. The chemical structure and physical characteristics of these animal-derived additives can vary depending on their source, influencing their properties and functions. Such additives include chitosan, collagen, and hyaluronic acid.

Chitosan, recognized as one of the most prevalent additives in clinical medicine, is derived from chitin, a ubiquitous biopolymer. The primary sources of chitin are marine organisms, predominantly shrimps and crabs, though it can also be extracted from lobsters, crayfish, and oysters. The quantity of chitin that can be extracted varies depending on the organism, with some species containing up to 70% chitin [86]. Chitosan exhibits inhibitory effects on certain bacteria, yeast, and fungi. However, this antimicrobial

activity is highly dependent on its molecular weight. When the molecular weight falls below a certain threshold, chitosan can instead promote the growth of bacteria such as *E. coli* and *S. aureus*. Additionally, chitosan demonstrates antitumor activity by directly inhibiting the proliferation of cancerous cells, either through the induction of apoptosis or by enhancing immune responses [87],[88].

Moreover, chitosan and its derivatives play a vital role in wound healing due to their beneficial biological properties. They promote the release of key growth factors essential for tissue repair. Additionally, chitosan's antimicrobial and immunomodulatory effects help control infection and regulate inflammation during the healing process [89].

In the context of dental applications, Tanaka et al. [90] developed a novel resin-based dental composite containing chitosan, and were evaluated for their biological and mechanical properties. The addition of chitosan particles to these composites did not cause cytotoxicity or genotoxicity in fibroblast pulp cells. Furthermore, the obtained composites exhibited antimicrobial properties against *S. mutans*, with no detectable chitosan release from the composites. In addition, the composites' mechanical properties remained stable, demonstrating that including chitosan submicrometer filler did not negatively impact these properties.

Collagen, a protein derived from marine animals, among other sources, is renowned for its beneficial properties in medicine. It is a crucial material in the wound-healing process and is extensively used in tissue engineering due to its capacity to promote cell proliferation. Certain types of collagen, such as that extracted from *Rhopilema esculentum* jellyfish, exhibit remarkable similarity to human collagen, making them highly desirable for scaffold applications [91]. Collagen is also recognized for its bone-repairing capabilities and is utilized in drug delivery systems. Depending on the medical application, collagen can be formulated into various forms, including sponges, spheres, membranes, or gels [92].

In a study by McGrath et al. [93], a bilayered scaffold consisting of an antimicrobial collagen/chitosan film and a collagen–glycosaminoglycan scaffold showed significant potential for enhancing diabetic wound healing. Its structural stability, favorable mechanical properties, and resemblance to native skin, along with its ability to

inhibit *Staphylococcus aureus* and support epidermal cell proliferation, make it a promising candidate for this application.

Hyaluronic acid (HA), a prominent component of the extracellular matrix in vertebrate connective tissue, exhibits intrinsic biocompatibility, hydrophilicity, and bacteriostatic properties, making it an ideal biomaterial for wound dressings. Recent advancements highlight HA-based dressings endowed with antimicrobial properties [94],[95].

Zamboni et al. have demonstrated that HA and its derivatives effectively inhibit bacterial adhesion and biofilm formation. For instance, crosslinked HA films show greater bacteriostatic activity in high molecular weight forms compared to low molecular weight variants. HA coatings on medical implants such as titanium have also shown promise in reducing bacterial density and adhesion, suggesting potential applications in orthopedics and dental surgery [96].

Moreover, HA particles conjugated with antibiotics have been developed for sustained release, effectively inhibiting various bacteria, including *Pseudomonas aeruginosa* and *Staphylococcus aureus*, without exhibiting cytotoxic effects on eukaryotic cells. These findings highlight the potential of HA-based materials in preventing infections and promoting effective wound healing in clinical settings [97].

Furthermore, Michalska-Sionkowska et al. [98] developed thin films from collagen, chitosan, and hyaluronic acid with added gentamicin sulfate. Findings showed these films inhibit both Gram-negative (*E. coli*, *P. aeruginosa*) and Gram-positive bacteria (*S. aureus*), suggesting their potential as effective antimicrobial materials in biomedical applications.

Although animal-derived substances possess a diverse range of properties that can enhance the functionality of various medical applications, their use is often limited by ethical concerns, supply chain stability, and, in some instances, cultural restrictions. Consequently, research is increasingly focusing on sourcing bioactive substances from plants. Plant-derived substances offer several advantages, including broad availability and renewability, simpler and more scalable cultivation processes, and the absence of



ethical issues associated with animal use. These factors make plant-derived substances a more attractive and viable option for many applications, including medical ones.

### 2.3.2. Plant-derived additives

The utilization of plants in medicine for their therapeutic properties dates back thousands of years, with ancient civilizations depending on herbal remedies to treat various diseases. Nowadays, the emergence of antibiotic-resistant bacteria and the need for more sustainable medical practices have sparked significant scientific interest in exploring plant-based antibacterial substances. Plants synthesize a diverse array of secondary metabolites as part of their defense mechanisms against pathogens. Understanding these defensive mechanisms could be vital to developing new, effective antibacterial therapies [99].

Plants are abundant in compounds that exhibit desirable bioactivity for the medical field, including antimicrobial activity and promoting cell proliferation. These compounds primarily include polyphenols, terpenoids, and alkaloids, often found in commercially available extracts and essential oils.

Polyphenols are among the most well-known chemical compounds, characterized by one or more aromatic ring structures naturally occurring in plants, as classified in Figure 2.6. These compounds are primarily responsible for the organoleptic and nutritional properties of plants. Their health benefits depend on their specific type and level of bioactivity [100],[101].

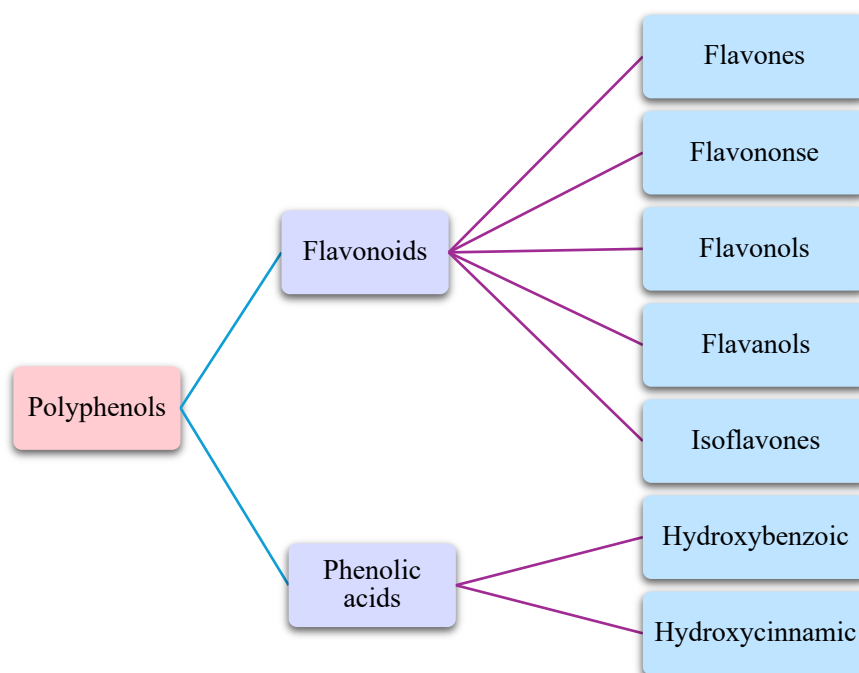


Figure 2.6. Classification of polyphenols [100]

Conversely, terpenoids are the primary constituents of volatile oils, with more than 50,000 terpenoids isolated from plants. These compounds play crucial roles in plant growth, development, and photosynthesis. Many terpenoids are utilized in cosmetics, flavorings, and pesticides. In health applications, terpenoids are valued for their anti-inflammatory and antimicrobial activities, as well as their anti-aging, antioxidant, and neuroprotective properties [102],[103].

Lastly, alkaloids are heterocyclic nitrogen compounds commonly isolated from plants, though they are also found in insects, animals, and microorganisms. The presence of alkaloids in plants deters insects and chordate animals from consuming them. These natural products have played a critical role in preventing and treating cancer and other diseases. Alkaloids exhibit various biological activities, including antitumor, antidepressant, anti-inflammatory, anti-angiogenic, and anti-dementia properties [104]–[106].

The concentration of the aforementioned substances in various plants fluctuates based on the plant's genus, the experimental methodology employed to determine the content, the region of cultivation, and the harvesting period. This section will focus on selected plants rich in these compounds, exploring their bioactivity and potential medical applications.

*Thymus vulgaris* L. (thyme) is the most extensively used and studied species within the *Thymus* genus. This herbaceous, perennial aromatic, and medicinal plant is widely consumed both as a herbal infusion and as a condiment. Thyme is cultivated for use in the food, pharmaceutical, and cosmetic industries. It contains 0.8% to 2.6% essential oil characterized by high chemical polymorphism and predominantly features thymol and carvacrol chemotypes. The synergistic effects of thymol and carvacrol significantly contribute to its antimicrobial properties. Notably, thyme exhibits substantial antimicrobial activity against Gram-positive bacteria and yeasts, although Gram-negative bacteria such as *Escherichia coli* and *Klebsiella pneumoniae* are less sensitive to thyme's bioactivity [107],[108].

Moreover, thyme is rich in bioactive compounds, including rosmarinic acid (avg. amount 1.18 mg/g DW), luteolin (0.27 mg/g DW), thymol (3.34 mg/g DW), apigenin (0.19 mg/g DW), caffeic acid (0.10 mg/g DW), and their derivatives, which demonstrate antioxidant, antimicrobial, anti-inflammatory, and anti-tumoral properties [109]. The content and type of active compounds vary among different plant parts, with the highest concentration found in thyme leaves [110]. In traditional medicine, thyme is utilized for treating asthma, serving as a disinfectant for the stomach and urinary tract, and functioning as a diuretic and anti-inflammatory agent. Thymol found in thyme inhibits platelet adhesion, potentially preventing thrombosis and atherosclerosis, and has shown efficacy against antibiotic-resistant bacteria [111],[112].

A study by Mohammed et al. [113] on the effects of thyme alcoholic extract on *Staphylococcus aureus*, a causative agent of acne, indicated that higher concentrations of the extract and essential oil increased bacterial inhibition zones. The alcoholic extract demonstrated superior antibacterial activity compared to thyme oil, suggesting that thyme extracts could serve as effective antimicrobial agents against pathogenic bacteria, particularly in treating acne.

*Salvia officinalis* L. (sage) belongs to the mint family *Lamiaceae*, subfamily *Nepetoideae*, tribe *Mentheae*, and genus *Salvia*, and it can grow up to 60 cm in height. As the largest genus in the *Lamiaceae* family, sage comprises approximately 1000 species, distributed across Europe, particularly around the Mediterranean, as well as in Southeast Asia, as well as Central and South America. Sage's leaves have traditionally been used for various medicinal purposes, including reducing perspiration, treating sore throats,

treating seizures and ulcers, combating gastroenteritis and other infections, improving lipid status and liver function, enhancing appetite and digestion, and boosting mental capacity [114],[115].

The phytochemicals responsible for sage's antimicrobial, anti-inflammatory, and antioxidant properties include rosmarinic (9.23 mg/g DW) and caffeic acids (0.32 mg/g DW), luteolin-7-O-glucoside (0.26 mg/g DW), and terpenes such as carnosic acid (3.91 mg/g DW) and carnosol (8.40 mg/g DW) [116],[117]. Despite its traditional and industrial applications, sage consumption must be moderated due to the presence of chemical components such as thujone and camphor that can cause adverse effects (e.g., neurotoxicity) when ingested in high doses (above 5 mg/day) for a longer period, leading some countries to regulate its usage [118],[119].

In addition, scientists investigated the impact of drying methods on the concentration of phytochemical compounds found in thyme and sage. Results indicated that for thyme, drying at 35 °C yields the highest phenolic compounds; however, the differences between other drying methods (natural drying, freeze drying, and drying at 40 °C) were minimal. On the other hand, sage exhibited the highest yield of compounds when freeze-dried, with concentrations twice as high as those obtained from the other drying methods. This highlights the importance of the drying method prior to extraction, which further influences the total polyphenols content [120].

In a study by Choukairi et al. [121], scientists discovered that the total extract of *Salvia officinalis* exhibits cytotoxic effects on glioblastoma cells but not on cortical neurons, indicating a selective action. The study also highlighted a dose-dependent antioxidant activity correlated with high levels of phenols and flavonoids, which is highly dependent on the extraction method and the state of the herb (fresh or dried). Additionally, sage essential oil has been found to promote the healing process by shortening the inflammatory stage by reducing pro-inflammatory cytokine expression and stimulating cellular proliferation in the proliferation phase. *S. officinalis* also improves tissue antioxidant status and angiogenesis, further supporting its therapeutic potential [122].

*Rosmarinus officinalis* L. (rosemary) is a woody perennial herb in the *Lamiaceae* family, native to the Mediterranean region and cultivated worldwide; traditionally used in folk medicine to treat ailments such as headaches, epilepsy, poor circulation, and

muscle spasms. The phytochemicals responsible for rosemary's biological effects include rosmarinic (11.60 mg/g DW) and caffeic acids (13.14 mg/g DW), luteolin (8.09 mg/g DW), carnosol (21.50 mg/g DW), carnosic acid (177.30 mg/g DW), ursolic acid. (186.70 mg/g DW), and oleanolic acid. (97.10. mg/g DW) [123]. These compounds, found mainly in the leaves, acting synergistically, contribute to its anti-inflammatory, antioxidant, and cytotoxic properties [124],[125].

Rosemary essential oil, obtained through steam distillation, contains numerous bioactive compounds, notably 1,8-cineole,  $\alpha$ -pinene,  $\beta$ -pinene, camphor, caryophyllene, and D-limonene. These compounds contribute to its strong antioxidant and antimicrobial properties, as well as its wound-healing activity [124],[126]. Studies have shown that rosemary essential oil can promote healing by reducing pro-inflammatory cytokine expression and enhancing cellular proliferation, tissue antioxidant status, and angiogenesis. The essential oil's antibacterial efficacy against *Staphylococcus aureus* and *Escherichia coli* has been demonstrated, with minimum inhibitory concentrations and minimum bactericidal concentrations, highlighting its potential as a natural alternative to synthetic antibiotics [127].

*Mentha piperita L.* (peppermint) is a perennial aromatic herb belonging to the *Lamiaceae* family. It is a naturally occurring hybrid between spearmint (*Mentha spicata L.*) and water mint (*Mentha aquatica L.*), typically reaching a height of 30–90 cm [128]. Peppermint has a long history of safe use in medicinal preparations, particularly its leaves, which are employed in the treatment of various diseases, including digestive disorders and nervous system issues. This efficacy is due to its antitumor, antimicrobial properties, chemopreventive potential, renal actions, and antiallergenic activities [129]. These therapeutic properties are attributed to the bioactive chemical compounds present in peppermint, such as rosmarinic acid (10.51 mg/g DW), caffeic acid (0.63 mg/g DW), tannic acid (0.88 mg/g DW), and luteolin (0.56 mg/g DW) [130]. Much like the herbs mentioned above, the extraction method used significantly influences the concentration of these compounds. For instance, a study by Dorman et al. [131] demonstrated that different solvents markedly impact the yield of detected polyphenolic compounds. In their findings, the rosmarinic acid content in water extracts was approximately 12 mg/g DW, while methanol extracts yielded nearly 180 mg/g DW, showing a 15-fold increase.

Menthol, constituting approximately 45% of peppermint essential oil, along with other compounds such as menthone and limonene, exhibits varying degrees of antimicrobial activity [132]. A study by Camele et al. [133] tested the antimicrobial efficacy of essential oil extracted from peppermint leaves against selected fungi and bacteria. The results demonstrated that the essential oil exhibited significant antifungal properties against *Botrytis cinerea*, *Monilinia fructicola*, *Penicillium expansum*, and *Aspergillus niger*. However, it had minimal impact on *Clavibacter michiganensis*, *Xanthomonas campestris*, *Pseudomonas savastanoi*, and *P. syringae* pv. *phaseolicola*.

Additionally, mixing two essential oils obtained from *Mentha piperita* and *Mentha pulegium* achieved high antimicrobial activity against *Staphylococcus aureus* and *Escherichia coli*. The study identified the optimal ratios for combating these microbes as 54%/46%, 55%/45%, and 56%/44% [134]. These findings highlight the potential of specific combinations of essential oils in enhancing antimicrobial efficacy.

*Melissa officinalis* L. (lemon balm) is a perennial herb belonging to the *Lamiaceae* family, naturally occurring in the Mediterranean region, Western Asia, Europe, and North America [135]. The common name "lemon balm" derives from its distinctive lemon-like flavor. The plant typically reaches a height of 1 meter, with leaves measuring 2-8 cm in length, and is widely recognized as one of the most well-known medicinal herbs in traditional medicine. Its medicinal use is primarily attributed to its efficacy in treating depression, anxiety, insomnia, and stress [136]. In addition to its culinary use as a flavoring agent, lemon balm possesses various bioactive properties, including antimicrobial, antioxidant, anti-inflammatory, spasmolytic, antitumor, anti-hyperlipidemic, hepatoprotective, and anti-Alzheimer effects [137]. Caleja et al. [138] demonstrated the antimicrobial and antioxidant properties of the aerial parts of lemon balm, highlighting its potential health benefits.

The bioactivity of lemon balm is linked to its chemical composition, which includes compounds known for their antioxidant and antimicrobial activities, such as rosmarinic acid (13.37 mg/g DW), caffeic acid (0.27 mg/g DW), quercetin (0.17 mg/g DW), and coumaric acid (0.19 mg/g DW) [138],[139]. A study by Šic Žlabur et al. [140] investigated the total polyphenolic content in lemon balm leaves, reporting a high concentration of  $1977.45 \pm 4.53$  mg/L extract.

In research assessing the antimicrobial activity of lemon balm, the plant exhibited significant inhibition zones against Gram-negative bacteria (up to 14.21 mm with 4 mg/mL of lemon balm essential oil) and slightly smaller zones for Gram-positive bacteria (10.72 mm for the same concentration of essential oil), indicating its antibacterial efficacy against common pathogens [141]. However, Bouloumpasi et al. [142] found that, although lemon balm demonstrates antibacterial activity, its effectiveness is considerably lower than that of rosemary and sage, which can achieve up to 100% inhibition of bacterial growth depending on the strain and herb concentration, compared to a maximum of 30% for lemon balm.

Furthermore, the cytotoxic effects of lemon balm on human cells were evaluated, revealing that the herb selectively targets tumor cells (melanoma) without affecting healthy cells (keratinocytes). No vascular toxicity was observed even at concentrations as high as 1000 µg/mL, suggesting that lemon balm leaf extract could be a promising candidate for treating skin disorders characterized by impaired physiological skin parameters [143].

*Curcuma longa L.* (turmeric) is a medicinal plant from the ginger family *Zingiberaceae* cultivated throughout Asia. Its rhizome yields curcumin, a major component responsible for a variety of pharmacological activities. Turmeric is used as a spice, food preservative, and coloring agent. Its phytoconstituents include three curcuminoids: curcumin (responsible for the yellow color of the rhizome), desmethoxycurcumin, and bisdemethoxycurcumin, as well as volatile oils, proteins, sugar, and resins [144].

In traditional medicine systems, turmeric has been used to treat liver obstruction, ulcers, inflammation, dental issues, indigestion, blood purification, skin infections, asthma, wounds, bronchitis, tumors, piles, and hepatic disorders. Modern research emphasizes the need to explore the therapeutic potential of turmeric in comparison to curcumin, especially through clinical trials. Both the plant and curcumin exhibit antioxidant, antimicrobial, anti-inflammatory, neuroprotective, cardioprotective, anticancer, hepatoprotective, immunomodulatory, antiallergic, and antidermatophytic properties [145],[146].

The chemical composition and antimicrobial properties of *Curcuma longa* essential oil have been investigated by de Oliveira Filho et al. [147]. Significant antibacterial activity against *Staphylococcus aureus* and *Escherichia coli* has been revealed, suggesting its potential as a natural alternative to synthetic antibiotics. Scientists also highlight the influence of drying temperature and solvent extraction on the bioactive compound content and turmeric extracts' antioxidant, antimicrobial, and cytotoxic activities. The results indicate that the most efficient conditions for phenolic compound extraction involve using a methanol/water solvent from plants dried at 60 °C. Conversely, the highest flavonoid content is yielded using the same solvent for turmeric dried at 40 °C. Moreover, extracts prepared using an ethanol/water solvent exhibited higher antimicrobial efficiency regardless of drying temperature compared to other extraction solvents. In conclusion, turmeric's rich profile of secondary metabolites, including flavonoids and terpenes, supports its extensive use in traditional medicine and potential applications in medical and pharmaceutical industries [148].

*Zingiber officinale* Roscoe, known as ginger, is a perennial plant from the *Zingiberaceae* family widely used as a spice and traditional medicine. Extensively cultivated, ginger has been the subject of numerous studies focusing on its chemical composition and biological activities. The rhizome contains a variety of bioactive compounds, including 194 types of volatile oils, 85 types of gingerols, and 28 types of diarylheptanoids. Key components like gingerols, shogaols, and paradols are responsible for ginger's antioxidant, antimicrobial, anti-inflammatory, and anticancer properties. Ginger also shows promise in managing diseases such as cardiovascular and neurodegenerative disorders, diabetes, obesity, and respiratory issues [149],[150].

Research by Gao et al. [151] has highlighted ginger's gastrointestinal-protective, anticancer, and obesity-preventive effects, with gingerol analogs being rapidly metabolized. The composition of ginger essential oil, which is influenced by the harvesting season, has been shown to yield the highest content of essential oil when harvested at five months of maturity. Moreover, it exhibits various bioactive properties, including antibacterial, antifungal, anti-ulcer, analgesic, and immunomodulatory activities [152]. Clinical trials have demonstrated ginger's efficacy in reducing early pregnancy-related nausea and vomiting, although its long-term safety requires further investigation [153].



Moreover, compounds such as gingerol, geraniol, shogaol, zingiberene, zingiberenol, and zingerone have shown potential as antiviral agents with good oral bioavailability [154]. Studies have also revealed that phenolic extracts from ginger exhibit significant anti-inflammatory and healing properties. Experiments with rats showed that ginger extract substantially reduced edema and enhanced wound healing, underscoring their therapeutic potential. These findings emphasize the need for additional research to fully explore ginger's medicinal applications and optimize its bioactive compounds' use in pharmaceuticals and cosmetics [151],[155].

Table 2.2 presents a summary of the aforementioned plants, categorizing them based on their similarity in polyphenolic compounds, availability and cultivation conditions, antimicrobial activity, and overall health benefits. This analysis served as the basis for selecting fillers in the experimental part of the study. It should be noted that the term "polyphenols similarity" refers to plants sharing a significant number of common major constituents. "Cultivation conditions" encompass the requirements for growing and harvesting the plants, as well as their year-round availability in Poland. The evaluation of antimicrobial activity focused primarily on the efficacy of these plants against microbes causing infections, such as those in wounds. Health benefits refer to properties that promote overall patient health in addition to antimicrobial activity.

Table 2.2. A summary of selected plants

Plant	Property			
	Polyphenolic compounds	Cultivation and availability	Antimicrobial activity	Health benefits
Thyme	✓✓✓	✓✓✓	✓	✓✓
Sage	✓✓✓	✓✓✓	✓✓✓	✓
Rosemary	✓✓✓	✓✓	✓✓	✓✓
Peppermint	✓✓	✓✓✓	✓	✓
Lemon balm	✓✓	✓✓✓	✓	✓
Turmeric	✓	✓	✓	✓✓✓
Ginger	✓	✓	✓✓✓	✓✓✓

To summarize, plant-based compounds exhibit a wide array of bioactivities that are essential for medical applications, particularly in wound healing and its protection. Consequently, they can function as fillers that supply bioactive substances. A distinct challenge is the effective dispersion of these compounds within the polymer matrix, with the objective of enhancing the functional properties of the polymers while leveraging the bioactive attributes of the plant-derived compounds. Such materials require specialized research tailored to their specific application areas. This approach is anticipated to significantly improve wound healing outcomes and provide more effective protection and treatment in medical applications.

## **2.4. Materials testing methods of polymers used in the medical industry**

Before being utilized in any application, materials must undergo a series of tests to confirm their suitability for the intended purpose. This process is especially rigorous in the medical field, where materials require additional testing due to their potential impact on the human body. Medical application testing protocols are supplemented with extra precautions to ensure biocompatibility and safety. This includes conducting several additional tests to assess the material's interaction with biological systems, thus guaranteeing that it does not pose any harm when in contact with human tissue. Depending on the intended field and possible application, different tests are required; however, for a material to be used in contact with the human body, biocompatibility is the most essential property it needs to fulfill.

Biocompatibility refers to a specific set of properties a material must possess to ensure safe use within a biological organism. These properties include being non-carcinogenic, non-pyrogenic, non-toxic, non-allergenic, blood-compatible, and non-inflammatory. Operationally, biocompatibility can be defined by the material's ability to be used without causing harm to the patient; if the patient remains alive and unharmed, the material can be considered biocompatible [156].

To determine a material's biocompatibility, it must undergo a series of tests tailored to its intended application, whether it involves contact with skin, blood, or internal tissues. One of the most fundamental tests is the cytotoxicity assay, which involves exposing the material to cell lines relevant to its future application and evaluating the ability of these cells to grow and propagate. For applications that involve direct or indirect contact with blood, hemocompatibility assays are essential. These tests assess the material's interaction with blood cells and plasma. Additional evaluations, such as hypersensitivity and genotoxicity tests, are also conducted to ensure comprehensive biocompatibility assessment [157].

Although biocompatibility is the most crucial characteristic of a biomaterial, it must also meet basic functional properties and, depending on the application, additional features such as broadly understood bioactivity. Mechanical properties, including stiffness, strength, and hardness, are primarily evaluated using universal testing machines

and durometers to determine whether the material can withstand the stresses encountered during its function. Furthermore, environmental factors and loading conditions, such as tension or compression, and whether the load is continuous or cyclic, must be considered during testing to ensure the material's performance under realistic conditions. In addition, tests such as wear resistance are important when friction is crucial in the intended application.

The characterization of physical and chemical properties is crucial from both the production standpoint and in terms of working conditions. For example, density and permeability are critically important in drug release or gas exchange applications. Chemical properties, on the other hand, are essential for assessing the material's susceptibility to degradation, particularly during sterilization, which is a vital step to ensure a contamination-free and safe application. Understanding these properties ensures that the material will perform reliably and safely in its intended environment.

The bioactivity of a biomaterial is a feature that enhances its applicability in medicine. Bioactivity refers to the interactions between the material and cellular responses, which subsequently lead to specific cellular behaviors. For instance, bioactivity refers to the material's ability to foster cell growth in applications where the medical device is expected to promote cell proliferation, such as in scaffolds and tissue engineering [158].

Conversely, antimicrobial activity becomes essential in applications where microbial adherence and biofilm formation are inevitable or highly likely. For example, assessments of antibacterial activity are carried out using various methods and protocols tailored to the specific material and its intended application. These tests may involve different bacterial strains based on the application's specific requirements.

## 2.5. Organic fillers-enriched composites with enhanced antimicrobial properties

Organic plant-derived fillers can be incorporated into a polymeric matrix in various forms. Depending on the type of matrix, the intended application, and the desired properties and outcomes, these additives may be introduced as essential oils, polyphenolic extracts, or in powdered form without prior extraction. This chapter examines different herbs and plant-derived fillers and their effects on modifying the bioactivity of polymers, with a focus on enhancing antimicrobial activity.

### 2.5.1. Materials modified with essential oils

Essential oils, including black pepper and ginger, are known for their remarkable antimicrobial, antioxidant, nutritional, and biomedical properties. Despite these benefits, their clinical application is often limited due to their poor aqueous solubility and instability, leading to reduced retention of their beneficial properties over time. To address these limitations, one study developed biocomposite films incorporating chitosan, gum arabic, and polyethylene glycol with aforementioned essential oils using a solution casting method at 60 °C. The films, dried for 40 min at 50 °C, exhibited rough surfaces, with essential oils droplets entrapped within the matrix, contributing to their structural integrity. Mechanical testing revealed that the films possessed significant mechanical strength, flexibility, and thermal stability. Notably, composites containing ginger oil exhibited superior tensile strength (7.58 MPa) and elongation (79.44%) compared to those based on black pepper oil. Additionally, the essential oil-incorporated films demonstrated high antimicrobial activity against *Bacillus cereus*, *Staphylococcus aureus*, *Escherichia coli*, and *Salmonella typhimurium*. The inhibition zones for composites with essential oils were 3-4 times larger compared to reference composites, suggesting their potential use in wound dressing materials. [159],[160].

In a similar study by Altaf et al. [161], hydrogel membranes were fabricated through the esterification of polyvinyl alcohol with starch, incorporating essential oils such as clove, oregano, and tea tree oil to enhance antibacterial activity and mechanical strength. Moreover, it was observed that the higher the content of these oils, the higher

the contact angle of the composites, indicating that the chemical composition of essential oils alters the surface wettability. The 0.1 mL clove oil-incorporated hydrogel exhibited optimal antibacterial activity against *S. aureus* and *E. coli* ( $39\pm 0.57$  mm and  $37\pm 0.29$  mm, respectively), tensile strength (19.36 MPa), and moisture retention (95.50%), marking it suitable for wound dressing applications.

In situ electrospun zein/thyme essential oil (TEO) nanofibrous membranes were developed to address the limitations of conventional wound dressings. The membranes containing 6 wt.% of TEO exhibited high gas permeability, reaching  $154\pm 20.9$  m<sup>2</sup>/s, superhydrophilicity with a 0° contact angle, and good antibacterial properties against *S. aureus* and *E. coli*. In vivo studies on mice demonstrated enhanced wound healing within 11 days, highlighting the efficacy of these membranes for wound management [162].

Moreover, thyme essential oil encapsulated in sodium caseinate nanomicelles was formulated into a gelatin nanocomposite hydrogel, which showed sustained release, enhanced antibacterial effects presented as bacterial cell wall and membrane disruption, and significant promotion of wound healing. This formulation is proposed as a multifunctional delivery system for thyme essential oil in wound healing applications [163].

In a similar work by Gheorghita et al. [164], researchers have succeeded in developing enhanced polymer compositions based on polyvinyl alcohol/polyvinyl pyrrolidone modified with 12 wt.% of essential oils, specifically mint, pine, fennel, and thyme oils, which exhibit promising properties for treating open wounds such as pressure ulcers. Moreover, these materials presented high antimicrobial activity against *Staphylococcus aureus*, *Enterococcus faecalis*, *Escherichia coli*, *Pseudomonas aeruginosa*, and *Candida albicans*.

Similarly, nanofibers based on collagen hydrolysate loaded with thyme or oregano essential oils were produced using electrospinning. These nanofibers exhibited antimicrobial properties and biocompatibility. Composites filled with thyme essential oil did not exhibit cytotoxicity up to a concentration of 1000 µg/mL, whereas those with oregano essential oil were non-cytotoxic up to 500 µg/mL. These properties make the

nanofibers promising candidates for applications in wound dressings, tissue engineering, and protective clothing [165].

Moreover, gelatin hydrogels loaded with *Salvia officinalis* essential oil were prepared by mixing gelatin and glycerol in a weight ratio of 1.25:1 and adding 0.2 wt.% of sage essential oil. This mixture was subjected to a microwave-assisted polymerization method and left to air dry for 4 to 5 days at room temperature. The resulting material demonstrated enhanced antibacterial activity and stability. The antibacterial activity of the hydrogels, assessed through the agar diffusion method, was comparable to that of silver nanoparticles and twice as effective as cinnamon essential oil against *S. aureus* and *E. coli* [166].

Lastly, polyurethane and cellulose acetate electrospun fibers encapsulating 3%, 5%, or 7% by weight of rosemary essential oil and silver nanoparticles were fabricated. These composites exhibited enhanced hydrophilicity, as indicated by a decrease in contact angle to  $62.8 \pm 0.9^\circ$  at the beginning of testing with higher loads of additives. They also showed increased PBS (phosphate buffered saline) absorption, reaching  $12.43 \pm 0.49\%$  for the highest content of additives after 5 days of incubation, and demonstrated superior antibacterial activity, with an increasing trend in activity correlating with higher contents of rosemary essential oil and silver nanoparticles. These composites mimic the natural extracellular matrix, promoting cell attachment and viability, indicating their potential utility in biomedical applications [167].

In conclusion, integrating essential oils into various biocomposite and hydrogel formulations offers promising advancements in antimicrobial and wound healing applications. These innovative materials, characterized by their enhanced mechanical properties, thermal stability, and significant antibacterial activity, present viable alternatives to conventional wound dressings.

### 2.5.2. Materials modified with polyphenolic extracts

Like essential oils, plant extracts are renowned for their significant bioactivity and diverse applications across various fields, particularly medicine. Numerous studies have investigated the effects of incorporating these extracts on the wound healing process and their protective benefits. For instance, *Moringa oleifera* extracts obtained using various water-to-methanol ratios were successfully incorporated into alginate films at concentrations of 0.1%, 0.5%, and 1% w/v. The cell viability results indicated that these extracts exhibited viability above 80%, deeming them non-toxic. Moreover, the wound scratch test results showed that due to the high amounts of vicenin-2, chlorogenic acid, and quercetin compounds present in the extracts, there was significant cell migration and proliferation. This led to the conclusion that these compounds facilitate the wound-healing process. Additionally, the tensile strength of the alginate films increased with higher extract concentrations, further supporting their potential use in wound healing applications. [168].

Sabando et al. [169] investigated pectin-based films for their biodegradable and biocompatible nature, which makes them suitable for wound dressing applications. A crosslinked pectin/starch blend loaded with bioactive extracts from *Gunnera tinctoria* and *Ugni molinae* leaves was developed, showing a controlled release of bioactive compounds and adequate water-uptake capacity (100-160%). Furthermore, it was concluded that adding extracts did not alter the mechanical properties of the hydrocolloid films. At the same time, they inhibited topical edematous responses and facilitated the complete closure of pressure ulcers within 17 days without adverse reactions, demonstrating their potential as effective wound dressings.

To address bacterial infections in wounds, *Tridax procumbens* extract was immobilized on polycaprolactone electrospun nanofibers, chosen for their beneficial surface properties and biocompatibility. The obtained nanofibers exhibited significant antibacterial activity (notably increased inhibition zone compared to fibers without the extract), enhancing wound healing and treating surfaces with pathogenic microorganisms, particularly in hospital environments [170].

Combining traditional Chinese herbal medicine with modern technology, Li et al. [171] fabricated an interactive and bioactive wound dressing using thyme extract



incorporated into polymeric nanofibers through electrospinning. Hemolysis tests demonstrated the dressing's hemocompatibility, with hemolysis rates remaining below 8%. In vitro studies further confirmed its cytocompatibility. The release kinetics analysis revealed that approximately 80% of the thyme extract was released from the nanofibers within the first 24 h. Additionally, animal studies indicated that the thyme extract-enriched nanofibers significantly enhanced the wound healing process.

To enhance the treatment of infections in chronic wounds, a nanofibrous mat composed of polyvinyl alcohol and chitosan, incorporating 10 wt.% thyme and ginger extracts, was developed. This mat exhibited excellent wettability, porosity, and liquid absorption capacity, with the latter increasing proportionally to the extract content, reaching 674% after 24 h. The mat provided a continuous and sustained release of active compounds for nearly 72 hours. It effectively inhibited the growth of both Gram-positive *S. aureus* and Gram-negative *E. coli* strains. The mat significantly accelerated cutaneous wound healing in bacterial-infected rats, reducing the wound area to  $0.05 \pm 0.01$  cm<sup>2</sup> by the 14th day [172].

Another study explored the development of electrospun poly(caprolactone)/poly(vinyl alcohol) core-shell nanofibers incorporated with 5% w/v thyme extract. Fourier transform infrared analysis indicated that incorporating thyme extract into the polymeric matrix did not alter its chemical backbone but affected certain peaks' intensity. Additionally, the inclusion of thyme extract reduced the water contact angle from approximately 83° to 76°, likely due to the presence of the polar compounds thymol and carvacrol, which increase hydrophilicity. Tensile testing revealed that incorporating thyme extract decreased the tensile strength of the matrix from 1.51 to 1.08 MPa but significantly increased the tensile strain almost twofold, from 74.14% to 143%. Cytotoxicity assays demonstrated that the thyme extract-enriched material was non-toxic to fibroblast cells, and antibacterial assessments showed high efficacy against both Gram-positive and Gram-negative bacteria. These findings suggest the potential application of this composite material in wound healing [173].

A study by Vasile et al. [174] investigated poly(lactic acid)-based multifunctional materials containing 3 and 6 wt.% chitosan and 0.5 wt.% rosemary extract. The composites containing only rosemary extract exhibited a slight decrease in tensile strength, around 27 MPa, which further decreased with the addition of 3 and 6 wt.%

chitosan, dropping to 24 MPa and 14 MPa, respectively. Conversely, the elongation at break for rosemary extract-enriched materials was higher than the reference, reaching approximately 9%. In comparison, the composite containing 6 wt.% chitosan and rosemary extract exhibited significantly higher elongation at break, exceeding 50%. Impact strength tests showed that the addition of rosemary extract increased the impact value of composites containing only 3 wt.% chitosan by 500%, highlighting the favorable impact of incorporating rosemary extract on the mechanical properties. The antibacterial evaluation revealed varied behaviors depending on the tested strain; however, after 48 h of incubation, all modified composites exhibited 100% inhibition. Water contact angle measurements indicated that composites containing only rosemary extracts had increased angles for all tested solutions, suggesting an influence on the wettability. The obtained materials demonstrated adequate properties, making them suitable for short-term biomedical implants and innovative drug delivery systems.

Carbomer-based hydrogel dressings incorporating 10% ethanolic extracts of *Rosmarinus officinalis* aerial parts and *Achillea millefolium* and *Calendula officinalis* flowers were developed. The rosemary extract-enriched material exhibited a firmer structure than the other extract-modified composites, reducing its stretchability by 10% compared to the reference. Additionally, this composite was the only one to demonstrate antibacterial activity against *Staphylococcus aureus*, *Pseudomonas aeruginosa*, and *Candida albicans*. Despite a slight decrease in pH and texture due to the extracts, the hydrogels proved effective as potential wound dressing materials, warranting further in vivo studies [175].

In conclusion, the incorporation of plant and herbal extracts into polymeric matrices has been extensively explored for various medical applications, both internal and external. This approach highlights the potential to develop biocompatible medical polymers with enhanced bioactivity while maintaining the required operational properties. However, the procedure of obtaining extracts and essential oils mainly necessitates chemical processes, leading to higher production costs and extended manufacturing times. Consequently, researchers are increasingly investigating the direct incorporation of plant parts into polymeric matrices to achieve materials with improved bioactivity.

### 2.5.3. Materials modified with powdered plants

The novel approach of incorporating powdered plants and herbs has the potential to yield composites with desirable properties and enhanced bioactivity, all while being environmentally friendly and generating no by-product waste. Additionally, this method facilitates the production of composites using off-the-shelf products, thereby accelerating the process and reducing costs.

Hybrid cellulose nanocomposite films were developed using cellulose from cotton as the matrix, with 5 to 25 wt.% of modified tamarind nut powder and copper nanoparticles as fillers. The results demonstrated that the addition of tamarind nut powder increased the crystallinity of the nanocomposites to 74.2% for those filled with 25 wt.%, compared to the 61.1% crystallinity of the cellulose matrix, without altering the chemical backbone of the matrix. The composites also exhibited enhanced antibacterial properties against *E.coli*, *P.aeruginosa*, *S.aureus*, *B. licheniformis* pathogens due to the presence of the phytochemicals found in tamarind nut powder and  $\text{Cu}^+$  ions [176].

Bazan et al. [177] investigated the modification of thermoplastic elastomer, specifically polyolefin (TPO), using various organic (horseradish root, ginger root, and chicory) and inorganic antibacterial additives at a weight percentage of 3%. The materials underwent injection molding, with a reduction of 10 °C in each zone's temperature for composites containing natural additives to prevent thermal degradation. The tensile testing results showed an overall increase in tensile strength for all modified TPO variants, particularly with organic additives demonstrating higher values (up to approximately 14.7 MPa for TPE with ginger root). Similar trends were observed in Shore D hardness measurements and flexural strength values. UV aging tests indicated that while only the matrix exhibited increased tensile strength, organic-modified composites showed a slight decrease after aging yet maintained higher or similar values compared to the reference. Specifically, the strain in ginger root-enriched TPO dropped to 80% after aging, whereas all materials achieved >300% strain both before and after aging. The study also assessed antimicrobial efficacy, noting varying degrees of bacterial survival reduction across different strains. Organic-modified composites exhibited greater effectiveness against Gram-negative bacteria and fungi than inorganic additives.

Furthermore, a study aimed to produce reinforced biocomposites using biomass-derived polypropylene with antibacterial turmeric for orthoses and medical equipment. Six hybrid composites with 5-15% basalt fibers, 5-15% microcellulose fibers, 2% turmeric powder, and 2% anhydride maleic compatibilizer were manufactured using injection molding. The resulting materials demonstrated increased tensile strength, achieving 35 MPa in composites modified with 10% basalt fibers, with a notable decrease in the strain at break by 94% compared to pure polypropylene. Similar trends were observed in bending tests, where fiber-modified materials exhibited bending strengths ranging from 40.2 to 54.2 MPa, surpassing the reference value of 34.6 MPa. Hydrothermal degradation testing conducted at 40 °C over 6 weeks indicated that the investigated materials retained their mechanical properties with minor deterioration. This study underscores the feasibility of producing functional biocomposites with enhanced strength and stiffness, thereby rendering them suitable for medical applications [178].

Chaaben et al. [179] developed a novel biocomposite for dental restorations consisting of poly(methyl methacrylate) resin and 30 wt.% *Salvadora persica* powder, commonly known as miswak. The filler was dried at room temperature and ground to a size under 40 µm. The mixture was cured in a pressure device at 60 °C for 10 minutes under 0.5 MPa. Antibacterial assessments revealed that the filler exhibited high activity, with an inhibition zone of approximately 22 mm against *Haemophilus influenzae*. However, the composite demonstrated a reduced inhibition zone of around 8 mm, suggesting that the incorporation of miswak limited its bioactivity due to the restricted release of the filler from the matrix. Despite this limitation, the observed antibacterial zone is still significant, indicating the composite's antibacterial characteristics. Furthermore, the composite did not present residual monomers that could cause oral inflammatory symptoms, highlighting its potential for dental applications.

In a similar study, a polylactic acid matrix composite reinforced with *Salvadora persica* was developed to address mechanical issues due to filler incompatibility. Miswak powder was added at concentrations of 5-20 wt.%. The addition of the filler increased the material's density with increasing filler content while decreasing the tensile strength and elongation at break values by 48% and 83%, respectively, for the maximum filler content. Similar trends were observed for flexural strength, with the value dropping from 89.15 to 47.79 MPa. However, it was concluded that composites with 5% miswak exhibited

excellent interlayer adhesion and mechanical strength, indicating their suitability for 3D printing applications. This suggests the potential for developing sustainable materials with antimicrobial benefits [180].

Moreover, chitosan-based biomaterials incorporating ginger, curcumin, and cinnamon were fabricated for wound healing applications. The fillers were dried at 50 °C and added to the chitosan mixture at 0.5 g each, forming thin films of 0.1 and 0.2 mm thickness. Morphology analysis revealed the presence of agglomerates throughout the matrix. Ginger-modified chitosan exhibited the highest surface roughness at 167.2 nm, followed by the curcumin composite at 63.1 nm and the cinnamon composite at 53.5 nm, with the lowest roughness observed for pure chitosan at 40.1 nm. Antimicrobial characterization demonstrated high efficacy against various microorganisms. Specifically, chitosan/ginger composites exhibited superior mechanical properties, with a tensile strength reaching 38.3 MPa, an approximate increase of 17%, along with enhanced antimicrobial activity, making them particularly suitable for wound dressings [181].

Lastly, Moopayak et al. [182] explored the use of *Garcinia mangostana L.* (mangosteen) peel and seed as bio-fillers in natural rubber latex products, such as medical gloves and transdermal patches. The peel and seed demonstrated excellent antibiotic properties. Gloves incorporating mangosteen peel powder exhibited hydrophobicity, with a water contact angle of  $130.67 \pm 2.08^\circ$ , and good mechanical properties, including high tensile strength ( $64.59 \pm 13.54$  MPa), elongation at break ( $815.72 \pm 54.67\%$ ), and stiffness ( $296.50 \pm 48.32$  N/m). These materials were also non-toxic to the skin, making them suitable for medical applications. Furthermore, the organic-enriched composites showed negligible cytotoxicity, whereas composites filled with higher concentrations of silver nitrate were deemed toxic. Natural rubber patches containing mangosteen seed exhibited high wettability, with a water contact angle of  $81.47 \pm 1.27^\circ$ , and mechanical properties similar to those of mangosteen peel-modified composites. These findings suggest their potential for antimicrobial and drug delivery applications.

In conclusion, this chapter focused on the outcomes of incorporating bioactive plant-based compounds into polymeric matrices and explored their potential utilization in the medical field, particularly for external applications. The primary emphasis was on obtaining materials with enhanced antibacterial properties. However, compared to materials enriched with essential oils and extracts, the direct incorporation of plant parts

in powder form into polymers for medical applications is limited, and few studies address the practical application of such materials. Although favorable results have been observed, this process can be constrained by the sensitivity of natural materials to the high temperatures often involved in production processes. This is particularly crucial because polyphenolic compounds are temperature-sensitive and can undergo degradation at elevated temperatures. Additionally, changes in crystallinity due to the cross-linking process may hinder the utilization of these materials due to their low functional properties, thereby limiting their use in applications where durability is required. Therefore, properties such as degradation temperature and chemical composition should be carefully considered when developing bio-based materials.

### 3. Literature review conclusions

Based on the conducted literature review, the following was concluded:

- Among elastomeric polymers, polydimethylsiloxane (PDMS) is widely employed in medical applications, both internal and external, due to its biocompatibility, high gas permeability, flexibility, and low reactivity. However, a notable limitation is its lack of antibacterial properties. The literature presents various methods for modifying PDMS to meet the specific requirements of medical applications.
- Wound dressings are the most common extracorporeal application of PDMS in medicine and can be classified as either passive or bioactive based on their intended use. These dressings often incorporate bioactive substances, such as drugs, nanoparticles, or monomers, to inhibit microbial adherence and biofilm formation while promoting wound healing by delivering substances that enhance cell proliferation.
- The rise of antibiotic-resistant bacteria necessitates the development of alternative solutions. Moreover, the production and incorporation of inorganic additives are often not financially efficient, involving complex and time-consuming synthesis processes.
- Naturally-derived compounds, both animal- and plant-based, exhibit a wide variety of bioactivities essential for medical applications, including antimicrobial properties and the promotion of cell growth. The inclusion of plant-derived fillers, such as essential oils and extracts, has been shown to be beneficial for the wound healing process and in combating microbial infections. Nevertheless, the preparation of these fillers can extend the biomaterial manufacturing process.
- The composition of plant additives is closely related to the conditions and environment of their cultivation. The specific plant part (root, stem, leaf, flower, or seeds) from which fillers are derived plays a significant role. Fillers from herbs are particularly promising due to their bioactive properties.
- The direct incorporation of plant or herbal powders into a polymeric matrix enhances the antibacterial activity and presents significant potential for creating bioactive materials. However, this approach has not been extensively studied. The use of organic fillers may be limited due to their thermal sensitivity, particularly the

bioactive polyphenolic compounds, and their potential impact on the polymerization process.

- There is a gap in research concerning the modification of the bioactive properties of PDMS while maintaining the performance characteristics of herbal powders. This area requires further investigation, which is the focus of this study.



## 4. PhD thesis and aims

Based on preliminary research and an extensive literature review, the thesis of this work was developed. **The introduction of specially prepared organic fillers, derived from selected parts of bioactive herbs, into polydimethylsiloxane significantly enhances its antibacterial activity while maintaining the necessary functional properties for external medical applications, such as dressings, i.e., mechanical and physicochemical properties, while at the same time ensuring long-term functionality and reliability in medical contexts.**

To address the put-forward thesis, this work aims to develop innovative biocomposites based on polydimethylsiloxane that exhibit superior antimicrobial properties. This research focuses on incorporating specific organic additives into the polymeric matrix and assessing their impact on selected physicochemical, mechanical, and biological properties. These additives are carefully selected for their ability to impart bioactive properties, effectively combating various pathogenic microorganisms. The work aims to ensure that, despite incorporating these bioactive fillers, the composites retain their essential functional characteristics, such as physicochemical stability, mechanical strength, and durability. This balance is crucial to meet the strict standards required for potential applications in medical and healthcare.

## 5. Methodology

The doctoral thesis required the development of biocomposites production technology, specifically focusing on the proper preparation of the fillers. The experimental part was divided into three phases, each followed by a multicriteria analysis to assess the extent of alterations and identify the most promising materials. The research methodology is delineated in Figure 5.1.

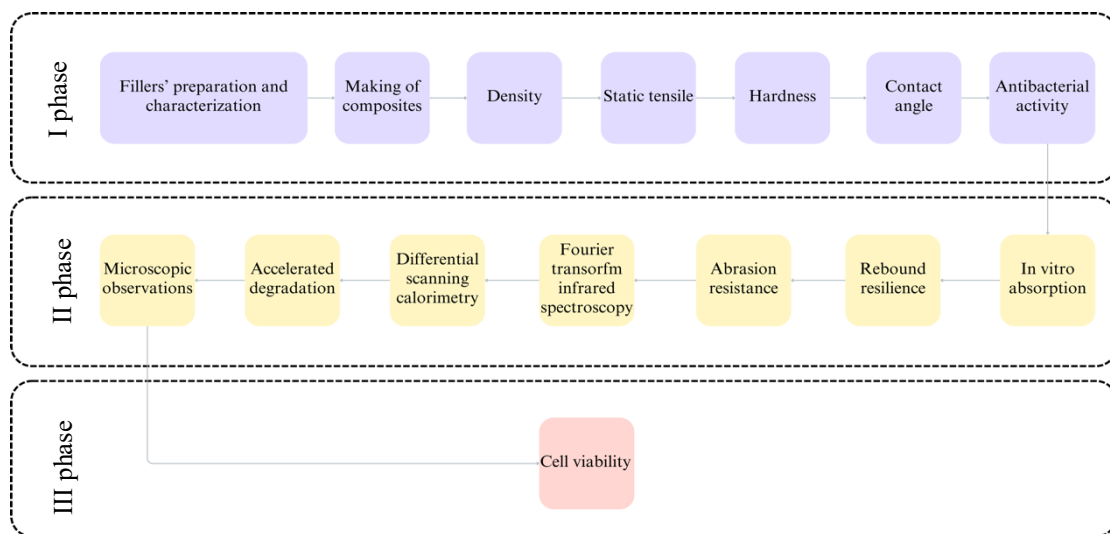


Figure 5.1. Research methodology

The scope of work covers:

- Identification and characterization of fillers – this step facilitates the selection of three promising herbal additives whose properties were tested to assess their influence on the resulting biocomposites.
- Preparation of biocomposites – detailed in Section 5.1.4.
- Physiochemical and mechanical properties– the selected experiments assess the impact of the fillers on the operational characteristics.
- Accelerated degradation tests in a simulated human body environment – this step assesses the long-term performance of the acquired materials.
- Bioactivity assessment – evaluation of the materials' antibacterial activity and cytotoxicity.
- Validation of the results, considering their potential medical applications.

Unless otherwise specified in individual studies, all experiments were performed in a laboratory maintained at a constant temperature of  $21\pm 2$  °C and a relative humidity of 40%. Furthermore, data curation and statistical analysis were conducted using OriginLab software (OriginLab Corporation, Northampton, MA, USA), with results reported as mean values with standard deviation.

## 5.1. Materials

### 5.1.1. Biocomposites' matrix

The matrix was a two-component, addition cross-linking, medical-grade polydimethylsiloxane (confirmed by infrared spectrum in Figure 5.2), where the linking agent is platinum(0)-1,3-divinyl-1,1,3,3-tetramethyldisiloxane under the commercial name Dragon Skin™ 30 (Smooth-On, Inc., Macungie, PA, USA). This material has a skin safety certificate, the properties of which are presented in Table 5.1 [183].

Table 5.1. Selected properties of PDMS [183]

Property	Value (unit)
Density	1.08 (g/cm <sup>3</sup> )
Viscosity	20 (mPa·s)
Hardness	30 (ShA)
Strain at break	3.45 (MPa)
Strain at break	364 (%)

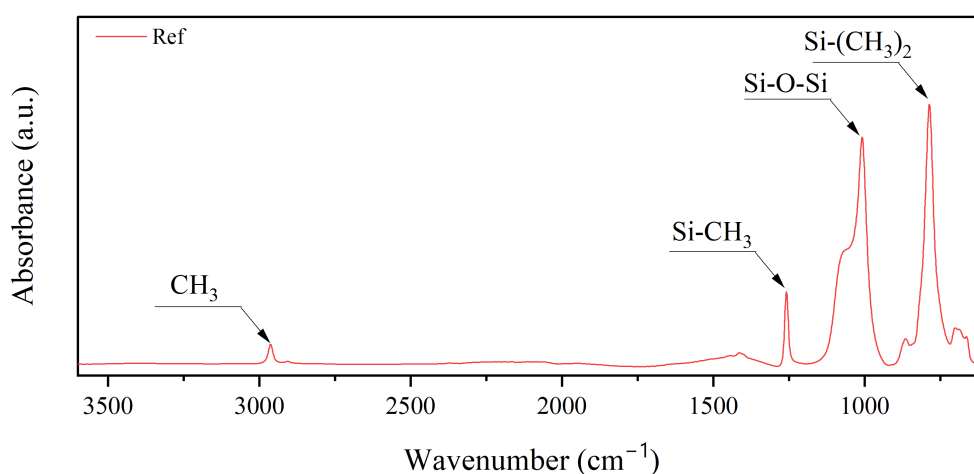


Figure 5.2. IR spectrum of the matrix

The matrix's IR spectrum displayed characteristic peaks of PDMS at  $786\text{ cm}^{-1}$  and  $1259\text{ cm}^{-1}$ , corresponding to the  $\text{CH}_3$  rocking and bending in  $\text{Si-CH}_3$ , respectively;  $1006\text{ cm}^{-1}$  for  $\text{Si-O-Si}$ ; and  $2967\text{ cm}^{-1}$  for C-H stretching in  $\text{CH}_3$  bands.

### 5.1.2. Fillers' preparation

Based on the literature review in Section 2.3.2, three herbs were selected as matrix modifiers: thyme, sage, and rosemary – Figure 5.3. All of the selected fillers were derived from herbal leaves.



Figure 5.3. Modifying fillers: thyme – a), sage – b), rosemary – c)

The leaves of the herbs were sourced from different regions: thyme from Turkey, sage from Poland, and rosemary from Morocco. Notably, in the case of sage, woody-like particles are visible, likely due to the presence of aged lignified petioles. The herbs were initially obtained in a dried state; however, they were further dried to a constant weight at  $20\pm 2\text{ }^\circ\text{C}$  in SLW 53 STD forced air dryer (Pol-Eko, Wodzisław Śląski, Poland). These

conditions allowed for the elimination of any residual moisture without significantly influencing the polyphenols, which are temperature-sensitive. Next, the fillers were ground in a four-blade grinder and separated into three groups: unmodified material (raw, ground herbs) – Figure 5.4.a,d,g, modified material (the proposed modification process is explained afterward) – Figure 5.4.b,e,h, and polyphenolic extracts – Figure 5.4.c,f,i.

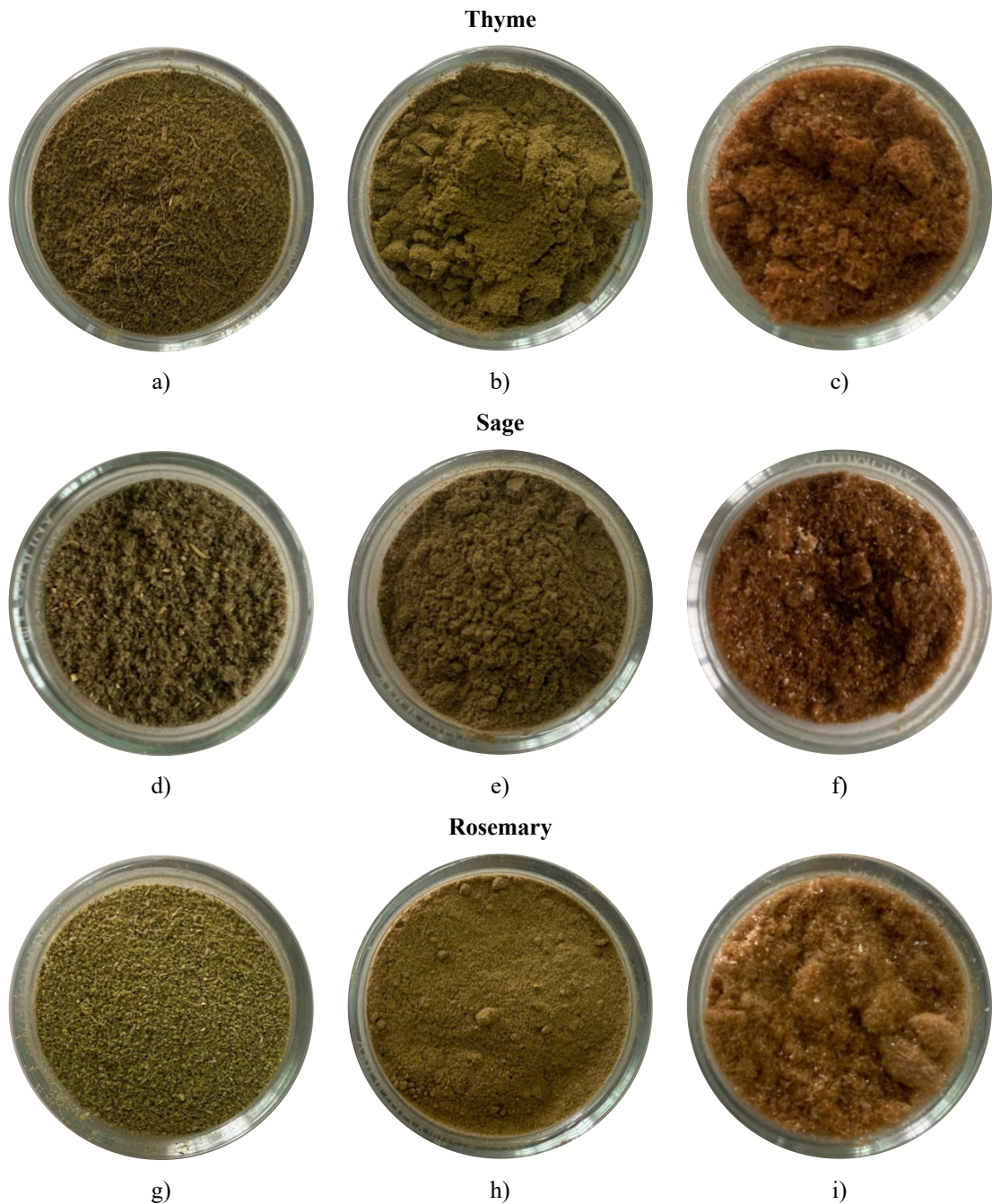


Figure 5.4. The selected fillers: raw material – a), d), g), modified material – b), e), h), polyphenolic extract – c), f), i)

The proposed modifications were implemented following a preliminary assessment of the raw material-silicone biocomposites. The algorithm detailing the selection process for these modifications is presented in Section 5.1.4. The second set of herbs underwent sieving using meshes with a size of 100  $\mu\text{m}$  using a Mutliserw sieve shaker (MULTISERW-Morek, Brzeźnica, Poland). Next, rosemary and sage were wetted with 90% ethanol for 4 h at room temperature and dried for 24 h at  $30\pm 2$  °C. This procedure facilitated the elimination of the adverse effects of fatty compounds on silicone polymerization, specifically the decrease in crosslinking density [184]. Furthermore, given the elevated concentration of terpenes and fatty acids in rosemary, a further step involved subjecting it to water vapor for 2 h, inducing the evaporation of these compounds. The modified rosemary filler was subsequently dried for 24 h at  $30\pm 2$  °C.

The last set of fillers constituted polyphenolic extracts obtained in cooperation with the Department of Biochemistry and Crop Quality, Institute of Soil Science and Plant Cultivation. The finely ground raw herbs (150 g of sage, 140 g of thyme, and 150 g of rosemary) underwent two extractions with boiling MiliQ water (3.5 L + 1.5 L), each lasting 5 min. Following the combination, the extracts underwent filtration using a Schott funnel and centrifugation (4500 rpm, 5 °C; Sigma 3-26 KL, Osterode am Harz, Germany) for 10 min. The aqueous extract contained significant levels of polar impurities, such as carbohydrates and organic acids, as confirmed by liquid chromatography-mass spectrometry (LC-MS) analysis.

The phenolic compounds were subsequently purified through solid-phase extraction on a short column (12 cm  $\times$  5 cm) packed with Cosmosil C18-Prep bed (140  $\mu\text{m}$ ; Nacalai Tesque Inc., Kyoto, Japan). Methanol and formic acid were introduced to the extract to achieve final concentrations of 2% and 0.1% (v/v), respectively. After filtration and loading (in five separate portions) onto a column stabilized with 2% MeOH (v/v), the ballast components were washed with 2% MeOH (v/v) containing formic acid. At the same time, the target compounds were eluted using 60% MeOH (v/v). The resulting polyphenol fractions were consolidated and subsequently lyophilized (Gamma 2–16 LSC, Christ, Osterode am Harz, Germany) following solvent evaporation on a vacuum evaporator (Laborota 20, Heidolph, Schwabach, Germany) at 40 °C. This process yielded 9.02 g, 9.19 g, and 16.67 g of thyme, sage, and rosemary polyphenolic

extract, respectively. The abbreviations utilized to describe the fillers are presented in Table 5.2.

Table 5.2. Fillers codes

	<b>Material</b>	<b>Code</b>
Thyme	Unmodified	UT
	Modified	MT
	Extract	ET
Sage	Unmodified	US
	Modified	MS
	Extract	ES
Rosemary	Unmodified	UR
	Modified	MR
	Extract	ER

### 5.1.3. Fillers' characterization

A thorough investigation of the fillers enabled the assessment of their impact on the resulting biocomposites. The morphology and size distribution of the grains significantly affect the integration between the additives and the matrix, thereby influencing the mechanical properties. Additionally, phytochemical analysis quantified and identified the chemical compounds in the fillers that may affect the cross-linking process of the matrix, subsequently impacting the tested properties.

The morphological characteristics of the selected fillers were examined utilizing a Zeiss Supra 35 scanning electron microscope (SEM) (Carl Zeiss AG, Oberkochen, Germany). Prior to analysis, the filler particles were coated with gold powder for 90 s to enhance their conductivity and visualization under the microscope. The results are presented in Figure 5.5.

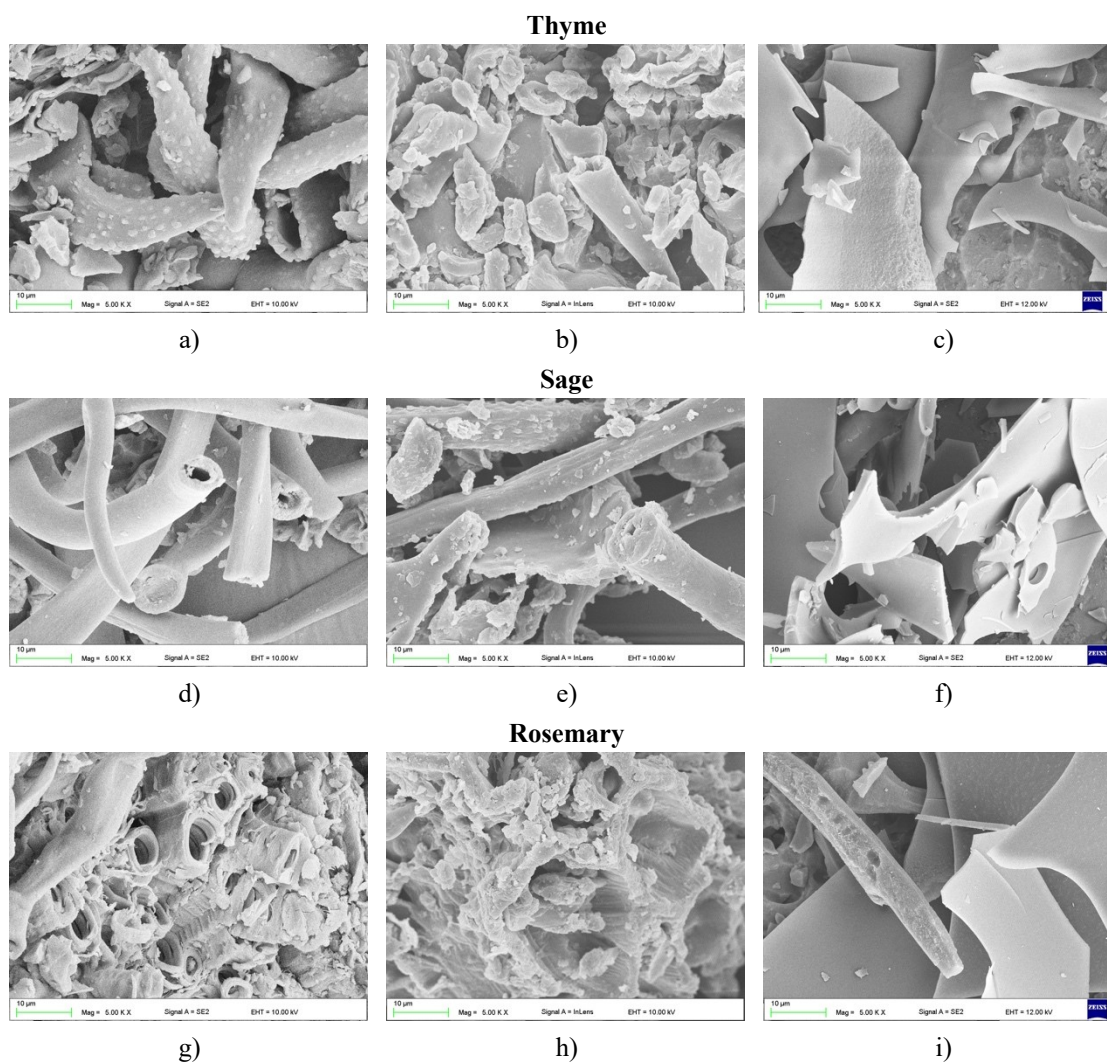


Figure 5.5. SEM micrographs of the tested fillers: raw material – a), d), g), modified material – b), e), h), polyphenolic extract – c), f), i)

The tested fillers exhibit uneven, variably shaped particles with visible stomas and trichomes. For thyme, the trichomes are short, with multiple glands on their surface, whereas for sage, they are long and smooth. Additionally, rosemary grains are noticeably larger, with irregular shapes and larger open particles. As can be seen, modification of the fillers does not visibly alter the morphology of the grains. On the other hand, the extracts are characterized by thin yet large particles with irregular shapes and smooth surfaces. Although the high surface roughness caused by the irregularity of the particles and the presence of numerous open stomas and glands may adversely affect the wetting of fillers by the polymer, the well-developed surface of the particles increases the contact area between the matrix and the filler, thereby could enhance mechanical adhesion.

The particle size and distribution of the grains were assessed through laser diffraction (LD) employing a Fritsch Analysette 22 Micro Tec Plus system (FRITSCH



GmbH, Idar-Oberstein, Germany). The results are depicted in Figure 5.6 and Table 5.3, in which the 10<sup>th</sup> (D<sub>10</sub>), 50<sup>th</sup> (D<sub>50</sub>), and 90<sup>th</sup> (D<sub>90</sub>) percentiles of the fillers size are presented.

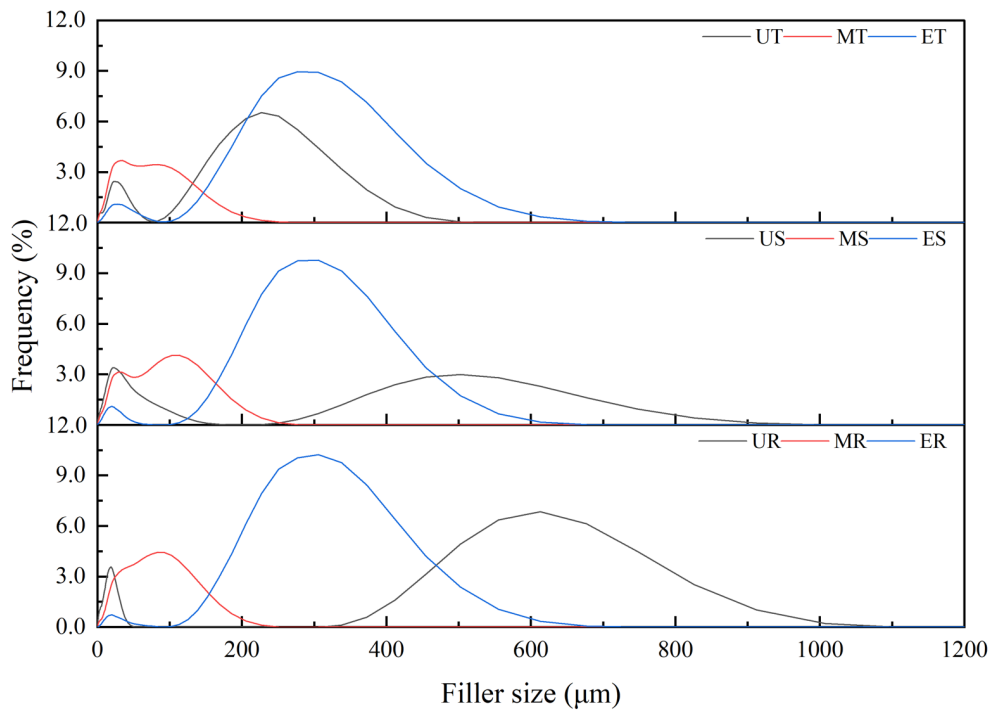


Figure 5.6. Fillers' particle size

Table 5.3. The average size of the fillers' particles

Average particle size, µm	Filler								
	UT	MT	ET	US	MS	ES	UR	MR	ER
D <sub>10</sub>	6.14	8.28	21.19	3.66	6.65	15.81	3.13	8.67	50.51
D <sub>50</sub>	133.70	39.48	239.01	25.41	41.33	244.75	20.62	44.04	258.72
D <sub>90</sub>	281.73	126.50	388.52	471.12	131.21	380.71	657.53	116.21	398.44

Compared to all other fillers, the largest particles characterize unmodified rosemary, followed by sage. For thyme, the largest particles are found in the extract, whereas the smallest are in the modified herb. In general, all unmodified herbs exhibit a bimodal distribution. Therefore, it can be deduced that the sieving made the distribution more uniform. Extracts of the fillers are all characterized by a similar particle size distribution. The results in Tabl 5.3 indicate that at the 90<sup>th</sup> percentile, unmodified rosemary (UR) has the largest particles, while modified rosemary (MR) has the smallest ones, demonstrating that the modifications had the greatest impact on rosemary.

Measurements were performed using a gas pycnometer, specifically the AccuPyc II 1340 model (Micromeritics, Norcross, GA, USA), to determine the grains' density. This analysis was repeated five times for each type of filler to ensure the accuracy and reliability of the density data obtained. The results are presented as mean values with standard deviation in Figure 5.7.

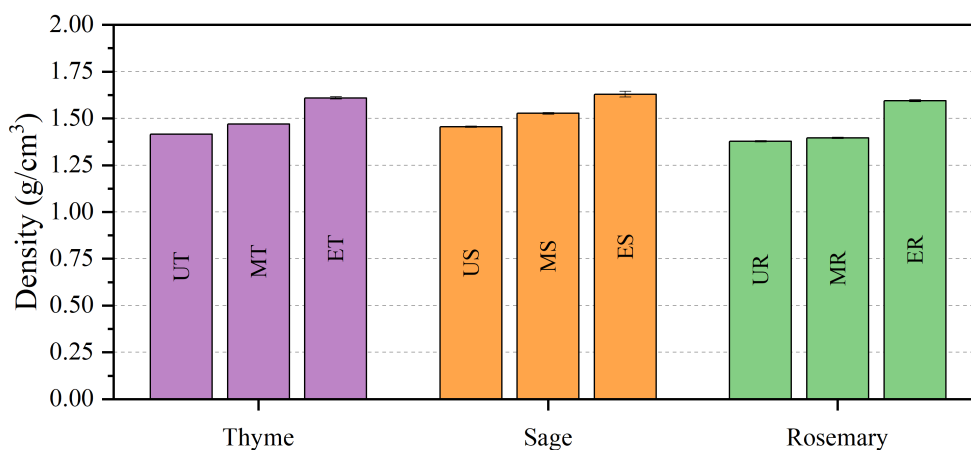


Figure 5.7. Fillers' density

An unequivocal behavior emerges for the density of the fillers, indicating that the modification of the filler leads to an increase in its density. This increase is attributed to the exclusion of larger particles, allowing space for a greater number of smaller particles, thereby enhancing the density. Additionally, the extracts are characterized by the highest densities, with rosemary exhibiting the most significant increase in density following extraction, approximately 16%.

The total phenolic content of the evaluated herbs (TPC) was quantified using the Folin-Ciocalteu assay. The test involved adding 100  $\mu\text{L}$  of Folin-Ciocalteu reagent to 1.6 mL of an appropriately diluted sample (0.2–1.0  $\mu\text{g}/\text{mL}$ ) or Gallic acid standard solution, which comprised six concentrations ranging from 1.0 to 10  $\mu\text{g}/\text{mL}$ . Subsequently, 0.3 mL of  $\text{Na}_2\text{CO}_3$  (15% w/v) was introduced to the mixture, which was then incubated in a water bath at 40  $^\circ\text{C}$  for 30 min. Absorbance was recorded at 765 nm against a blank sample using an Evolution 260 Bio spectrophotometer (Thermo Fisher Scientific, Waltham, MA, USA). The TPC of the samples was derived from the linear calibration curve of Gallic acid ( $R^2 > 0.998$ ) and expressed as milligrams of Gallic acid equivalents per gram of dry weight (mg GAE/g DW). The results are presented in Table 5.4.

Table 5.4. Total phenolic content of the tested fillers

<b>Material</b>		<b>TPC (mg GAE/g DW)</b>
Thyme	UT	69.71 ± 6.22*
	MT	69.45 ± 2.65*
	ET	453.48 ± 10.65 <sup>#</sup>
Sage	US	44.65 ± 2.90*
	MS	59.05 ± 4.36*
	ES	381.87 ± 8.71 <sup>#</sup>
Rosemary	UR	70.22 ± 4.81*
	MR	86.91 ± 1.88*
	ER	471.55 ± 11.29 <sup>#</sup>

\*calculated on plant dry matter; <sup>#</sup>calculated on extract dry matter

The TPC results indicate that the modification of the fillers enhanced the polyphenolic compound content in both sage and rosemary, with rosemary exhibiting a higher TPC. This suggests that the proposed modification effectively facilitated the extraction of phenolic compounds. As thyme underwent only sieving with no additional chemical or thermal modification, the changes in TPC value are negligible, and the values fall within the standard deviation range. Furthermore, for the extracts, rosemary demonstrated the highest TPC, while sage exhibited the lowest.

The phytochemical compositions of the fillers were characterized using a Thermo Ultimate 3000RS chromatography system (Thermo Fisher Scientific, Waltham, MA, USA) with a corona-charged aerosol detector (CAD) and a Bruker Impact II HD quadrupole-time of flight (Q-TOF) mass spectrometer (MS) (Bruker, Billerica, MA, USA). Both raw and modified herbs were extracted with 80% methanol using an ultrasonic bath for 15 minutes, yielding extracts with a final concentration of 20 mg/mL. Freeze-dried polyphenolic extracts were reconstituted in 80% methanol to a 5 mg/mL concentration. After centrifugation (12,000 rpm for 3 min), samples were separated on an HSS C18 column at 45 °C. A 30-minute linear gradient from 5% to 85% acetonitrile water (0.1% formic acid) at a 0.4 mL/min flow rate was used for separation. Mass spectrometry analysis in ESI(−) ion mode included a scanning range of 50–1800 m/z, capillary voltage of 3.0 kV, dry gas flow of 10 L/min at 220 °C, nebulizer pressure of 2.0 bar, collision RF at 750 Vpp, transfer time at 100 μs, and prepulse storage time at 10 μs. MS/MS spectra were acquired with a collision energy of 35 eV, stepping at 60% and 120% of CE. Data was calibrated internally using sodium formate. Data processing was done with DataAnalysis 4.4 software. Figure 5.8 presents the chromatography of rosemary fillers, which proved to be the most challenging herb to introduce into the PDMS matrix.

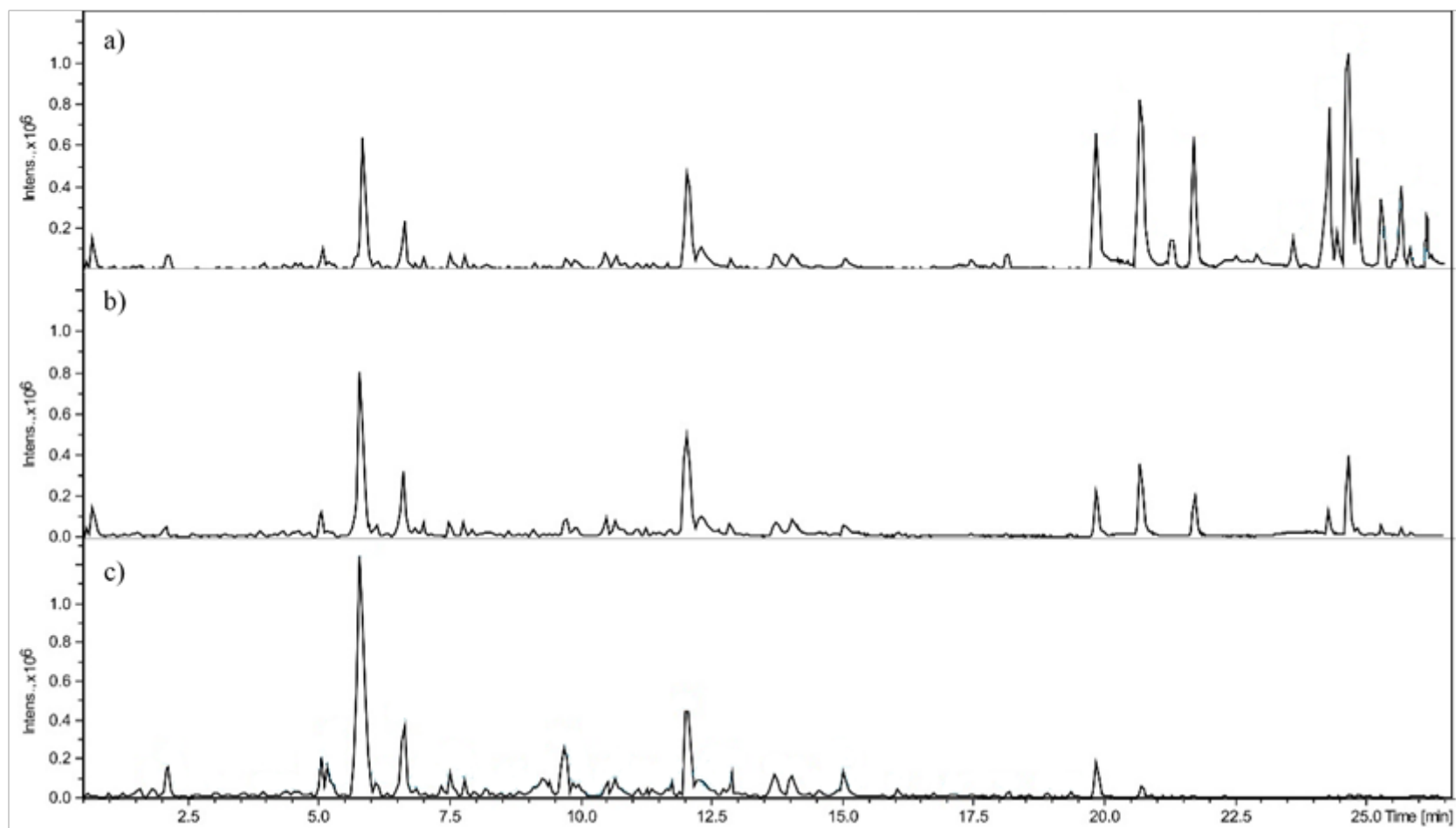


Figure 5.8. Phytochemical composition of rosemary: unmodified – a), modified – b), extract – c)

The most essential identified compounds and their respective percentages are presented in Tables 5.5 – 5.7.

Table 5.5. Selected detected compounds in thyme, expressed as percentages (%)

Compound	Thyme		
	UT	MS	UT
Apigenin	0.94	0.89	1.04
Caffeic acid	1.58	1.5	3.89
Gallocatechin	5.91	5.84	13.81
Luteolin	2.05	2.02	3.55
Quercetin	2.32	2.25	1.55
Rosmarinic acid	11.81	11.74	10.81
Tuberonic acid	4.33	4.29	5.99
Remaining polyphenolic compounds	47.03	47.27	55.46
Carnosic acid	2.62	2.57	2.31
Carnosol	0.87	0.77	–
Oxoctadecadienoic acid	1.85	2.01	–
Trihydroxyoctadecadienoic acid	2.37	2.23	–
Remaining terpenes and fatty acids	16.32	16.62	1.59

Table 5.6. Selected detected compounds in sage, expressed as percentages (%)

Compound	Sage		
	US	MS	ES
Apigenin	0.98	1.52	0.66
Caffeic acid	0.29	0.61	0.64
Luteolin	1.57	3.86	6.98
Quinic acid	0.41	0.4	4.2
Quercetin	1.13	1.66	2.65
Rosmarinic acid	9.76	16.56	10.18
Salvianic acid	0.35	4.19	5.96
Salvianolic acid	2.14	3.96	1.4
Tuberonic acid	1.42	2.1	4.88
Remaining polyphenolic compounds	14.24	42.52	60.98
Carnosic acid	17.27	4.98	–
Carnosol	11.15	2.69	–
Oxoctadecadienoic acid	4.54	0.82	–
Remaining terpenes and fatty acids	35.73	15.65	2.13

Table 5.7. Selected detected compounds in rosemary, expressed as percentages (%)

Compound	Rosemary		
	UR	MR	ER
Apigenin	0.15	0.14	0.73
Caffeic acid	0.56	0.17	1.34
Gallocatechin	4.39	11.09	19.07
Luteolin	3.10	6.89	4.94
Rosmarinic acid	5.47	11.42	9.12
Tuberonic acid	0.50	4.56	2.01
Remaining polyphenolic compounds	15.05	37.25	55.59
Carnosic acid	2.35	1.96	–
Carnosol	2.78	0.38	–
Rosmadial	2.35	0.91	–
Rosmanol	13.89	8.00	1.06
Rosmanol methyl ether	1.39	1.46	–
Remaining terpenes and fatty acids	48.02	14.77	6.14

The analysis presents the varying concentrations of selected metabolites identified in the tested fillers, indicating that the modification applied to sage and rosemary significantly impacts the levels of these compounds. Notably, the modification facilitated the dissolution of higher quantities of certain compounds, such as rosmarinic acid, with its concentration increasing by approximately 70% in sage and 108% in rosemary. Additionally, the modification led to a reduction in the overall content of fatty acids and terpenes. These findings are consistent with the total phenolic content (TPC) results presented in Table 5.4. In contrast, the alterations made to thyme resulted in minimal differences, as it underwent only sieving without further modification. This approach was chosen because additional modifications had a detrimental impact, leading to a reduction in the tested properties. Furthermore, the analysis reveals that rosemary contains the highest levels of fatty acids and terpenes, followed by sage and thyme. Trace amounts of terpenes were detected in the extracts, though their total concentration did not exceed 7.2%.

#### 5.1.4. Making of biocomposites

The biocomposites that were further tested were made according to the scheme presented in Figure 5.9, which provided an algorithm describing the modification method to achieve the assumed criteria. Three iterations were conducted. The first iteration involved only sieving the filler; the second involved sieving and wetting with alcohol; and the third involved sieving, wetting with alcohol, and subjecting to water vapor. After each iteration, the obtained materials were tested. If the results were deemed satisfactory, subsequent tests were conducted. It should be noted that the testing of biocomposites with unmodified thyme and sage was preliminary, and only the materials with the highest content of fillers (10 wt.%) were assessed for their antibacterial activity. This step was made to evaluate the activity of the materials where the incorporation of the filler was most challenging due to its large amount in the matrix.

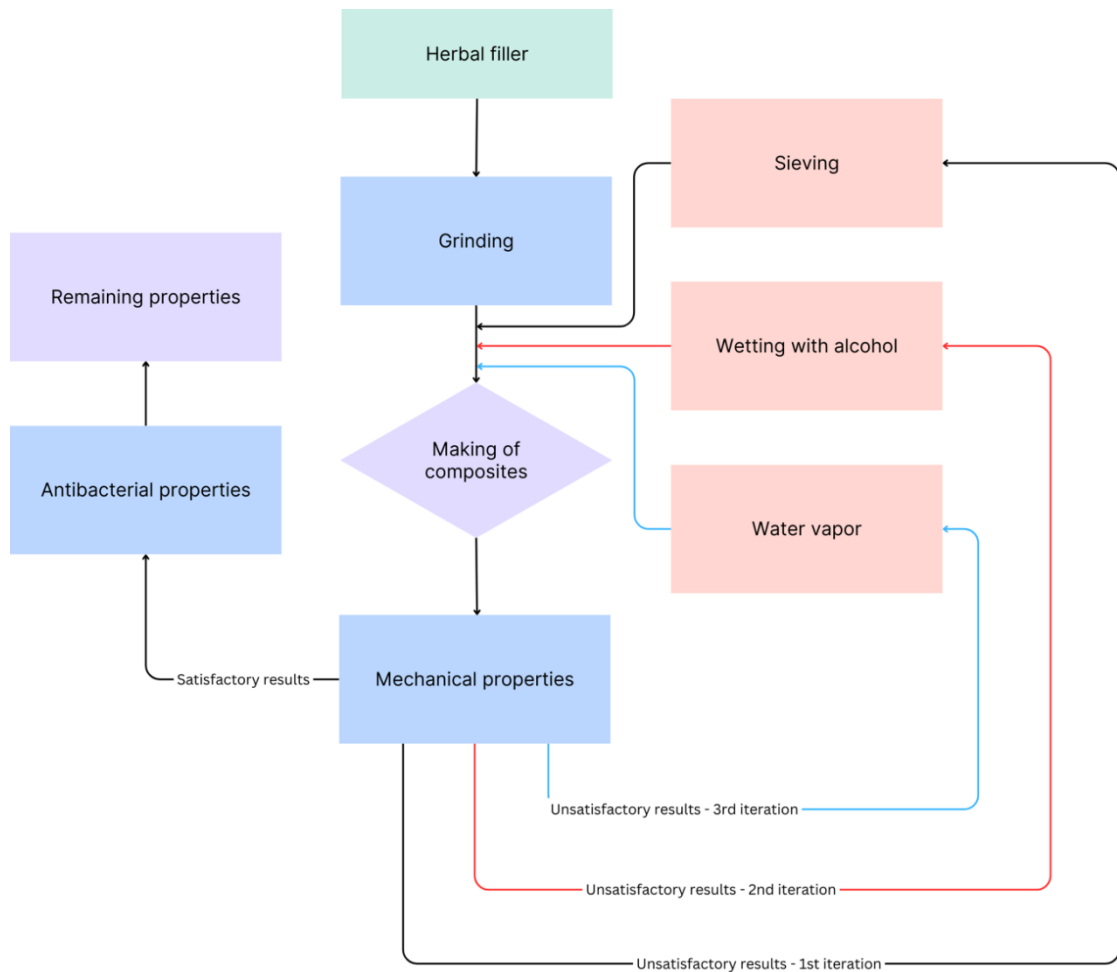


Figure 5.9. The algorithm employed for acquiring the biocomposites

Given that the developed materials are composites in which the modifier is a naturally derived filler, the term "biocomposites" was used to describe them. The silicone base (part A) was combined with the modified herbs and extracts at weight percentages of 2.5%, 5%, 7.5%, and 10%. Next, the catalyst (platinum(0)-1,3-divinyl-1,1,3,3-tetramethyldisiloxane – part B) was added to the blend at a 1:1 ratio with the base. Only two mass concentrations were prepared for unmodified thyme and sage: 5 wt.% and 10 wt.%. Due to the substantial influence of fatty acids and terpenoids in rosemary, particularly rosmadial and rosmanol, as presented in Table 5.7, which may impede the cross-linking process of PDMS by decreasing the crosslinking density, the fabrication of biocomposites using raw, unmodified rosemary was deemed infeasible. In the case of extracts, the amount of filler introduced into the matrix was determined based on the quantity of polyphenolic compounds present in the raw herbs, with calculations performed according to the extraction efficiency. This approach was chosen because the primary focus of the work was to assess the influence of bioactive polyphenolic compounds on the physicochemical and antibacterial properties, distinguishing these effects from those of other compounds found in the herbs. The mixtures were processed using a high-speed dis-solver Dispermat LC30 mixer (VMA-Getzmann GmbH, Reichshof, Germany) at a speed of 150 rpm for 3 min, followed by vacuum degassing for 4 min to eliminate any air bubbles and ensure a homogenous structure. The prepared biocomposites were gravity cast into 150 mm × 210 mm molds, on which a thin layer of polyvinyl alcohol was applied to facilitate easy demolding of the materials (Figure 5.10).



a)



b)

Figure 5.10. Making of biocomposites: rotary mixing – a), gravity casted material – b)



The curing period lasted 24 h at room temperature, with an additional post-curing phase of 2 h at  $60\pm 2$  °C. Subsequently, the biocomposites, along with the reference material, were thermally conditioned for 2 h at  $80\pm 2$  °C following the manufacturer's specifications. The materials' preparation process was conducted at a temperature of  $21\pm 2$  °C and a humidity of 40%

Table 5.8 outlines the classification of the materials produced, whereas Figure 5.11 illustrates the prepared testing samples.

Table 5.8. Obtained materials abbreviations and fillers' mass concentration

<b>Filler</b>	<b>Content (wt.%)</b>	<b>Abbreviation</b>
Reference material	–	Ref
Thyme	unmodified	5
		10
	modified	2.5
		5
		7.5
		10
	extract	2.5
		5
		7.5
		10
Sage	unmodified	5
		10
	modified	2.5
		5
		7.5
		10
	extract	2.5
		5
		7.5
		10
Rosemary	modified	2.5
		5
		7.5
		10
	extract	2.5
		5
		7.5
		10

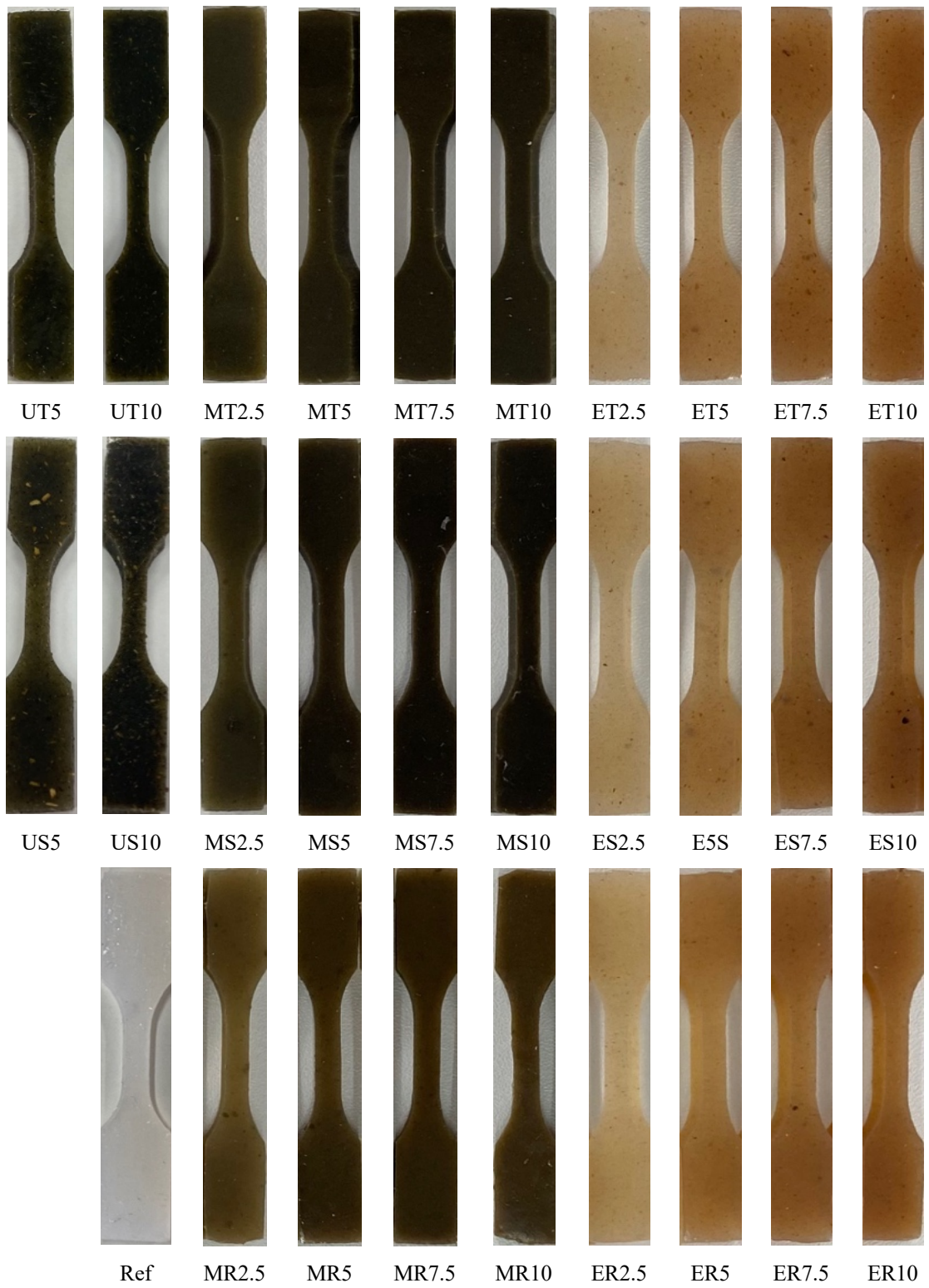


Figure 5.11. The obtained materials in the shape adapted for tensile testing

## 5.2. Biocomposites testing methods

### 5.2.1. Density

The density of the obtained materials was determined utilizing an analytical balance equipped with a hydrostatic density measurement kit presented in Figure 5.11 (Ohaus Adventurer Pro, OHAUS Europe GmbH, Greifensee, Switzerland), adhering to the protocols stipulated in the ISO 1183-1 standard [S1].

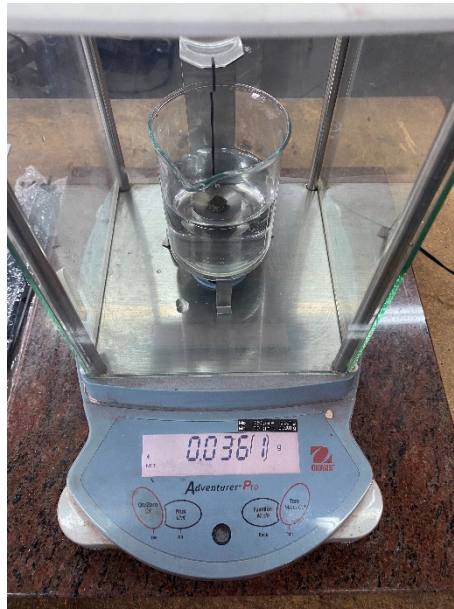


Figure 5.12. Density measurements apparatus

The evaluation was executed by employing the immersion method in distilled water on five cubic-shaped specimens of each material, with each side measuring 4 mm in length. The density  $\rho$  ( $\text{g}/\text{cm}^3$ ) of the materials was calculated based on the following equation (6.1):

$$\rho = \rho_w \frac{m_1}{m_1 - m_2}, \quad (6.1)$$

where  $m_1$  (g) is the sample mass in air,  $m_2$  (g) is the sample mass in distilled water, and  $\rho_w$  ( $\text{g}/\text{cm}^3$ ) is the density of distilled water taken as  $0.998 \text{ g}/\text{cm}^3$ .

### 5.2.2. Contact angle

The surface wettability of the samples was determined by measuring the contact angle, utilizing Attension Theta Flex tensiometer in conjunction with OneAttension software (Biolin Scientific, Gothenburg, Sweden). These measurements adhered to the EN 828:2013 standard [S2] and were carried out employing the sessile drop method, using distilled water as the medium (Figure 5.13). For each test sample, five droplets, each with a volume of 2  $\mu\text{L}$ , were deposited on the surface. The duration of each measurement was 60 s, with a sampling frequency of 1 Hz. The test was conducted on round samples with a diameter of 16 mm and a thickness of 4 mm.

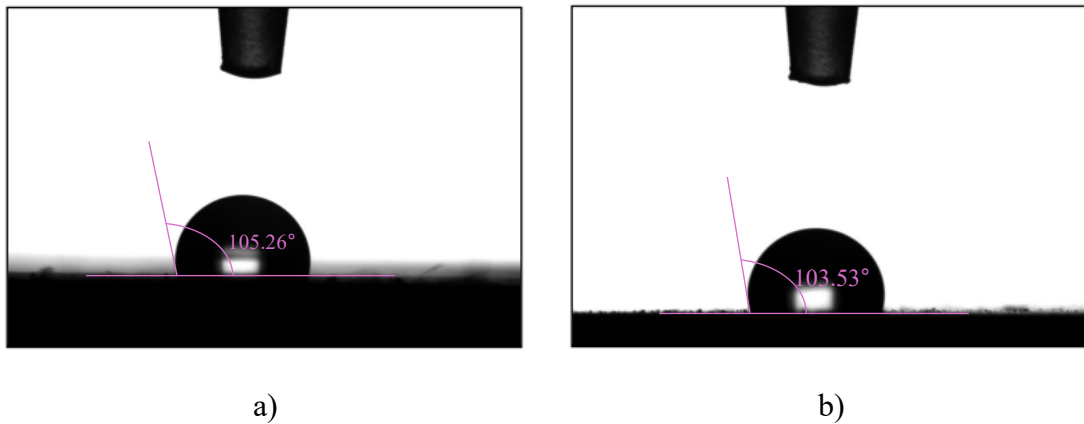


Figure 5.13. The post-test drops of reference – a) and MT2.5 – b)

### 5.2.3. In vitro absorption

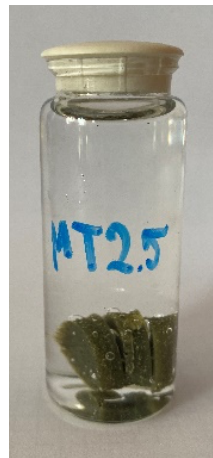
Absorption assessment was conducted on samples submerged in an artificial plasma solution, prepared following the ISO 10993-15 standard – Table 5.9 [S3], mimicking human extracellular fluid and approximating operational conditions. The samples underwent a 7-day incubation period at  $35 \pm 1$  °C in a laboratory incubator IMC18 (Thermo Scientific, Waltham, MA, USA). Every 24 h, three samples of each material were retrieved, weighed on the balance presented in Figure 5.12, and then returned to the solution for further observation (Figure 5.14). The test was performed adhering to the ISO 62 standard [S4]. Absorption  $A$  (%) was calculated based on the following equation (6.2):

$$A = \frac{m_B - m_A}{m_A} \times 100, \quad (6.2)$$

where  $m_A$  (g) is the sample mass before incubation and  $m_B$  (g) is the sample mass after incubation.

Table 5.9. Artificial plasma composition [S3]

Chemical name	Chemical formula	Concentration (g/L)
Sodium chloride	NaCl	6.800
Potassium chloride	KCl	0.400
Calcium chloride	CaCl <sub>2</sub>	0.200
Magnesium sulphate	MgSO <sub>4</sub>	0.100
Sodium hydrogen carbonate	NaHCO <sub>3</sub>	2.200
Sodium hydrogen phosphate	Na <sub>2</sub> HPO <sub>4</sub>	0.126
Sodium hypophosphite	NaH <sub>2</sub> PO <sub>2</sub>	0.026



a)



b)

Figure 5.14. The setting of the in vitro absorption experiment: tested sample – a) and incubator – b)

#### 5.2.4. Rebound resilience

The elasticity of the prepared biocomposites was assessed through a rebound resilience test conducted on the Schob machine (Heckert, Chemnitz, Germany). Prior to the evaluation, test samples underwent mechanical conditioning involving two impacts from a pendulum-like mechanical oscillatory device striking at a speed of 2.0 m/s. The indenter measured 15 mm in diameter and weighed 250 g. Subsequently, each sample measuring 50 mm × 50 mm × 4 mm was subjected to testing thrice, in alignment with the ISO 4662 standard [S5]. The measurements were conducted on the upper side of the

samples (opposite to the side where the fillers sedimented), where the potential application could interact with external factors. The results are expressed as the material's mean elasticity value in percentage. Figure 5.15 illustrates a representative sample following testing.

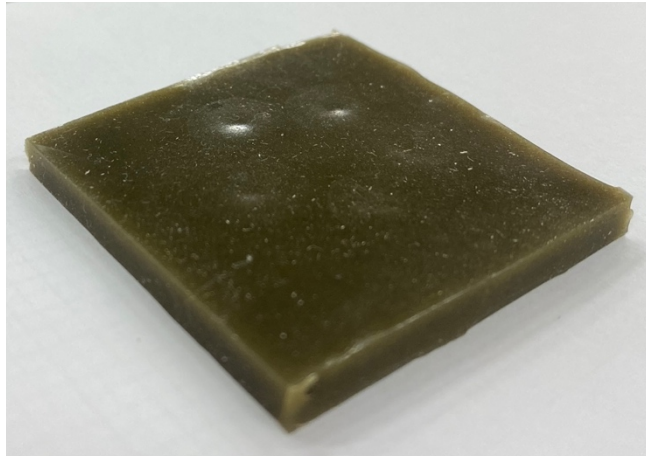


Figure 5.15. MT2.5 test sample for rebound resilience

#### 5.2.5. Hardness measurements

The hardness of the samples was evaluated using a Shore type A durometer (Zorn Stendal, Stendal, Germany), with the hardened steel rod indenter measuring 1.25 mm in diameter and applying a maximum force of 8.05 N. This assessment was conducted in accordance with the ISO 7619-1 standard [S6] on samples measuring 50 mm × 50 mm × 4 mm and consisted of five measurements for each type of material. The tests were conducted on both sides to assess whether the dispersion of results, particularly on the side where filler sedimentation may have occurred, significantly affects this property.

#### 5.2.6. Abrasion resistance

The abrasion resistance test was carried out employing the Schopper-Schlobach apparatus (APG Germany GmbH, Friedberg, Germany). The device consists of a rotating, 150 mm in diameter cylindrical drum rotating at approximately 40 rpm. Three samples measuring 16 mm in diameter and 10 mm thick of each material were pressed against a 60-grain sandpaper with a 10 N load. This setup ensures uniform contact between the sample and the abrasive. After completing the wear track measuring 40 m, the apparatus

automatically lifts the sample. Figure 5.16 presents an exemplary sample before and after the test conducted following the ISO 4649 standard [S7]. The measurements were conducted on the upper side of the samples, and the abrasion resistance was calculated as the volume loss  $\Delta V$  ( $\text{cm}^3$ ) of the materials based on the following equation (6.3):

$$\Delta V = \frac{m_I - m_{II}}{\rho_w}, \quad (6.3)$$

where  $m_I$  (g) is the sample mass before abrasion,  $m_{II}$  (g) is the sample mass after abrasion, and  $\rho_w$  ( $\text{g}/\text{cm}^3$ ) is the density of the test sample.



Figure 5.16. MT2.5 samples for the abrasion test

### 5.2.7. Tensile testing

The static tensile test was conducted utilizing AGX kN10D testing machine cooperating with Trapezium software (Shimadzu Corporation, Kyoto, Japan), in accordance with the ISO 527-1 standard [S8]. The test employed a crosshead speed of 500 mm/min and a DSES-1000 contact extensometer with a gauge length of 10 mm. The samples, adhering to ISO 527, type 5-B (as depicted in Figure 5.17), measured 60 mm in length and 4 mm in width along the 10 mm measuring area. Each material was tested 5 times, as presented in Figure 5.18, and the results of the test included stress at break ( $\sigma_B$ ) and strain at break ( $\epsilon_B$ ) obtained from the course of stress-strain curve as shown in Figure 5.19.

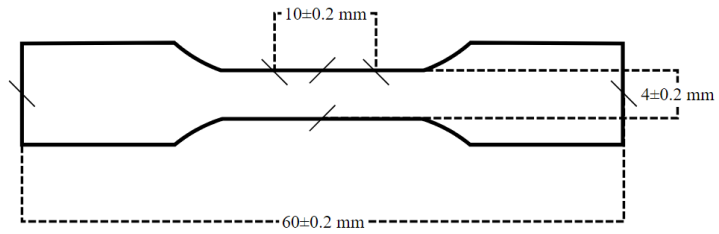


Figure 5.17. Tensile testing sample

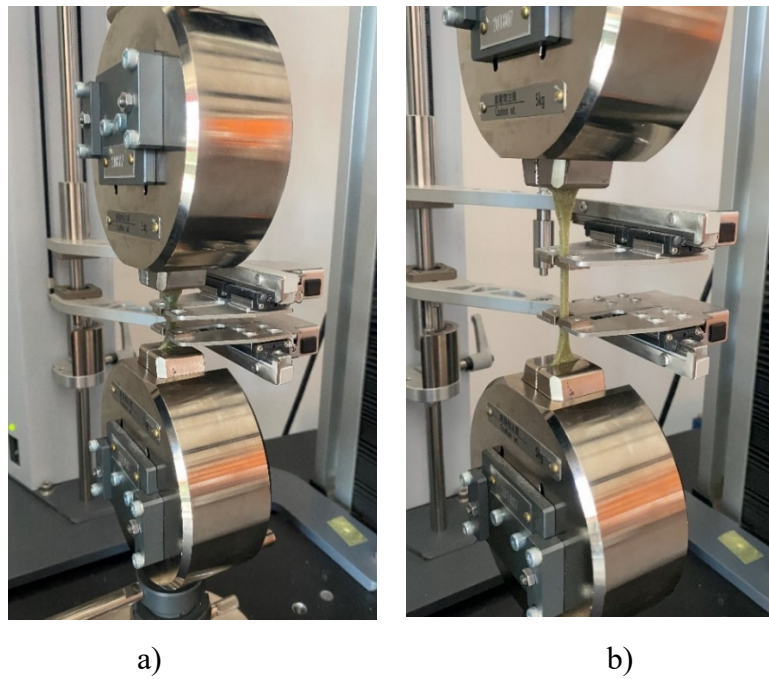


Figure 5.18. Tensile testing of MT2.5 sample: before – a) and during testing – b)

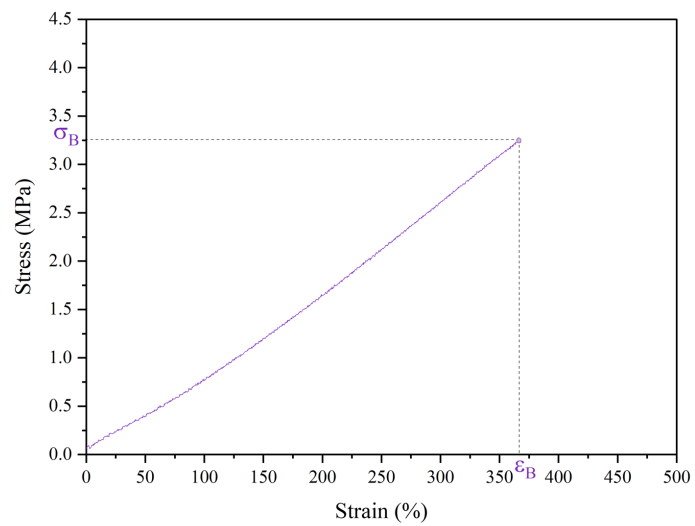


Figure 5.19. Stress-strain curve of MT2.5



### 5.2.8. Accelerated degradation

Accelerated degradation experiments were conducted under conditions simulating a biologically active environment to assess the material changes occurring during usage. The biocomposites underwent an accelerated degradation process through immersion in an artificial plasma solution (prepared for absorption determination). Given the materials' potential application in wound dressings, the samples underwent incubation for 2 and 7 days at  $70 \pm 2$  °C in SLW 53 STD forced air dryer (Pol-Eko, Wodzisław Śląski, Poland) in compliance with the ISO 10993-13 standard [S9]. These conditions fulfill the criteria for testing short-term polymeric medical materials (used for less than 30 days). Moreover, it should be noted that the samples were incubated in individual testing tubes to ensure unrestricted solution flow in all directions surrounding the sample, as illustrated in Figure 5.20.

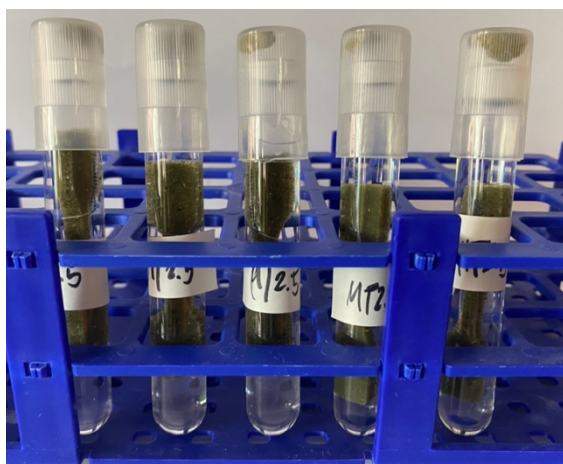


Figure 5.20. Incubated MT2.5 samples for accelerated degradation test

Degradation progression was evaluated by comparing mechanical (stress at break, strain at break, hardness) and chemical (chemical backbone – IR spectra) properties between the aged samples and their native counterparts. Variations observed facilitated qualitative and quantitative assessment of aging effects on the tested composites under the specified conditions.

### 5.2.9. Fourier transform infrared spectroscopy

FTIR spectra were acquired in attenuated total reflection (ATR) mode using the IRSpirit FTIR spectrophotometer cooperating with LabSolutions IR software (Shimadzu Corporation, Kyoto, Japan). The spectra were gathered over the mid-infrared range (4000–400  $\text{cm}^{-1}$ ) with a resolution of 4  $\text{cm}^{-1}$  and averaging 20 scans. Prior to testing, a background spectrum against air was recorded. Following each test, the ATR diamond crystal was cleaned with ethanol. Peaks corresponding to the characteristic features of PDMS were analyzed (Si-O-Si,  $\text{CH}_3$  rocking and bending in Si- $\text{CH}_3$ , and C-H stretching in  $\text{CH}_3$ ). The obtained spectra represent the average of three individual spectra taken from different material areas to ensure reliable results.

### 5.2.10. Differential scanning calorimetry

DSC analysis was conducted to determine the crystallinity degree of the obtained materials using DSC 1 model differential scanning calorimeter with the supplied STARe software (Mettler Toledo, Greifensee, Switzerland) in temperature scan mode. Specimens weighing between 20 and 21 mg were measured using XS105DU analytical balance (Mettler Toledo, Greifensee, Switzerland). Each sample was sealed hermetically in aluminum pans (40  $\mu\text{L}$  capacity), with a new pan utilized for every test. The samples underwent heating from  $-90\text{ }^\circ\text{C}$  to  $220\text{ }^\circ\text{C}$  at a rate of  $20\text{ }^\circ\text{C}/\text{min}$ , followed by cooling at the same rate in a nitrogen atmosphere ( $60\text{ mL min}^{-1}$ ). The entire procedure was carried out according to the guidelines outlined in the ISO 11357-1 standard [S10].

### 5.2.11. Microscopic observations

The topography of the tested samples and the fracture surfaces following tensile testing was examined using Leica DVM6 stereomicroscope (Leica microsystems, Wetzlar, Germany) and ZEISS Evo MA 10 scanning electron microscope – SEM (Carl Zeiss AG, Oberkochen, Germany) equipped with an X-ray energy dispersive spectrometry (EDS) system. Before SEM analysis, the samples were coated with gold particles for 90 s. EDS analysis was conducted to investigate whether compounds from

the artificial plasma degradation environment had been deposited or incorporated into the materials, as depicted in Figure 5.21.

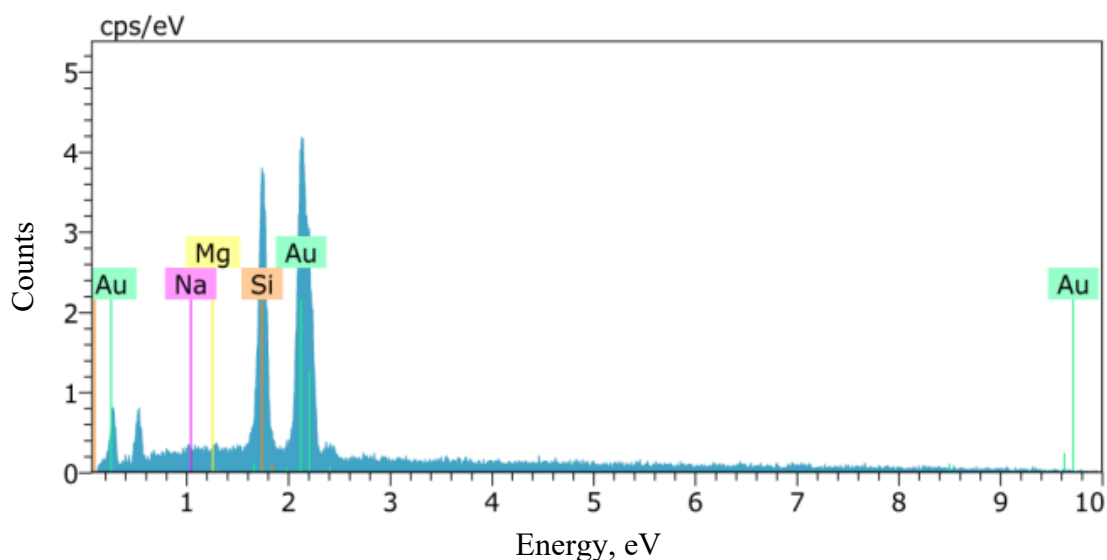


Figure 5.21. EDS analysis of MT2.5 performed after 7 days of incubation in artificial saliva under accelerated degradation conditions

#### 5.2.12. Antibacterial activity assessment

The antimicrobial efficacy was determined through an initial qualitative method followed by a quantitative study in cooperation with the Department of Biomaterials and Composites, AGH University of Science and Technology. This subsequent analysis was exclusively conducted on materials that demonstrated antibacterial activity in the qualitative assessment. It is important to note that the qualitative analysis was not conducted during the preliminary testing phase for composites based on unmodified herbs.

The Kirby-Bauer disk diffusion method was conducted for the qualitative analysis, adhering to the protocol established by the American Society for Microbiology. This involved using two commercial bacterial strains: the Gram-positive *Staphylococcus aureus* ATCC 6538P and the Gram-negative *Escherichia coli* ATCC 8739. Each bacterial strain was suspended in a saline solution, adjusting the concentration of the bacterial inoculum to match turbidity equivalent to 0.5 McFarland ( $\sim 1.5 \times 10^8$  CFU/mL) using DEN-1B Benchtop densitometer (Grant Instruments, Cambridge, United Kingdom). The bacterial suspension was uniformly applied over the agar surface using a sterile swab. Evaluations were conducted on Petri dishes containing Mueller-Hinton agar, chosen for

its ability to promote consistent growth of the tested bacterial strains. After positioning 5 mm diameter samples on the agar, the dishes were incubated at  $35 \pm 1$  °C for 24 h in a laboratory incubator IMC18 (Thermo Scientific, Waltham, MA, USA). Subsequently, the diameter of any zones of inhibition surrounding the samples was measured using colony counter Scan100 (Interscience, Saint Nom, France).

To further analyze the antibacterial effects of the developed materials, a detailed examination was performed in accordance with the ISO 22196 standard [S11], with modifications made to accommodate the size of the samples, as presented in Figure 5.22. Specimens with a diameter of 16 mm were tested against the *Staphylococcus aureus* ATCC 6538P strain. The initial step involved spreading the bacterial strain onto Mueller Hinton agar and incubating at  $35 \pm 1$  °C for 24 h. Subsequently, the specimens were sterilized using 70% ethanol and arranged in a multi-well plate. A bacterial suspension of *S. aureus* at a concentration of  $\sim 1.5 \times 10^8$  CFU/mL was prepared, and 1 mL of this suspension was applied to each sample. The specimens were then incubated at  $35 \pm 1$  °C for another 24 h. Following incubation, the samples were washed with 1 mL of soybean casein digest broth with lecithin and polyoxyethylene sorbitan monooleate (SCDLP broth), followed by serial dilutions. 0.1 mL from each dilution and the control were spread onto agar-filled Petri dishes – Figure 5.22. These dishes were then incubated at  $35 \pm 1$  °C for 24 h, after which the colonies were counted. The reduction in bacterial count was determined by comparing the colony counts from the materials tested to those of the control, calculating the logarithmic reduction  $R$  in bacterial colonies number based on the following equation (6.4):

$$R = (U_t - U_0)(A_t - U_0) = U_t - A_t, \quad (6.4)$$

where  $U_0$  (cells/cm<sup>2</sup>) is the log of viable bacteria recovered from the untreated sample after inoculation immediately,  $U_t$  (cells/cm<sup>2</sup>) is the log of viable bacteria recovered from the untreated sample after 24 h of inoculation and  $A_t$  (cells/cm<sup>2</sup>) is the log of viable bacteria recovered from the treated sample after 24 h of inoculation.

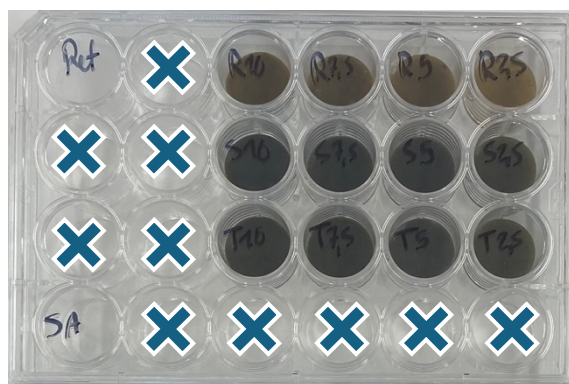


Figure 5.22. Inoculated samples for antibacterial activity assessment

### 5.2.13. Cell viability assay

The cell viability tests were conducted in cooperation with the Department of Microbiology and Immunology, Medical University of Silesia. Following the ISO 10993-5 standard [S12], extracts from selected biocomposites were prepared. Each material sample was individually placed in a plate containing 2 mL of the same culture medium employed for the L-929 fibroblast line (ATCC CCL-1). These plates were then incubated at  $37 \pm 1$  °C in a 5% CO<sub>2</sub> environment for 2 and 10 days, yielding extracts of these two durations. Identically, the culture medium was also incubated without biocomposites samples to serve as control media. The extracts and control media were preserved at  $-80$  °C until further use for assessing L-929 cell viability.

The *in vitro* experiments utilized mouse fibroblasts from the L-929 line, sourced from the American Type Culture Collection (Manassas, VA, USA). The L-929 line originates from the subcutaneous connective tissue of C3H/An strain mice. The cells were cultivated in Eagle's Minimum Essential Medium (EMEM) supplemented with 10% horse serum, penicillin (100 IU/mL), and streptomycin (100 µg/mL). Cultivation was conducted in 25 cm<sup>2</sup> polystyrene flasks (Nunc EasYFlasks™ Nunclon™ Delta, Nunc A/S, Roskilde, Denmark) in a controlled environment incubator (MCO-17 AIC, Sanyo, Japan) at  $37 \pm 1$  °C, with 5% CO<sub>2</sub> and 100% humidity. The cells were passaged every 2-3 days, and a cell suspension was prepared at a density of  $1 \times 10^5$  cells/mL for testing, assessed using a Burker chamber.

Following EN ISO 10993-5 guidelines, the cytotoxicity of the biocomposites was evaluated. L-929 fibroblasts were exposed to undiluted biocomposite extracts for 24 h. Cell viability was then assessed using the MTT (3-[4,5-dimethylthiazol-2-yl]-2,5 diphenyl tetrazolium bromide) assay, which measures mitochondrial dehydrogenase activity to determine the percentage of surviving cells, thereby assessing the cytotoxic potential of the biocomposites. A viability reduction greater than 30% compared to control cultures (viability under 70%) indicated cytotoxic effects.

For the assay, each well was filled with 100  $\mu\text{L}$  of L-929 cell suspension at a density of 10,000 cells per well in RPMI 1640 medium supplemented with 10% fetal bovine serum (FBS), penicillin (100 IU/mL) and streptomycin (100  $\mu\text{g}/\text{mL}$ ). After incubating for 24 hours at  $37\pm 1$   $^{\circ}\text{C}$  in a 5%  $\text{CO}_2$ , 100% humidity environment, the supernatants were removed, and 100  $\mu\text{L}$  of either the undiluted test extract or control medium was added. Following another 24-hour incubation under the same conditions, the wells received 1.1 mM of MTT solution in fresh medium. After 3 hours, the supernatants were removed, 200  $\mu\text{L}$  of DMSO was added to dissolve the MTT formazan, and after 20 min, 150  $\mu\text{L}$  from each well was measured for absorbance at 550 nm using Eon automatic plate reader (BioTek Instruments, Winooski, VT, USA). The resulting violet color intensity, indicating the amount of formazan formed, was directly proportional to the number of viable cells. The cell viability *Viab.* (%) was calculated based on the following equation (6.5):

$$Viab. = \frac{A_{test}}{A_{control}} \times 100, \quad (6.5)$$

where  $A_{test}$  is test sample absorbance and  $A_{control}$  is the control sample absorbance.

## 6. Results

### 6.1. Density measurements

The mean values of the density measurement results with the standard deviations are illustrated in Figure 6.1.

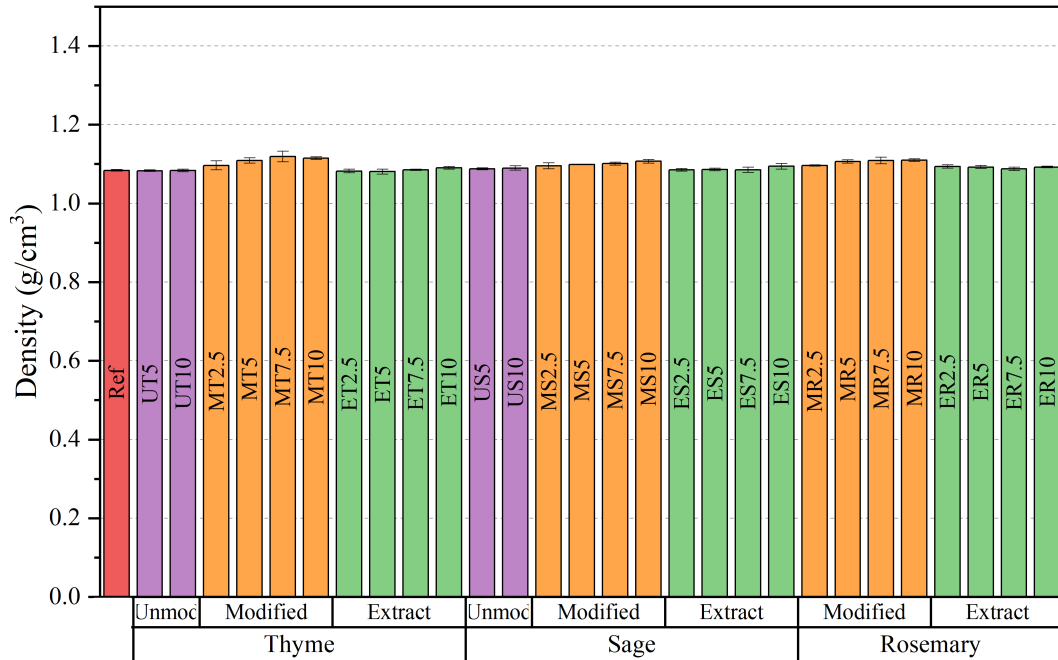


Figure 6.1. Density results

As can be seen, the addition of fillers marginally increased the density of the material. Furthermore, the density increment is proportional to the filler content, ranging between 1% and 3%. This is significant from a fabrication perspective, as the material's density influences its flow and solidification processes. Additionally, high density affects the gas permeability of the material by necessitating longer travel distances for gas molecules, thereby increasing resistance and reducing permeability. The exchange of gases, particularly oxygen, is essential for cell metabolism and tissue repair. Adequate oxygen supply to the wound site promotes faster healing [185]. Statistical analysis indicates the significant impact of filler incorporation on the tested property; however, post-hoc analysis reveals no significant effect for biocomposites with 2.5 wt.% filler, only for those with higher filler contents. Moreover, the modified herb-based biocomposites exhibit the highest alteration in density compared to unmodified and extracted herbs. In

addition, all extract-based materials present similar density values and fall within the same range of standard deviation.

Additionally, extracts containing larger and higher-density fillers exhibit a lower biocomposite density compared to those incorporating modified fillers. This phenomenon may be attributed to the absence of terpenes and fatty acids found in herbal powders, which could influence the density of the fillers and, consequently, affect the overall density of the materials produced. Furthermore, the displacement of the matrix by these larger and denser fillers, along with potential aggregation and poor dispersion, could create regions of lower density, ultimately reducing the overall density of the composite material.

## 6.2. Static tensile testing

The conducted static tensile test on the obtained materials allowed for the determination of their stress at break and strain at break values, and their mean values, along with the standard deviations, are presented in Figure 6.2 and Figure 6.3, respectively.

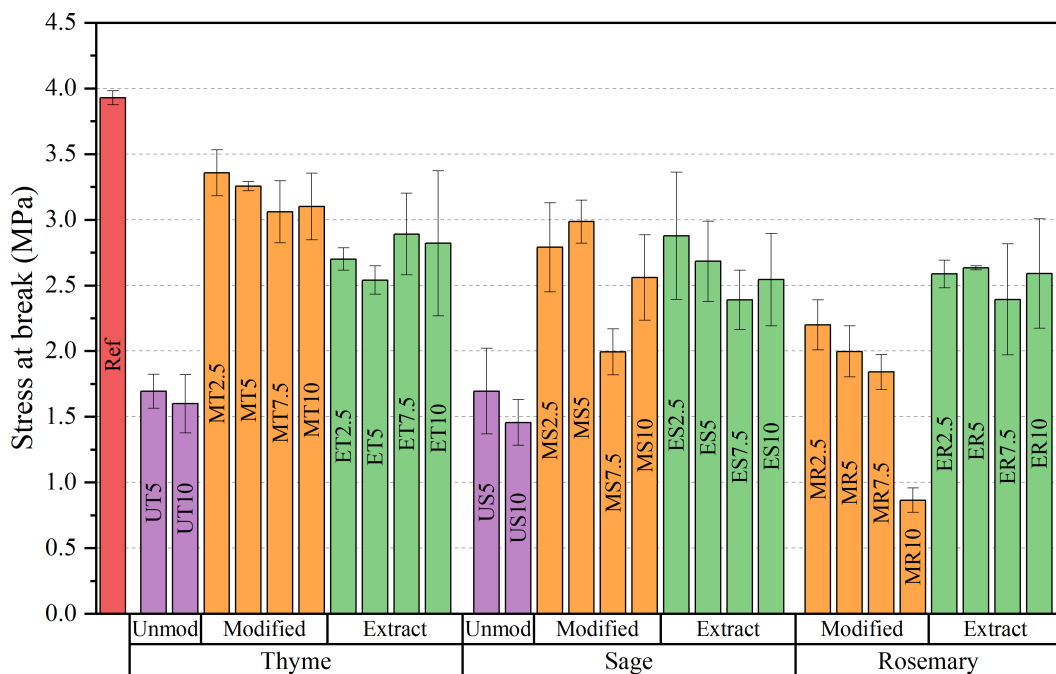


Figure 6.2. Stress at break results



For the reference material, these values exceed those provided by the manufacturer by approximately 12%, likely due to additional post-curing conditioning at 60 °C beyond the standard process. The addition of fillers generally reduces the stress at break value to varying extents. The greatest decrease in value is observed for MR10, with a reduction of 78%, while the smallest occurs for MT2.5, at just 15%. This phenomenon could be attributed to the inadequate wetting of the fillers by the hydrophobic PDMS, resulting in poor interfacial integrity between the filler and the matrix. This, in turn, impacts the mechanical properties of the obtained biocomposites. However, for wound dressing applications, biocomposites with modified thyme, modified sage, MR2.5, and extract-based fillers meet the required values [82],[186],[187].

Biocomposites containing unmodified fillers exhibit the lowest stress at break values, with reductions of over 50% compared to the reference sample. However, these values improve following modification, resulting in decreases of 17%, 21%, 24%, and 35% for the corresponding fillers and their respective contents. Furthermore, for thyme-based materials, the modification (sieving) resulted in a greater improvement in stress at break value (approximately 40%) compared to sage-based materials (approximately 30%). This suggests that the modifications positively impact this property, likely by reducing the presence of larger particles, as illustrated in Figure 5.6, which may compromise the filler's integrity with the matrix. Additionally, for sage- and rosemary-based composites, the performed modifications (wetting with ethanol and water vapor) may lessen the adverse effects of fatty compounds, confirmed by the conducted phytochemical analysis in Section 5.1.3. Unmodified thyme composites exhibit a decreasing trend with increasing filler content, while modified thyme composites show a decreasing behavior until the addition of 10 wt.%, where the stress at break minimally increases.

Similar trends are observed for both unmodified and modified sage composites. When 7.5 wt.% of modified sage is incorporated into PDMS, the stress at break decreases by over 50%, but this reduction diminishes to 35% with the addition of 10 wt.%. This decrease is likely due to the agglomeration of sage particles wetted with ethanol, which may detach during testing and create voids acting as notches, significantly affecting tensile strength.

For rosemary, the stress at break value decreases with increasing filler content, dropping by approximately 78% compared to the reference for the material with the

highest filler content. Despite additional modifications intended to reduce the influence of fatty compounds, the effect was limited. This could suggest that the presence and concentration of rosmanol and rosmadial in rosemary (Table 5.7) may impair the mechanical integrity between the filler and the matrix, further affected by the notable larger particle size relative to the other fillers. The absence of these compounds in rosemary extract resulted in higher stress at break values compared to the herb-based composites.

All extract-based composites exhibit similar values, ranging from 2.39 MPa for ER7.5 to 2.89 MPa for ET7.5. The addition of thyme extract results in a decrease of approximately 30% in the stress at break value, followed by sage extract with a 33% reduction and rosemary extract with a 35% decrease. This trend may be attributed to the increasing  $D_{50}$  of the filler size, as presented in Table 5.3, where smaller particles contribute to a more uniform filler distribution throughout the matrix. Moreover, it is noteworthy that thyme extract exhibits the lowest concentration of terpenes and fatty compounds, followed by sage and rosemary.

Similar to the modified thyme and sage composites, extract-based composites do not exhibit a clear relationship between filler content and stress at break value. Moreover, for sage and rosemary extract-based materials, the most significant decrease in stress at break value occurs with the addition of 7.5 wt.% filler, which lessens when the filler content is increased to 10 wt.%. This indicates that incorporating these extracts at levels above 5 wt.% significantly impacts the mechanical properties, while higher filler concentrations appear to improve structural integrity and stiffness. For ET7.5, higher stress at break value is observed compared to less filled materials, but increasing the filler concentration further leads to a decrease in this value. However, these changes remain within a similar range. Nevertheless, it should be noted that although the extracts contain mainly polyphenolic compounds, the stress at break value decreases compared to reference material. This leads to the conclusion that polyphenols (such as rosmarinic acid and gallic acid – the main components of extracts) also significantly influence tensile strength in addition to terpenes and fatty compounds. This finding paves the way for future research in this area.

Furthermore, the standard deviation range for the obtained materials varies depending on the type of filler and its content. These variations can be attributed to several

factors, including the methods used to prepare the fillers and their incorporation into the matrix, sedimentation, potential formation of agglomerates, and their subsequent detachment during testing, which can lead to inconsistent tension behavior. Additionally, the formation of concave sides along the measuring length during the punch-cutting of samples for testing may have influenced the measured properties. These factors underscore the significance of the manufacturing process on the tested properties. However, no correlation is found between the conducted modifications and the range of the standard deviation values.

Similar to the stress at break, the incorporation of fillers altered the strain at break value to varying degrees depending on the filler type and content, as presented in Figure 6.3.

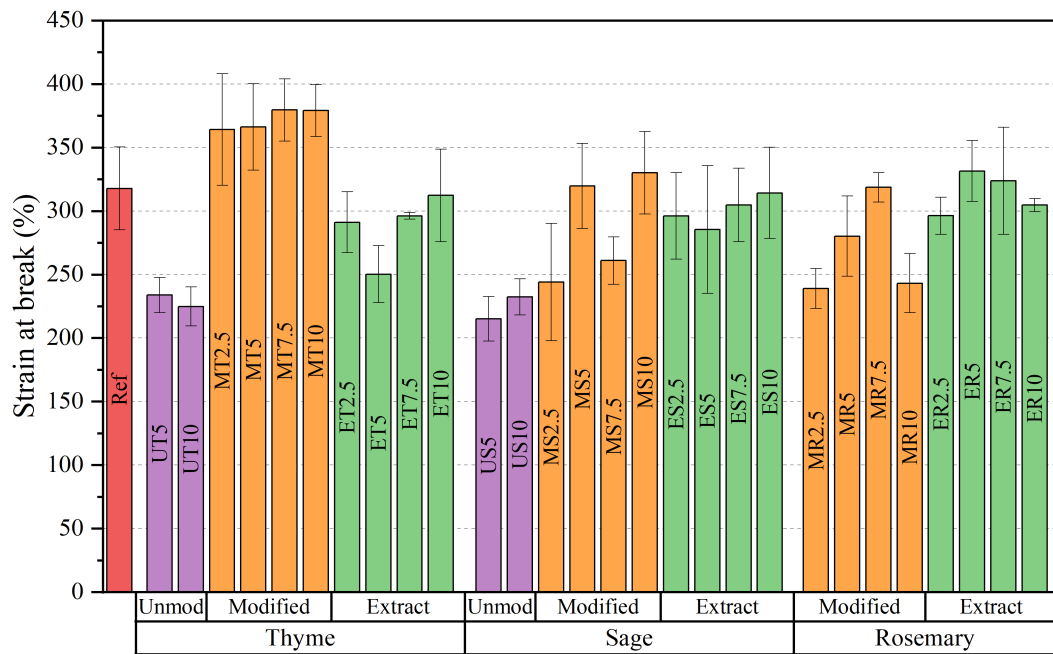


Figure 6.3. Strain at break results

The most significant decrease is observed in biocomposites with unmodified herbs, indicating the beneficial impact of fillers' modifications. Additionally, modified thyme composites display higher strain at break values compared to the reference samples, with an increase of up to 20%. This improvement trends upward with rising filler content, accompanied by a decrease in the standard deviation range. This suggests that the proposed modification and production technology resulted in improved distribution of the filler. Furthermore, thyme is characterized by the smallest particles, which contribute

to a more even distribution within the matrix. This could account for the higher stress at break values observed compared to the other materials.

The behavior of the other modified herbs is less clear; however, a decrease in strain at break value is observed after incorporating 7.5 wt.% of modified sage into PDMS, similar to the trend seen with stress at break. Although the tests were repeated, the results consistently exhibited similar behavior. Moreover, with the exception of MS7.5, all modified sage composites show a decreasing range of standard deviation with increasing filler content. On the other hand, a significant reduction in strain at break value is noted for MR10 compared to MR7.5, exceeding 23%. This could be attributed to the increased brittleness associated with higher filler concentrations. Although such materials can endure greater stresses, their elongation capabilities are reduced. No correlation between filler content and the standard deviation range is observed.

In the case of extract-based materials, a trend opposite to that of stress at break is observed. This may be related to the behavior and structure of these materials during tension, where large filler particles could detach, thereby reducing the tensile strength. Concurrently, the matrix could be subjected to further tension without a corresponding increase in stress value. Generally, rosemary extract composites exhibit higher values (by 7% for ER5) or only slightly decreases compared to PDMS. In contrast, sage extract composites show reduced values, with a further reduction observed in thyme extract composites, decreasing by over 21% for ET5. In addition, thyme and sage extract composites exhibit a similar pattern, with an initial decrease in strain at break value after incorporating 5 wt.% of the filler, followed by an increase. Furthermore, no unequivocal correlation between the filler type and content on the scatter of results is observed for all extract-based materials

From a potential application perspective, the material's flexibility is crucial for ensuring patient comfort. Despite the incorporation of fillers, the strain at break values are comparable to, or even exceed, those reported in the literature [82],[188]. Nevertheless, the performed statistical analysis unequivocally indicates the significant impact of the filler's type and content on the stress at break and strain at break value ( $p < 0.05$ ).

### 6.3. Hardness measurements

The mean values and standard deviations of the measured hardness are presented in Figure 6.4.

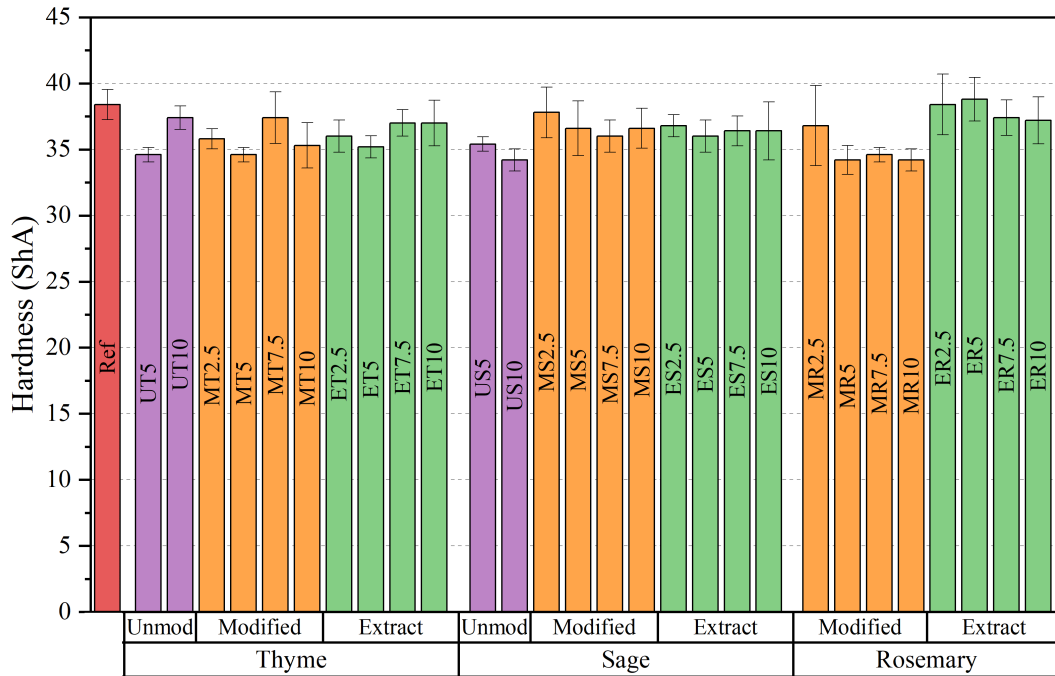


Figure 6.4. Hardness measurements results

As observed, the behavior of all biocomposites is not unequivocal, and no clear correlation is found between the filler content or type and the measured hardness. The significance of the filler's impact on the material's hardness was confirmed ( $p < 0.05$ ). Among the tested materials, ER5 exhibits the highest hardness value, which is slightly higher (by 1%) compared to the reference, while US10 shows the lowest hardness, decreasing by over 10%. For thyme-based materials, the extracts generally show the smallest decrease in hardness, followed by the unmodified herb, with the modified thyme showing the greatest decrease. A similar pattern is observed for rosemary-based composites, although the changes are more pronounced. In contrast, the modification proves beneficial for sage-based materials, with the extracts displaying similar hardness values. The varying range of the standard deviation is attributed to the distribution of fillers in the matrix and the adopted testing method. It should be noted that measurements were conducted on both sides of the samples, and the mean value was calculated. Consequently, sedimentation of the filler increased the likelihood of

encountering particles on one of the tested sides. Furthermore, modified sage- and rosemary-based composites exhibit decreasing hardness and increasing standard deviation with higher filler content. This phenomenon may be attributed to the distribution of potential agglomerates throughout the matrix. Moreover, the harder the additive, the broader the scatter of results, which is related to the dispersion of the filler in the matrix. During measurements, stiffer particles can be encountered, while subsequent measurements might be taken from a matrix with fewer large, rigid particles. In materials with lower filler content, variability in the concentration and distribution of the filler, as well as potential agglomerates, can lead to inconsistent measurements. As filler content increases, this variability decreases, with higher concentrations on the sedimented side leading to a more uniform distribution. For biocomposites containing 5 wt.% of thyme and sage, the modification of the filler did not result in a significant change in hardness ( $p > 0.05$ ). However, for biocomposites filled with 10 wt.%, a significant change in hardness was observed ( $p < 0.05$ ). This difference is likely due to the higher concentration of the filler and its sedimentation compared to those with a lower filler content.

Comparable hardness results are observed between the modified and extract fillers of thyme and sage, as both types of fillers exhibit similar average particle sizes. Conversely, rosemary extract-based composites show higher hardness values due to the presence of larger particles. Compared to smaller particles, the likelihood of encountering these larger particles contributes to increased material stiffness. From the perspective of wound dressing applications, the results meet the requirements, as higher hardness is preferable to prevent the dressing from adhering to the wound, thereby enhancing the healing process [189],[190].

## 6.4. Water contact angle measurements

The water contact angle (WCA) mean values and standard deviations are presented in Figure 6.5.

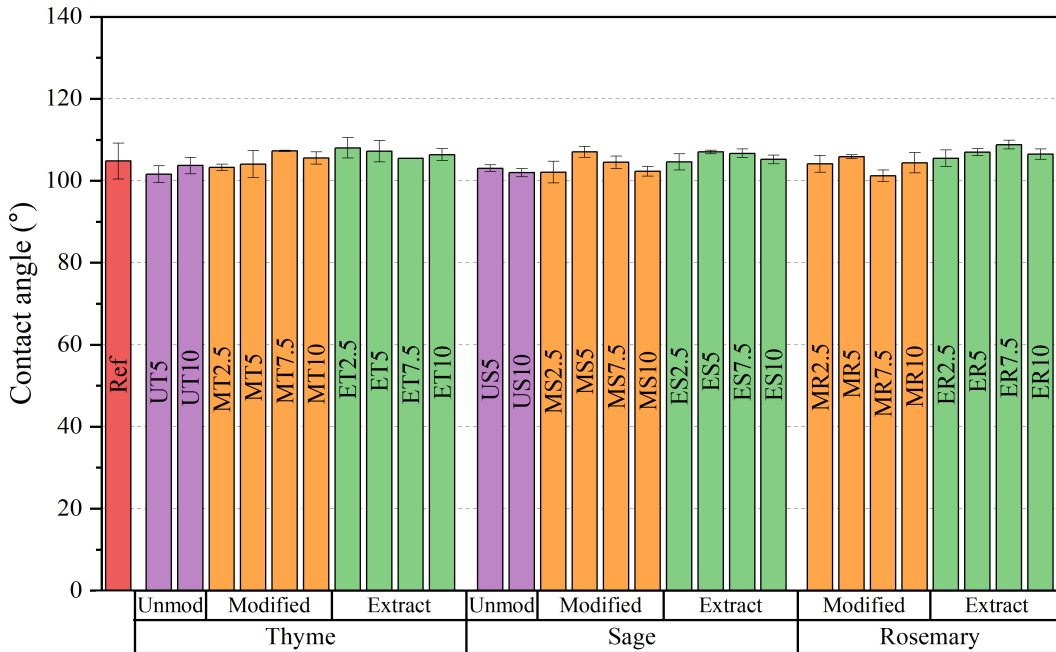


Figure 6.5. Water contact angle measurement results

The results unequivocally indicate that the incorporation of the selected fillers did not alter the nature of PDMS from hydrophobic to hydrophilic. The hydrophobic character of the surface is crucial for antifouling properties, specifically in limiting bacterial adhesion. Literature reports indicate that silicone surfaces with a WCA up to around  $110^\circ$  inhibit or limit the adhesion and biofilm formation of *S. aureus*, whereas higher contact angles favor the proliferation of *E. coli* [191],[192].

In general, among the modified fillers, the highest WCA is exhibited by thyme composites, followed by sage and rosemary. This suggests that the higher the polyphenols content, as detailed in Table 5.4, the lower the contact angle values. This is mainly due to the hydrophilic character of polyphenols. Moreover, the performed modifications of the filler demonstrated their beneficial impact on the tested property. For thyme-based composites, MT5 shows an increase of approximately 2.5% compared to UT5, while for sage, MS5 increased by almost 4% compared to US5. Additionally, extract-based composites exhibit higher water contact angle values compared to those with unmodified

and modified fillers. Although polyphenolic compounds are known for their hydrophilicity, it is important to note that the actual mass of introduced extracts is significantly lower than that of powdered fillers. As a result, their impact on the water contact angle may not be as prominent. Furthermore, despite the fillers being highly hygroscopic, this characteristic did not significantly affect the contact angle values, and the observed changes fall within the standard deviation of the reference material.

A one-way ANOVA confirmed the significance of the tested property ( $p < 0.05$ ); however, post-hoc analysis revealed no significant differences between the biocomposites and the reference. However, significant differences were observed among the biocomposites themselves, particularly in the rosemary-based materials.

## 6.5. Antibacterial activity assessment

Preliminary antibacterial activity tests were conducted on biocomposites filled with 10 wt.% of unmodified herbs, and the results are presented in Table 6.1. These tests represent initial steps in assessing the potential antibacterial properties of the obtained materials, facilitating the development of the algorithm shown in Figure 5.1.

Table 6.1. Antibacterial activity assessment results – part I

Material	Reduction log	
	<i>S. aureus</i>	<i>E. coli</i>
UT10	4.4	0.45
US10	4.4	0.75

According to the literature, a reduction log in bacterial cell viability above 2 indicates antibacterial activity, specifically bacteriostatic properties [193]. A log reduction equal to or exceeding 3 is typically considered bactericidal [194]. However, some studies suggest that a reduction log exceeding 5 is necessary for a material to be deemed truly bactericidal [195]. Based on these criteria, both tested materials exhibit significant antibacterial activity against the *S. aureus* strain but show negligible activity against the *E. coli* strain. This discrepancy may be attributed to the morphology of the Gram-negative bacteria, which possesses an additional outer layer that acts as a barrier, impeding the penetration of bioactive substances [196].



Following the initial tests, a qualitative assessment of the antibacterial activity of the remaining materials was conducted. For powder herb-based composites, all filler contents were tested, while for extract-based composites, only the maximum filler contents were examined, similar to the unmodified herb-based samples. The results are depicted in Figure 6.6.

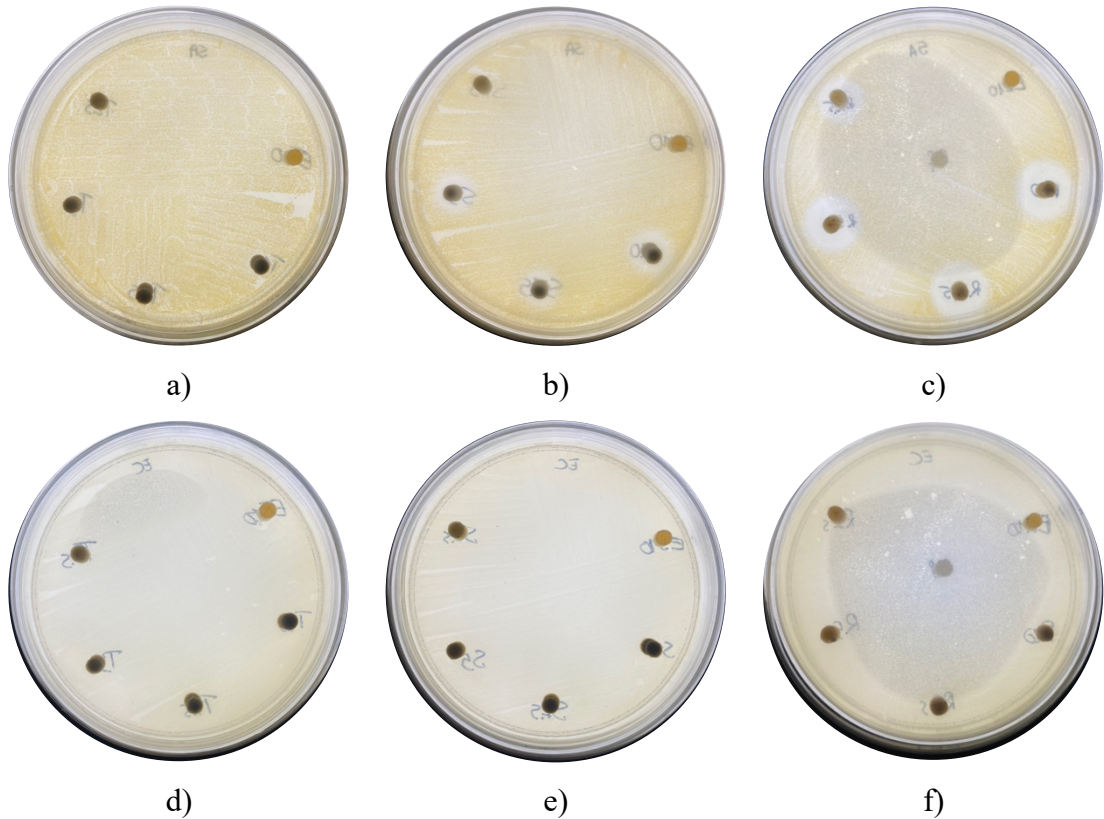


Figure 6.6. Kirby-Bauer test results for *S. aureus*: thyme – a), sage – b), rosemary – c) and *E. coli*: thyme – d), sage – e), rosemary – f)

The findings unequivocally demonstrate that herb-based materials exhibit antibacterial activity against *S. aureus* but no activity against the *E. coli* strain. The inhibition zone observed in thyme-based composites is very minimal; thus, these materials require further testing to accurately determine their antibacterial behavior. In contrast, extract-based composites did not show antimicrobial activity against either tested strain.

Additionally, the same test was conducted on the extracts themselves, and the results indicate that the tested fillers exhibit significant inhibition zones against both Gram-negative and Gram-positive strains. This suggests that the filler content within the matrix may be too low to affect the material's biological properties. These findings

indicate that the applied modifications do not significantly decrease the antibacterial activity of the herb-based composites. However, a comprehensive quantitative examination was subsequently conducted to assess the modifications' impact on this property.

For the second part of the test, only the modified herbs-based composites were taken into account, and the results are presented in Table 6.2.

Table 6.2. Antibacterial activity assessment results – part II

<b>Material</b>	<b>Reduction log</b>
Ref	0.06
MT2.5	2.78
MT5	2.09
MT7.5	2.06
MT10	2.39
MS2.5	3.96
MS5	3.90
MS7.5	3.43
MS10	2.56
MR2.5	2.90
MR5	3.36
MR7.5	3.52
MR10	3.34

The test was conducted only on the Gram-positive strain, following the no-exhibited activity against *E. coli* from the Kirby-Bauer test. As can be noticed, the highest reduction is observed for MS2.5, reaching almost 4, while the lowest is observed for MT7.5. Nevertheless, all tested biocomposites exhibit bacteriostatic activity against *S. aureus*, while the reference material exhibits none. For sage composites, the higher the filler content, the lower the antibacterial activity. On the contrary, for rosemary, the relationship is reversed; however, when surpassing the content of 7.5 wt.%, the reduction of bacteria decreases by only 5%. On the other hand, opposite to rosemary's behavior, thyme exhibits decreasing activity with increasing filler content, where after surpassing the content of 7.5 wt.%, the antibacterial activity increases by 16%.

Moreover, despite the modified fillers having higher total phenolic content (Table 5.4), the results indicate that the modification of the fillers decreases the antibacterial activity of the biocomposites due to the altered phytochemical composition of the herbs. This suggests that the eliminated fatty compounds and terpenes possess

significant antibacterial properties. However, these modifications were implemented following preliminary tests, which ensured improved mechanical properties and facilitated the successful crosslinking of rosemary-based materials. Nevertheless, the modified herbs-based materials achieve the minimum reduction log required for antibacterial properties.

Although literature reports that the water contact angle is an essential factor for bacterial adhesion [197], many studies highlight the importance of surface roughness in this phenomenon, impeding the correlation of the obtained results solely to WCA [198].

## **6.6. Biocomposites assessment – I analysis**

After the first phase of the work, a multicriteria analysis was conducted to evaluate the acquired materials, as detailed in Table 6.3 where 'C' refers to the criterion and 'V' to the value. The evaluation was conducted by assigning values to properties deemed significant from an application perspective on a scale from 1 to 6, reflecting the specific requirements for materials intended for use as wound dressings. Each criterion was evaluated by assigning a value on a scale from 1 to 9, with the outcome derived from multiplying the criterion by the property weight. The assessment was based on the analysis of the obtained results for density, stress at break, strain at break, hardness, water contact angle, and antibacterial activity. The materials were categorized based on the primary processes used to acquire the fillers. It was assumed that the biocomposites, which will be further examined alongside the reference, should achieve a minimum score of 100.

Following the multicriteria analysis, biocomposites based on modified herbs emerged as the most promising group of materials. While antibacterial activity is the primary focus of this work, it is essential to ensure that the appropriate operational requirements are met. The selected materials demonstrated both satisfactory antibacterial activity and adequate mechanical properties. Consequently, these materials were subjected to further investigation to assess the influence of the fillers on specific physicochemical and biological properties, as well as to evaluate their extended mechanical characteristics.

Table 6.3. I multicriteria analysis results

Property	Weight	Material																			
		Ref		Thyme						Sage						Rosemary					
				Unmodified		Modified		Extract		Unmodified		Modified		Extract		Modified		Extract			
		C	V	C	V	C	V	C	V	C	V	C	V	C	V	C	V	C	V		
Density	1	9	9	8	8	3	3	6	6	7	7	2	2	5	5	1	1	4	4		
Stress at break	3	9	27	2	6	8	24	7	21	1	3	4	12	6	18	3	9	5	15		
Strain at break	4	7	28	2	8	9	36	3	12	1	4	5	20	6	24	4	16	8	32		
Hardness	2	9	18	4	8	2	4	4	8	1	2	7	14	6	12	5	10	8	16		
Water contact angle	5	9	45	2	10	8	40	1	5	4	20	7	35	5	25	6	30	3	15		
Antibacterial activity	6	1	6	8	48	5	30	4	24	9	54	7	42	3	18	6	36	2	12		
$\Sigma$		<b>124</b>		<b>80</b>		<b><u>134</u></b>		<b>70</b>		<b>83</b>		<b><u>123</u></b>		<b>97</b>		<b><u>101</u></b>		<b>90</b>			

## 6.7. In vitro absorption

The obtained materials incubated in artificial plasma exhibit varying degrees of absorption, as depicted in Figure 6.7.

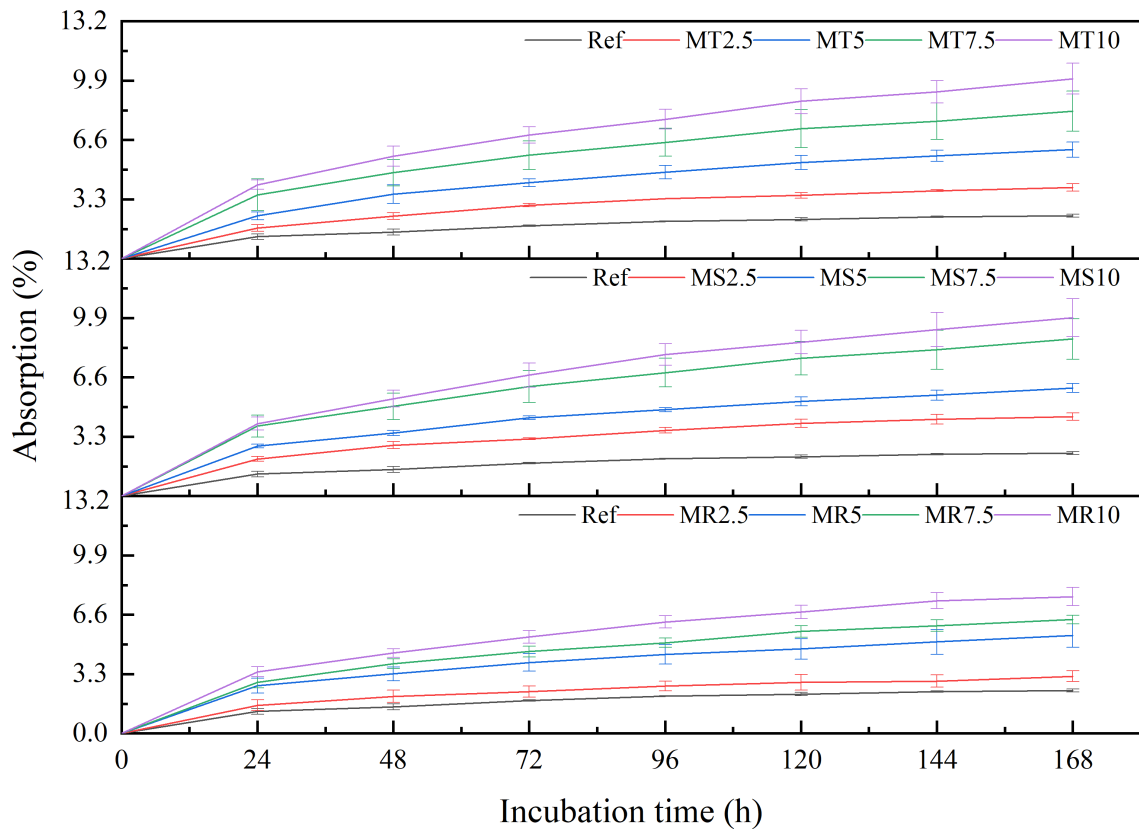


Figure 6.7. Absorption results

All tested biocomposites are characterized by higher absorption compared to the reference samples. After the first 24 h of incubation, the highest rate of absorption is observed for all materials. The reference material displays an initial steep increase, nearing a plateau but continuing to show a slight upward trend. Conversely, this behavior is not seen in the biocomposites, which exhibit a steady increase in absorption at each 24-hour interval. This behavior is attributed to the highly hygroscopic nature of the filler, leading to greater absorption of the artificial plasma solution. However, these changes become less pronounced after 72 h for the lowest filler content. The absorption level increases with higher filler content. Sage- and thyme-based materials demonstrate the highest absorption rates among the biocomposites. After 168 hours of incubation, thyme-based materials exhibit an increase in absorption ranging from 66% to 318%, while sage-

based materials show an increase from 84% for MS2.5 to 318% for MS10. In contrast, rosemary-based materials exhibit a smaller increase, ranging from 32% to 218%. This difference is primarily related to the nature of the introduced herbs. Sage leaves are covered with dense trichomes, enhancing their ability to retain water. A similar characteristic is observed in thyme, while rosemary leaves are more rigid and have a waxy surface, which reduces their water absorption capacity. Furthermore, thyme and sage particles exhibit a highly porous structure (opened trichomes – Figure 5.5), significantly enhancing the surface area for moisture retention. Moreover, the higher the filler content and the longer the incubation period, the greater the scatter of results. This variability could be attributed to the distribution of the filler within the matrix, as well as the fact that samples for testing were obtained by cutting, which exposed the fillers to the incubation solution. This exposure could lead to inconsistent absorption rates, contributing to the observed scatter in the results.

Absorption is significant for the wound-healing process. Increased moisture promotes even re-epithelialization, while dry wounds result in uneven repair due to epithelial cells following moisture tracks. Wound exudate, containing essential healing agents, is less present in dry wounds, delaying healing. Excessive moisture can cause skin maceration and bacterial colonization. Therefore, an optimal moisture level is crucial, requiring dressings that moisten the wound surface while absorbing excess exudate [185],[199].

## **6.8. Rebound resilience**

The rebound resilience mean values with the standard deviations, illustrated in Figure 6.8, demonstrate the effect of incorporating fillers into the PDMS matrix.

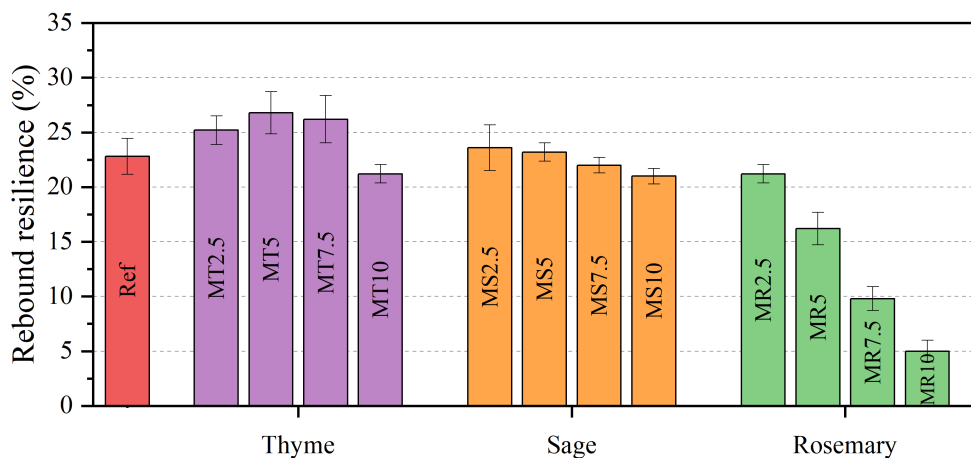


Figure 6.8. Rebound resilience measurement results

An increase in filler content for sage- and rosemary-based composites leads to decreased rebound resilience. Specifically, for sage, the difference reaches 11% for MS10 compared to MS2.5, while for rosemary, the decrease is nearly 77%, with MR10 showing a reduction of more than 78% compared to the reference. In contrast, thyme-based composites exhibit an increase in rebound resilience up to a filler content of 5 wt.%, with a rise of almost 18% compared to PDMS. Beyond this point, a decline is observed. Similar rebound resilience values are noted for MT10, MS10, and MR2.5. This behavior may be related to the stiffness of the fillers: thyme and sage have less rigid leaves, while stiffer ones characterize rosemary. This leads to increased stiffness of the biocomposite and consequently reduces its ability to return to its original shape [200]. Furthermore, the higher rebound resilience values of thyme-based composites can be attributed to this filler's smaller average particle size (Table 5.3), leading to a more uniform stress distribution within the matrix. However, at higher filler contents, this relationship reverses due to increased stiffness and, consequently, lower flexibility.

Durability is crucial for wound dressing applications to minimize the need for frequent dressing changes, which can disrupt the wound-healing process. High rebound resilience also enhances patient comfort by ensuring that the dressing adapts to the body's movements without losing shape, thereby reducing irritation and pressure on the wound. Therefore, the observed decrease in rebound resilience for rosemary-based materials containing the filler above 5 wt.% may limit their potential application as wound dressings.

## 6.9. Abrasion resistance

As depicted in Figure 6.9, the incorporation of organic fillers results in a reduction of abrasion resistance, which further decreases with increasing filler content.

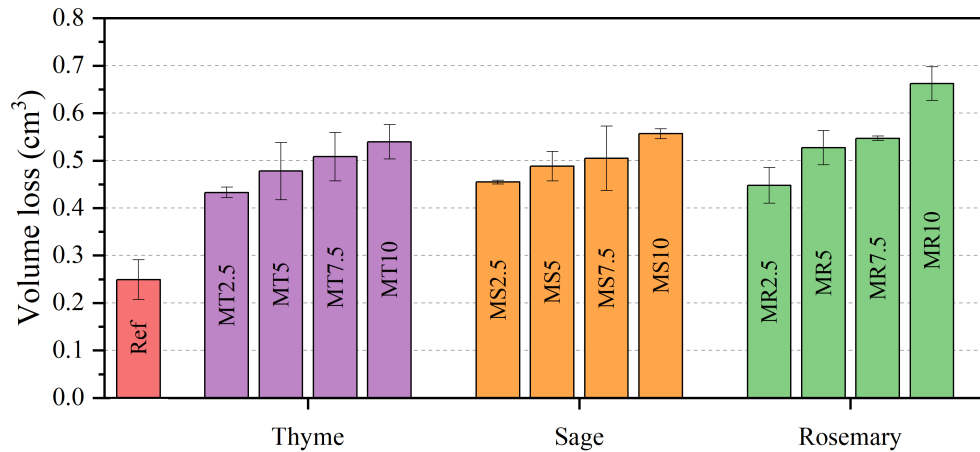


Figure 6.9. Abrasion resistance results

The most significant decrease in abrasion is observed in rosemary-based composites (approximately 170% for MR10), whereas sage- and thyme-based materials exhibit similar volume loss rates (approximately 70% higher than the reference for MT2.5). This reduction is attributed to the inadequate binding force between the filler particles and the matrix, which adversely affects the mechanical properties and durability of the biocomposites [201]. Moreover, during testing, all materials showed a tendency for edge wear and detachment of material pieces, as depicted by the traces visible in Figure 5.16, with this phenomenon being more pronounced in biocomposites containing higher filler content. For rosemary-based materials, the highest increase in volume loss is observed for MR10, with an increase of approximately 48% compared to the lowest filler content. This can be attributed to the potential presence of agglomerates, which, when detached, leave voids and increase the mass loss of the samples. In addition, the lower the hardness, as shown in Figure 6.4, the greater the volume loss. This occurs because reduced deformation resistance makes the material more susceptible to wear when in contact with a rigid surface. Additionally, the varying degree of result scatter can be attributed to differences in particle size and distribution. Furthermore, it is observed that the higher the terpene and fatty acid content, the greater the volume loss, suggesting their potential influence on the integrity between the filler and the matrix.



In the context of wound dressing applications, it is crucial that the dressing protects the wound from external factors, including forces that could cause rapid wear of the patch, necessitating frequent replacement. For long-short-term dressings, a very high level of abrasion resistance would render the material unsuitable. On the other hand, in short-term applications, such high values do not constitute grounds for material exclusion. Additionally, the conditions specified by the ISO 4649 standard for abrasion resistance are considerably more severe than those encountered in actual use.

## 6.10. FTIR analysis

The IR spectra obtained from the FTIR analysis are illustrated in Figure 6.10.

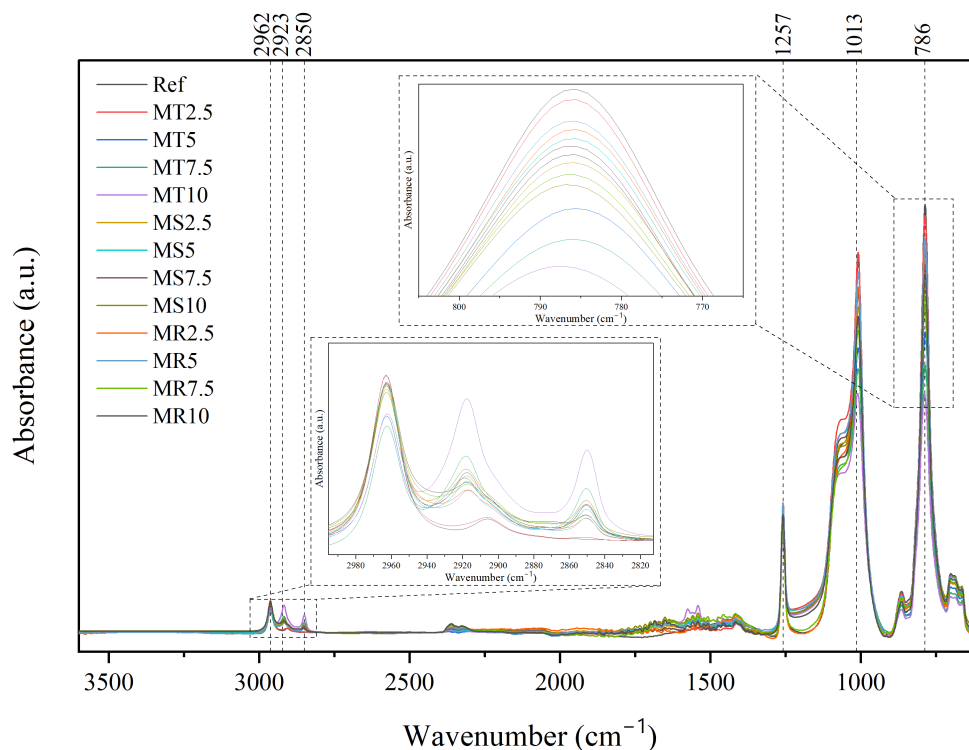


Figure 6.10. FTIR analysis results

The incorporation of herbs into the PDMS matrix did not introduce new peaks; however, it did alter the intensity of the characteristic peaks of polydimethylsiloxane. Specifically, the peaks at  $786\text{ cm}^{-1}$  and  $1013\text{ cm}^{-1}$  decreased with the addition of fillers. This reduction in peak intensity for individual biocomposites corresponds to a decline in the mechanical properties observed during tensile testing, as the siloxane bond is crucial

for the material's strength. Notably, this decrease is not proportional to the amount of filler introduced.

A similar trend is observed for the asymmetric stretching of CH<sub>3</sub> groups at 2962 cm<sup>-1</sup>, whereas the opposite is noted for the symmetric stretching of the same groups at 2850 cm<sup>-1</sup>. Increased intensity of CH<sub>3</sub> stretching correlates with higher hydrophobicity of the material due to its contribution to lower surface energy. These findings are consistent with the water contact angle results. Furthermore, the minimal changes observed in the -OH band indicate that the biocomposites exhibit limited moisture absorption from the surrounding environment.

## 6.11. DSC analysis

The results of the DSC analysis are presented in Figure 6.11.

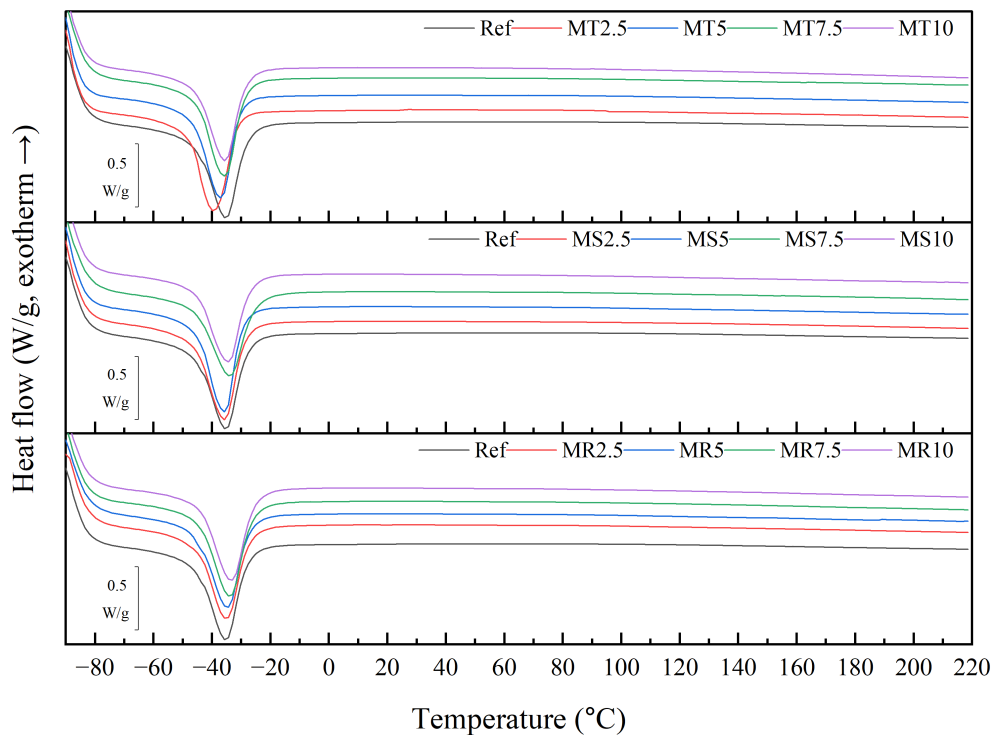


Figure 6.11. DSC analysis results

Based on the obtained thermograms, polydimethylsiloxane exhibits an endothermic peak around -40 °C, a temperature corresponding to a single crystalline structure, which is consistent with reported literature findings [202],[203]. Moreover, the

thermograms indicate that introducing herbal fillers into the PDMS matrix does not change the thermal behavior of the material. Additionally, no significant alterations or shifting of the melting temperatures are observed. Furthermore, no additional exo- or endothermic peaks are noted. This indicates a similar crystalline structure of all obtained materials.

The degree of crystallinity was calculated using the enthalpy of fusion for 100% crystalline PDMS, which is 61.19 J/g and presented in Table 6.4.

Table 6.4. Crystallinity degree calculated based on the DSC thermograms

<b>Material</b>	<b>Crystallinity degree (%)</b>
Ref	40.09
MT2.5	41.98
MT5	41.23
MT7.5	38.88
MT10	38.55
MS2.5	40.56
MS5	40.28
MS7.5	38.55
MS10	37.44
MR2.5	39.53
MR5	39.14
MR7.5	39.83
MR10	39.75

As can be noticed, the crystallinity of PDMS aligns with values reported in the literature [204]. Additionally, the crystallinity varies depending on the type and content of the filler. For thyme-based composites, the material filled with 2.5 wt.% exhibits the highest recorded crystallinity degree, which decreases with increasing filler content. Similar behavior is observed for sage-based composites. This suggests that the chemical compounds present in thyme and sage may influence the chemical structure by enhancing the nucleation process in the polysiloxane, leading to improved mechanical properties and stiffness. However, this enhancement depends on the filler content, with the effect diminishing when the amount surpasses a certain threshold.

In contrast, rosemary-based composites exhibit a lower degree of crystallinity, which further decreases with the addition of 5 wt.% rosemary, increases after adding 7.5 wt.%, and then decreases again after adding 10 wt.%. This results in a material with a more amorphous structure, contributing to higher gas permeability due to reduced

resistance to molecular diffusion. It should be noted that filler distribution plays an essential role in shaping the thermal properties and impacting the degree of crystallinity. Moreover, the biocomposites' results correlate with the siloxane peaks presented in Figure 6.10, where high peak intensity corresponds to a high crystallinity degree.

## 6.12. Accelerated degradation

The degree of accelerated degradation impact is evaluated based on the changes in the chemical backbone (Figures 6.12 – 6.15) and tensile properties (Figures 6.16 – 6.21). For the purpose of this work, samples that underwent degradation are referred to as aged samples. It should be noted that prior to testing, samples were drained from excess water.

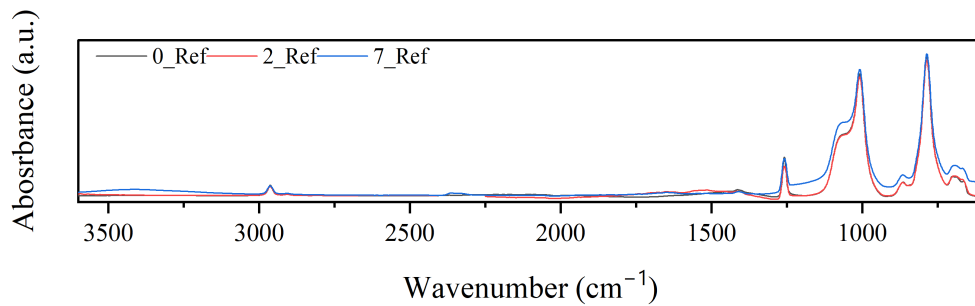


Figure 6.12. FTIR spectra of aged reference samples

In the reference samples, the intensity of the characteristic peaks shows a slight decrease after two days of incubation in artificial plasma at an elevated temperature (70 °C), indicating minimal degradation of the polymer. After seven days of incubation, the material exhibits higher peak intensities, including a notable increase in the broad -OH group peak. This suggests the presence of water from the artificial plasma solution, as confirmed by the *in vitro* absorption results in Section 6.7.

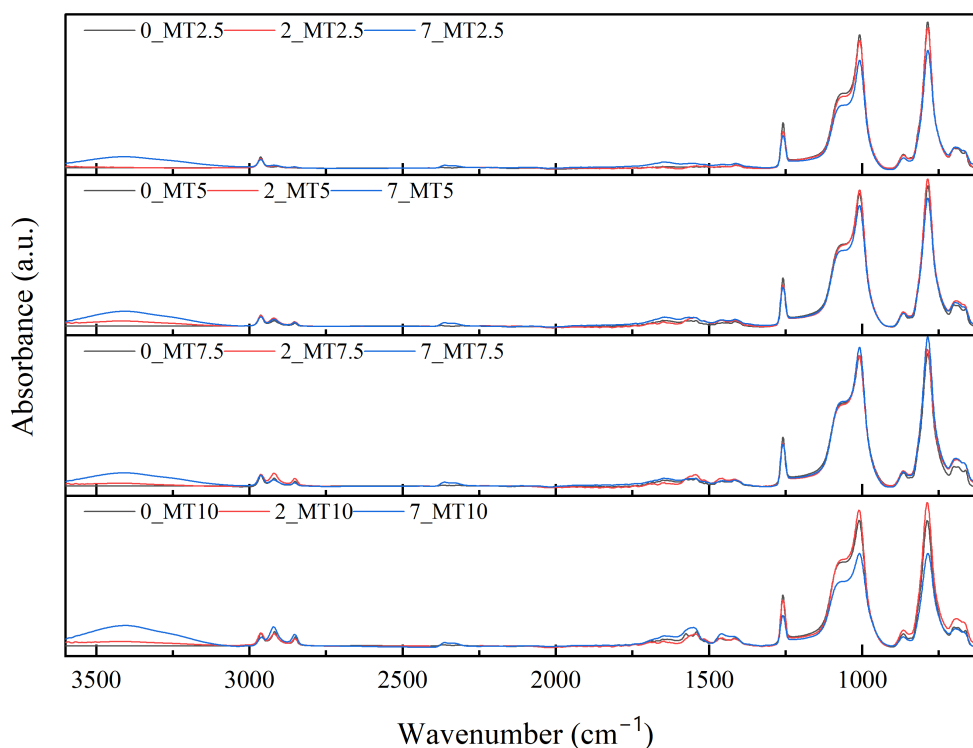


Figure 6.13. FTIR spectra of aged thyme-based composite samples

The filler content influences the changes in the chemical backbone of thyme-based composites. For MT2.5, as the incubation period increases, the intensity of the peaks decreases, indicating material degradation and the dissolution of the siloxane bond, resulting in lower mechanical properties. Additionally, no stretching of symmetric  $\text{CH}_3$  is observed, suggesting reduced flexibility of the material both before and after accelerated degradation. MT5 and MT10 exhibit a similar trend, where the peaks increase after 2 days of incubation but decrease after 7 days. In contrast, MT7.5 behaves similarly to reference PDMS, with an initial decrease in peak intensity followed by an increase. Furthermore, all materials showed the presence of the  $-\text{OH}$  group, with its amount increasing with both the incubation period and filler content, consistent with the absorption results.

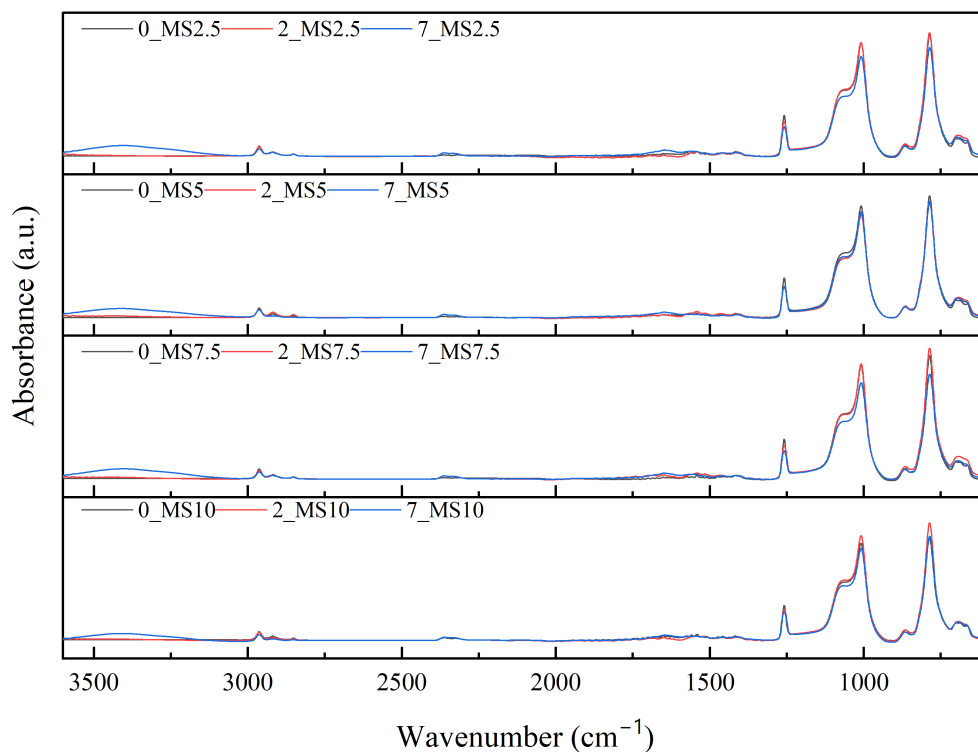


Figure 6.14. FTIR spectra of aged sage-based composite samples

In the case of sage-based composites, MS2.5, MS7.5, and MS10 behave similarly to PDMS, while MS5 exhibits decreasing peak intensities with an increasing incubation period. However, it should be noted that these changes are very negligible. Similar to thyme-based composites, sage-based composites display a broad band of the -OH group, indicating its incorporation into the polymeric chain.

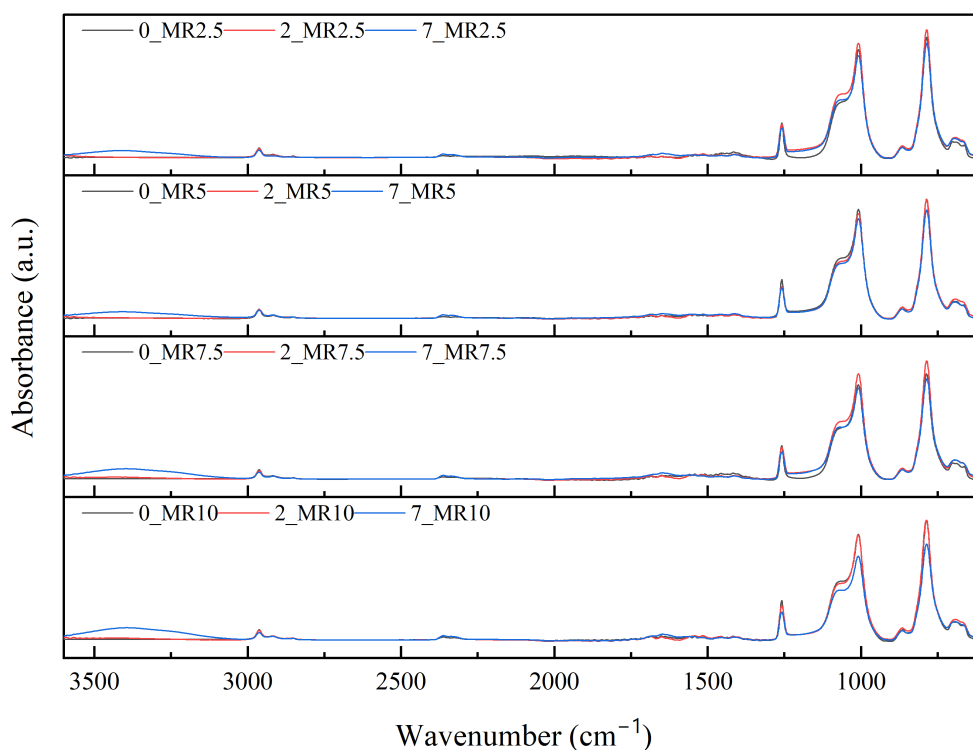


Figure 6.15. FTIR spectra of aged rosemary-based composite samples

Only in the case of rosemary-based materials do all biocomposites consistently exhibit an increase in peak intensity after 2 days of incubation, followed by a decrease after 7 days. Similar to the other biocomposites, rosemary-based materials also show a peak indicating the incorporation of -OH due to incubation in a water-based solution.

Overall, the accelerated aging of the tested materials affects the intensities of the characteristic polydimethylsiloxane peaks. However, no components from the artificial plasma were incorporated into the polymeric chain, except for water, as indicated by the presence of the -OH group. This suggests that the changes in the chemical backbone were induced by high temperatures and the liquid solution rather than by the compounds present in the solution.

To comprehensively characterize the changes in materials under tension, tests were conducted on samples taken every 24 hours for up to 7 days. However, only data from 2 and 7 days of incubation, following the ISO 10993-13 standard, are evaluated.

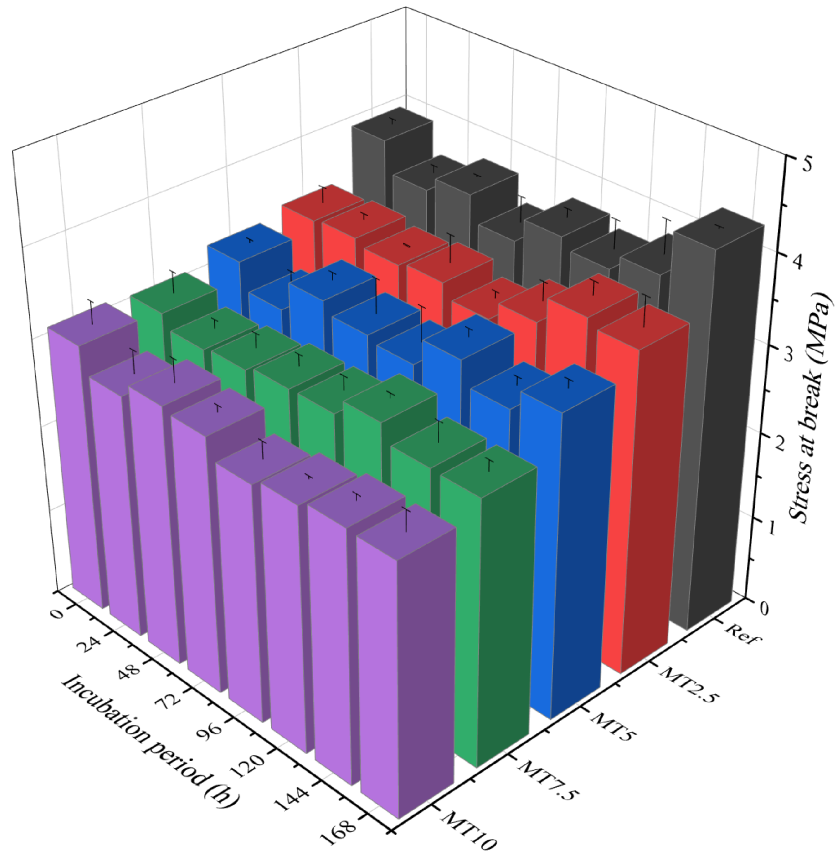


Figure 6.16. Stress at break results for aged thyme samples

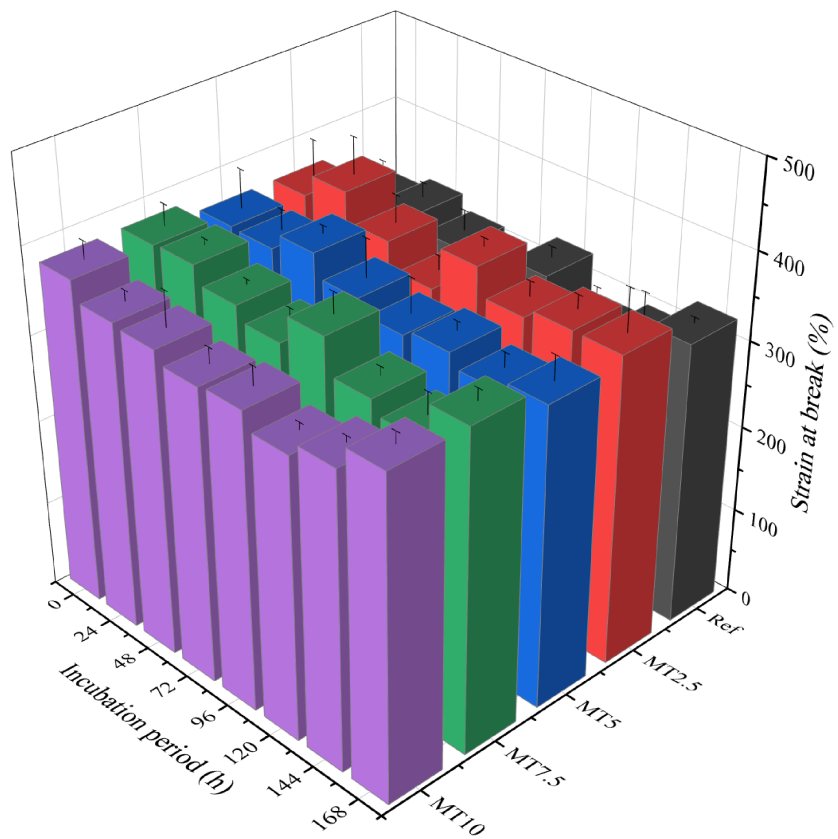


Figure 6.17. Strain at break results for aged thyme samples



For the reference material, there is an initial decrease in stress at break value, followed by an increase after 7 days of incubation. This suggests minimal initial degradation, with further incubation leading to increased cross-linking and higher values. These findings are consistent with the IR spectra. For thyme-based composites, a similar trend is observed across all samples except MT10, where prolonged incubation results in a consistent decrease in stress at break value. This indicates that beyond a certain threshold, above 7.5 wt.% of incorporated filler, the biocomposites' behavior changes due to the increased amount of terpenoid compounds affecting the cross-linking of the material. Furthermore, no direct correlation between stress at break value and the chemical structure of these biocomposites is found, suggesting that changes are strictly related to the filler content and its distribution within the matrix. In terms of strain at break, the reference material (PDMS) shows an initial decrease followed by an increase. For thyme-based composites, only MT2.5 shows a decreasing trend, while the others show an increase. This could be associated with the increasing peak of symmetric  $\text{CH}_3$ , indicating higher material flexibility.

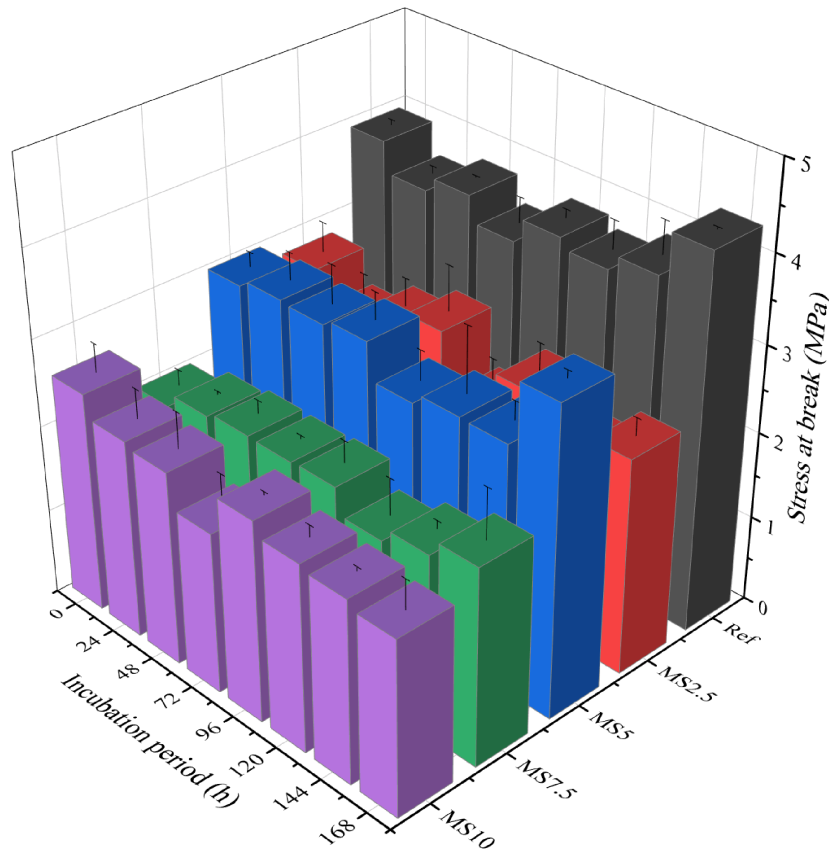


Figure 6.18. Stress at break results for aged sage samples

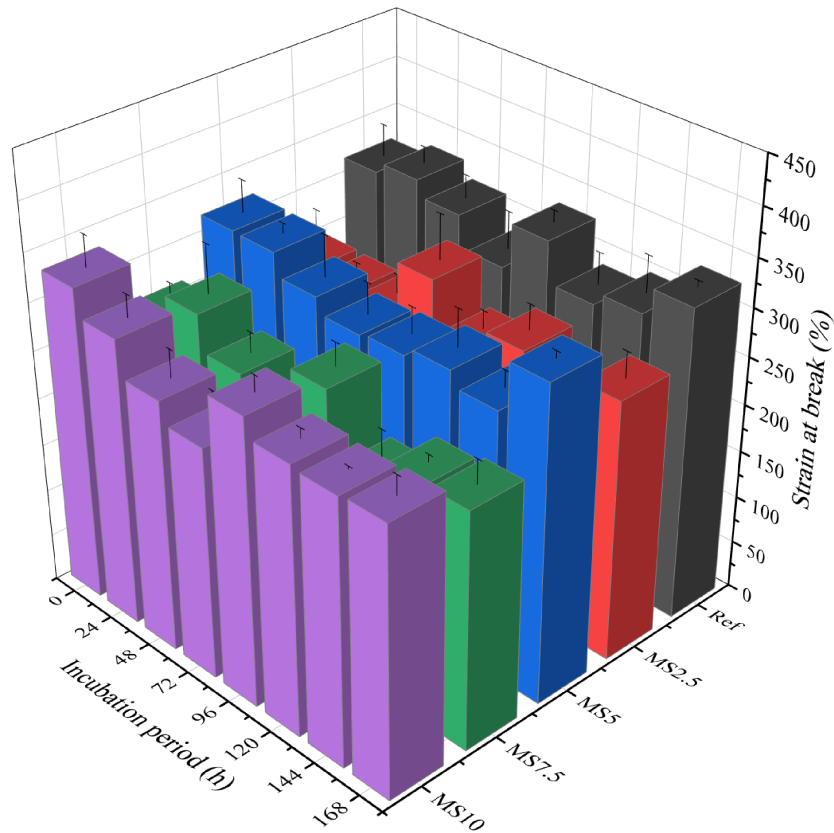


Figure 6.19. Strain at break results for aged sage samples

Sage-based composites exhibit different behaviors depending on the filler content. MS2.5 shows an overall decreasing trend, while MS5 and MS7.5 demonstrate an increasing one. Similar to MT10, MS10 displays a decreasing behavior, indicating that a high filler content negatively impacts the degradation process. Additionally, no correlation with chemical changes was observed in the IR spectra. MT2.5 and MT5 exhibit increasing trends for strain at break, whereas MT7.5 and MT10 show decreasing trends. Sage-based composites display a higher range of standard deviation, likely due to the behavior of the filler within the matrix, including its distribution and mechanical adhesion. The release of bioactive compounds from the biocomposite may also affect the integrity between the filler and the matrix, resulting in varied values. Despite these changes, all measured values fall within the same standard deviation range.

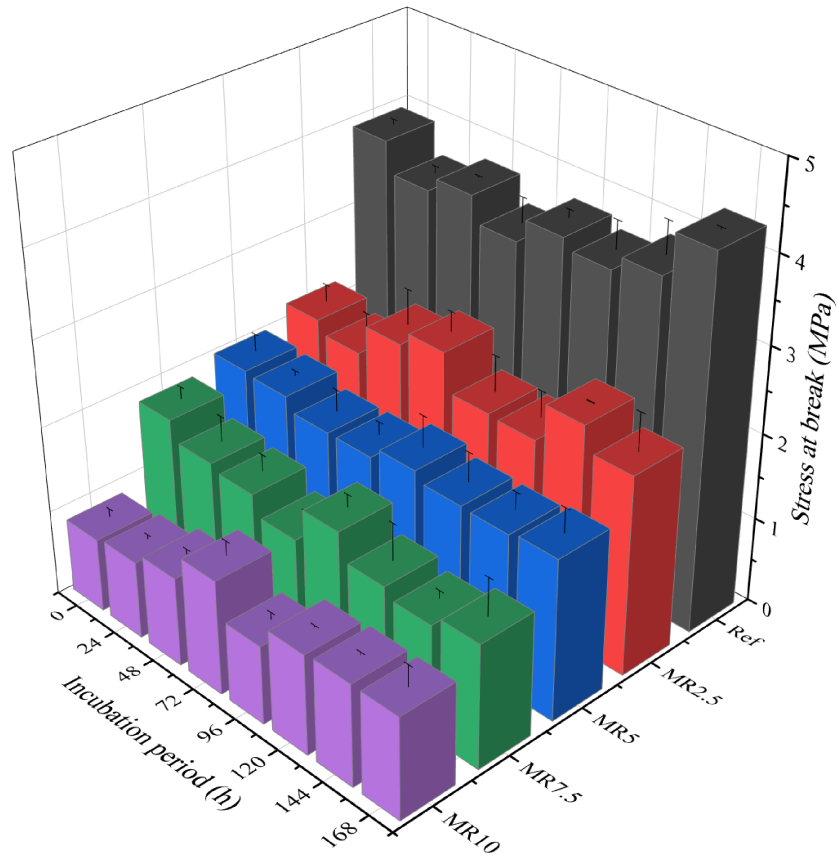


Figure 6.20. Stress at break results for aged rosemary samples

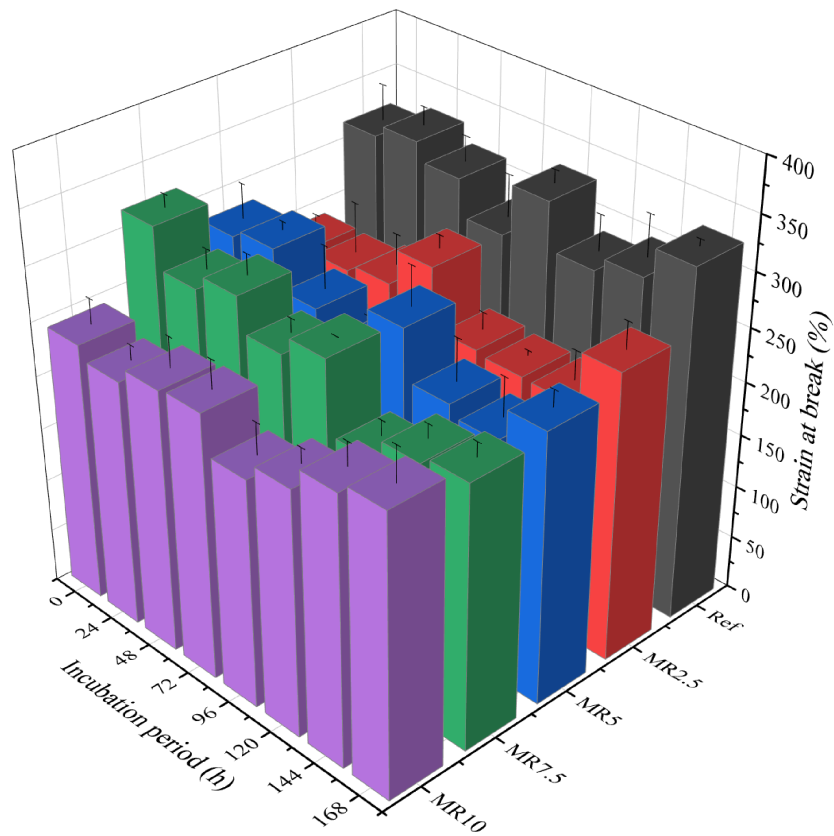


Figure 6.21. Strain at break results for aged rosemary samples

Rosemary-based composites exhibit the lowest stress at break and strain at break values. Specifically, MR2.5 and MR10 show increasing characteristics, while MR5 and MR7.5 display a decreasing trend. This suggests that incorporating 10 wt.% of rosemary into polydimethylsiloxane may induce further cross-linking due to the presence of some bioactive compounds. However, similar to sage-based composites, these changes in characteristics fall within the standard deviation range. Additionally, the higher the rosemary content, the more pronounced the decrease in overall biocomposites performance during tension, as evidenced by the declining stress at break values. This indicates that while rosemary filler can affect the mechanical properties of the biocomposites, its impact becomes detrimental at higher concentrations, reducing the material's ability to withstand tensile stress.

In conclusion, accelerated degradation impacted the mechanical properties of the materials to varying degrees, depending on the type and content of the filler. However, from the perspective of wound dressing applications, the most critical feature is the material's flexibility. This property remained at a satisfactory level even after degradation at elevated temperatures, which do not occur under normal daily conditions.

### **6.13. Microscopic topography analysis**

The micrographs shown in Figures 6.22 – 6.24 depict the fracture surfaces of unaged modified thyme-, sage-, and rosemary-based materials after tensile testing. In these figures, the SEM analysis is shown on the left, while those on the right show the corresponding stereoscopic images. This comprehensive analysis enabled the examination of fracture characteristics, the evaluation of filler integration with the matrix, and the assessment of structural alterations under tensile stress. For biocomposites, the microscopic images reveal the initiation zone of tensile stress, identified by the smoother surface, as well as the direction of crack propagation, which is indicated by the presence of white structure flaking, resulting in an interfacial peeling. Furthermore, it can be observed that the biocomposites exhibit a ductile fracture mechanism, which becomes more pronounced as the filler content increases. At the same time, the reference sample displays a brittle fracture mechanism. This suggests that incorporating organic fillers changes the crack propagation behavior under tensile stress. The results indicate that

higher filler content results in more jagged fracture surfaces. Additionally, it is observed that sage and rosemary particles tend to form agglomerates within the matrix (seen as dark or bright areas in Figures 6.23a and 6.24, respectively), which notably influences the fracture surface characteristics and consequently alters the mechanical properties of these materials, as discussed in Section 6.1. With increasing filler content, larger particles tend to detach from the matrix, creating voids that act like notches. This greatly influences the tensile behavior of the materials, leading to variable results depending on the filler distribution within the matrix. Despite protective measures during fabrication to prevent contamination, some impurities were observed in the reference samples. Furthermore, the presence of clusters within the matrix indicates uneven mixing of the base and catalyst. This irregularity could be attributed to insufficient mixing time or inadequate mixing speed, potentially resulting in greater variability in the testing outcomes. However, after performing accelerated degradation, these clusters underwent further cross-linking, leading to a more homogenous structure and increased stiffness, confirmed by the results of tensile testing.

For aged samples, only selected examples are presented because of their unclear behavior during testing. As illustrated in Figure 6.25, color changes indicate the release of polyphenolic compounds responsible for the herbs' color into the artificial plasma solution. In the case of MT5, an even distribution of longer trichomes is visible, explaining the increased tensile strength after aging. Conversely, MT10 exhibits the formation of voids due to filler detachment, leading to decreased tensile strength. This detachment is likely due to the hygroscopic nature of the filler, which absorbs the solution, causing particle enlargement and subsequent detachment during tension. A similar trend is observed for aged sage-based composites. Although the higher magnification of MS10 shows a more even surface, lower magnification reveals increased surface jagginess and enlarged particles due to absorption. The micrographs display a highly uneven fracture surface for rosemary-based composites filled with 10 wt.% filler, which may account for the varying tensile behavior during testing and decreased mechanical properties. The EDS analysis confirmed the absence or negligible presence of artificial plasma components adhered to or incorporated into the matrix, thereby eliminating their impact on the tested properties.

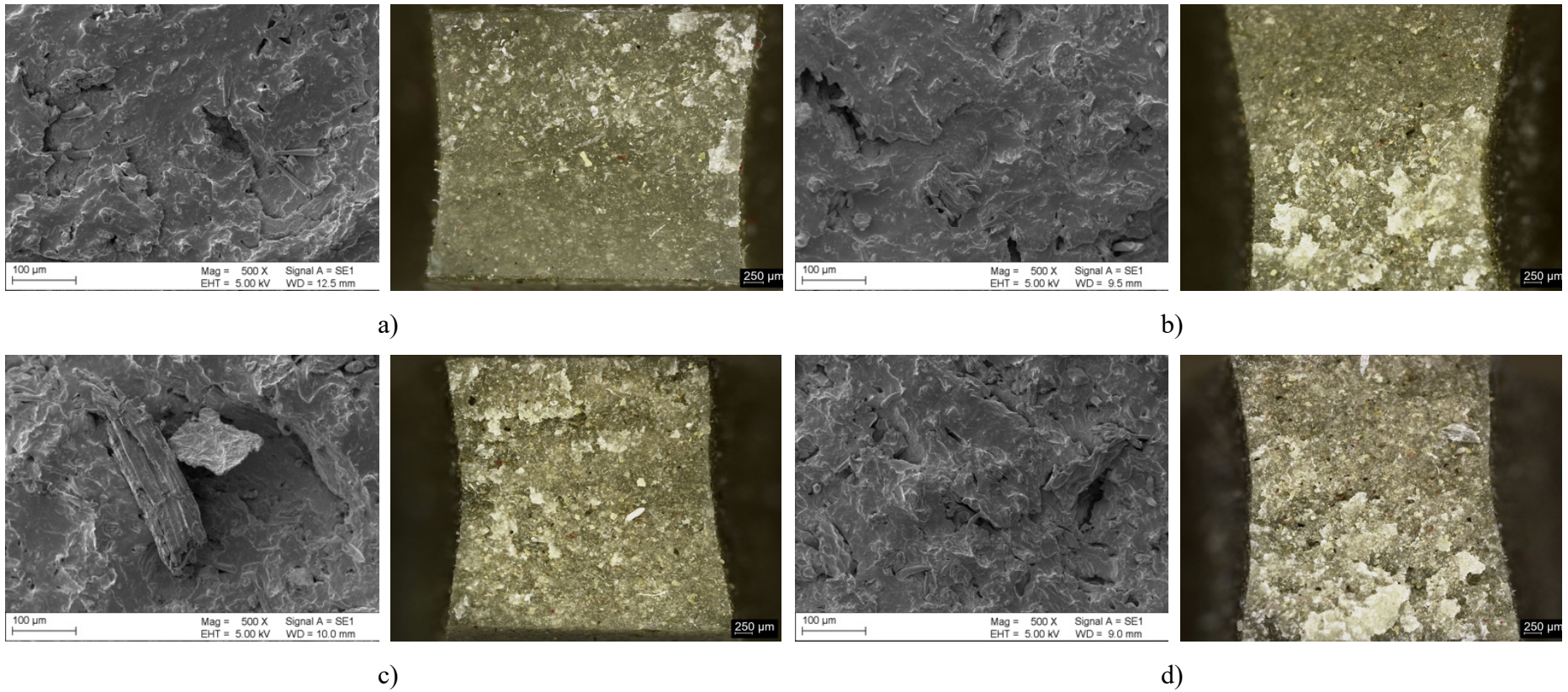


Figure 6.22. Fracture surface micrographs of modified thyme composites: MT2.5 – a), MT5 – b), MT7.5 – c), MT10 – d)

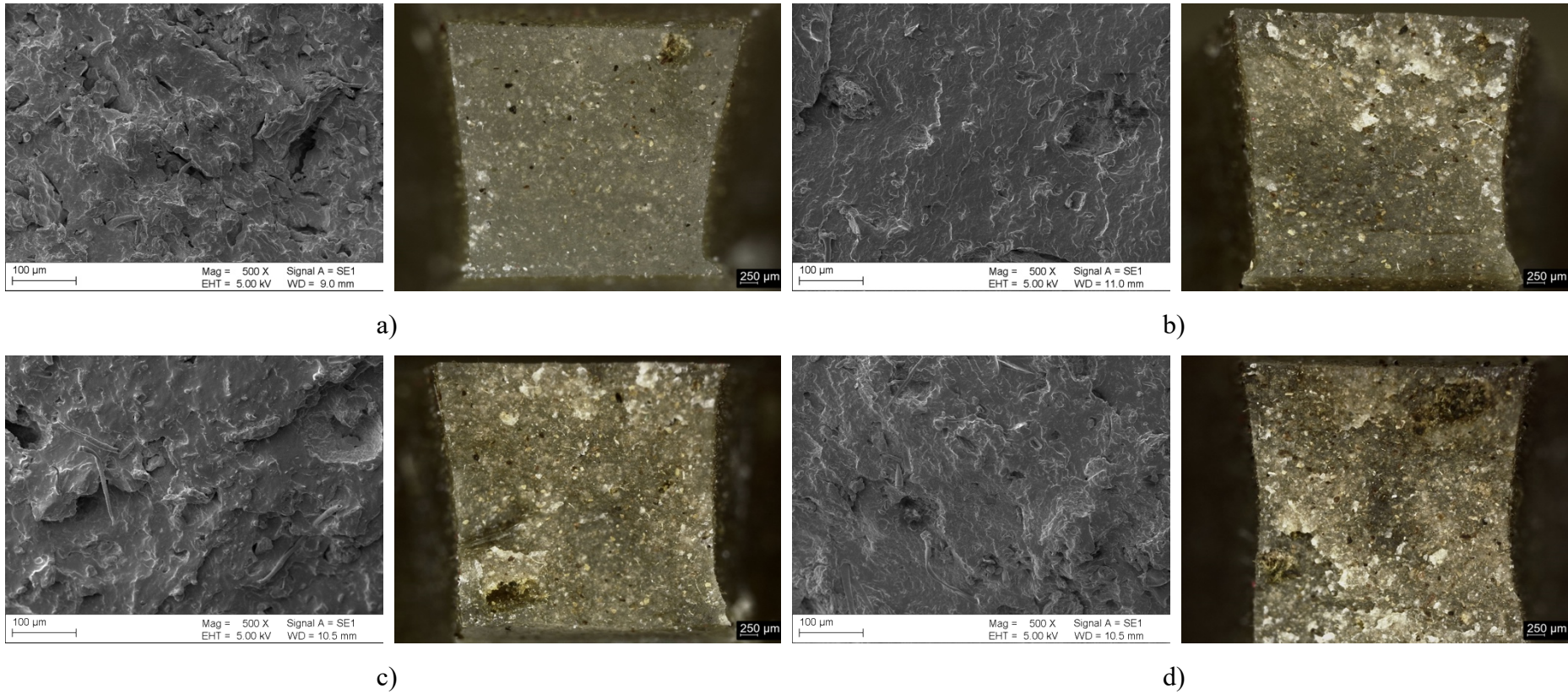


Figure 6.23. Fracture surface micrographs of modified sage composites: MS2.5 – a), MS5 – b), MS7.5 – c), MS10 – d)

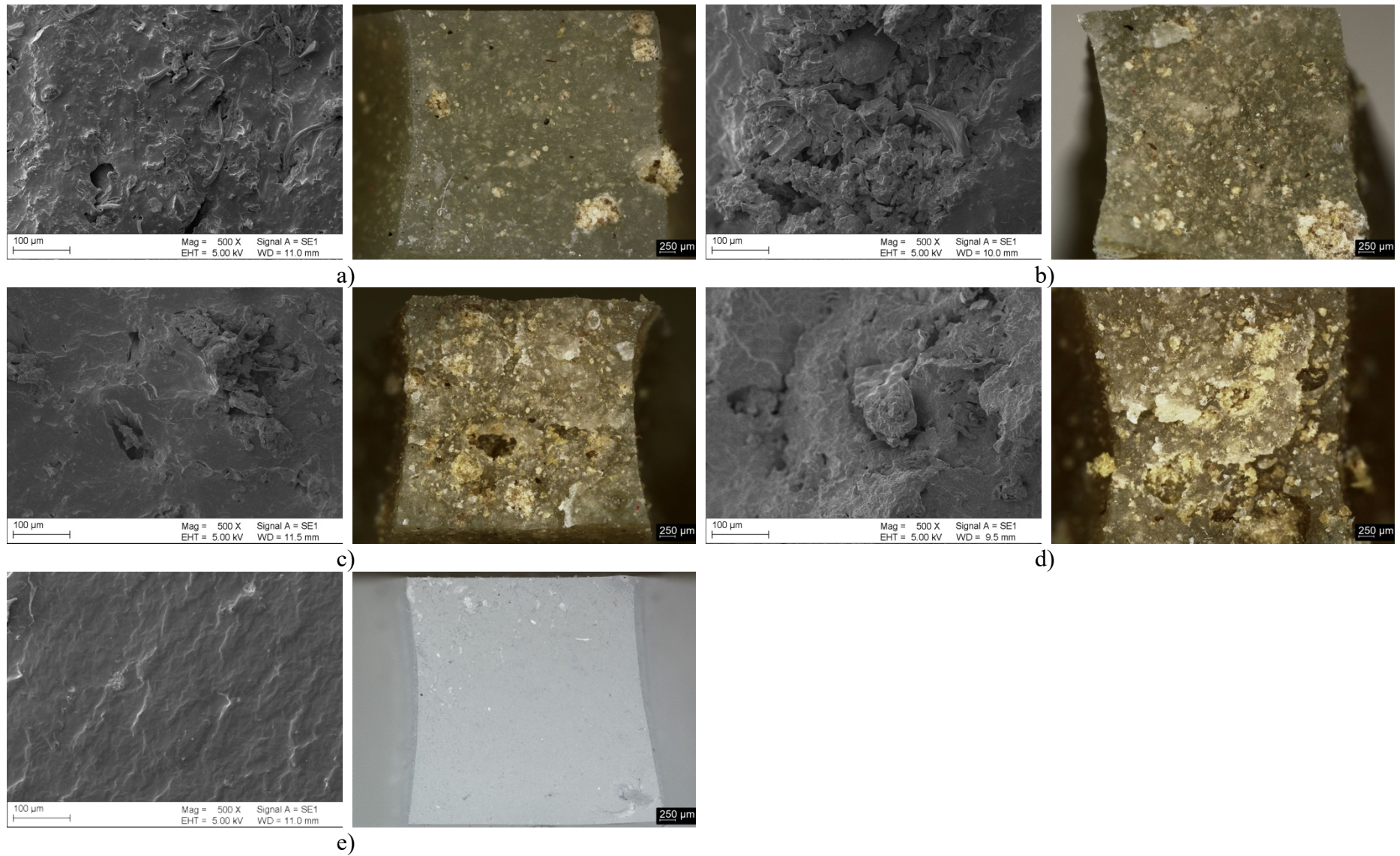


Figure 6.24. Fracture surface micrographs of modified rosemary composites: MR2.5 – a), MR5 – b), MR7.5 – c), MR10 – d), reference – e)



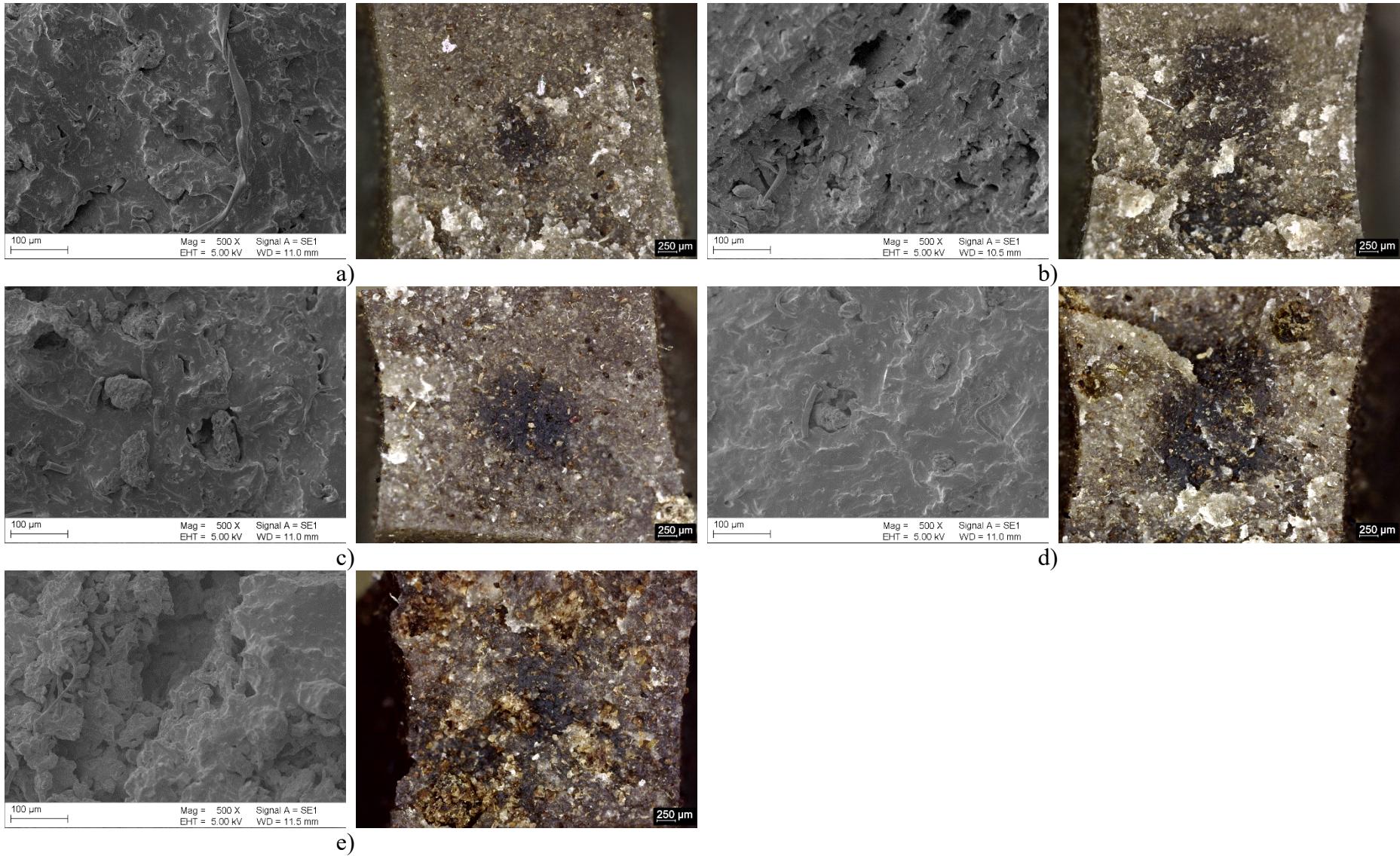


Figure 6.25. Fracture surface micrographs of selected 7-day aged samples: MT5 – a), MT10 – b), MS7.5 – c), MS10 – d), MR10 – e)

#### **6.14. Biocomposites assessment – II analysis**

Upon completion of the second phase of the work, another multicriteria analysis was conducted to select the materials for the final phase, which involves assessing cell viability. This analysis evaluated each modified filler-based material individually compared to PDMS. However, for the subsequent phase, two herb-based composites were chosen. The assessment was based on the analysis of the obtained results for absorption, rebound resilience, abrasion, and accelerated aging. The results of the second multicriteria analysis are displayed in Table 6.5. As with the first analysis, the evaluation was based on the significance of the requirements for wound dressing materials, with values assigned on a scale from 1 to 13. Although the materials were initially assessed individually, subsequent testing incorporated all variations of the chosen biocomposites to evaluate the dependence of the results on filler concentration.

Based on the results of the second analysis, thyme-based composites achieved the highest score, followed by sage- and rosemary-based composites. Therefore, for the final phase, testing was conducted on the materials with the greatest application potential: thyme- and sage-based composites.

Table 6.5. II multicriteria analysis results

Property	Weight	Material																									
		Ref		MT2.5		MT5		MT7.5		MT10		MS2.5		MS5		MS7.5		MS10		MR2.5		MR5		MR7.5		MR10	
		C	V	C	V	C	V	C	V	C	V	C	V	C	V	C	V	C	V	C	V	C	V	C	V	C	V
<b>Absorption</b>	3	5	15	12	36	11	33	7	21	1	3	13	39	10	30	6	18	2	6	3	9	9	27	8	24	4	12
<b>rebound</b>	2	8	16	13	26	12	24	11	22	4	8	10	20	9	18	7	14	5	10	6	12	3	6	2	4	1	2
<b>resilience</b>																											
<b>Abrasion</b>	1	13	13	12	12	9	9	6	6	3	3	11	11	8	8	7	7	2	2	10	10	5	5	4	4	1	1
<b>resistance</b>																											
<b>Accelerated</b>	4	13	52	12	48	10	40	9	36	8	32	7	28	11	44	5	20	4	16	6	24	3	12	2	8	1	4
<b>degradation</b>																											
<b>Σ</b>		<b>96</b>		<b>122</b>		<b>106</b>		<b>85</b>		<b>46</b>		<b>98</b>		<b>100</b>		<b>59</b>		<b>34</b>		<b>55</b>		<b>50</b>		<b>40</b>		<b>19</b>	

## 6.15. Cell viability assay

The viability of L-929 line cells of the tested materials is depicted in Figure 6.26, where the red line indicates the minimum required cell viability percentage – 70%.

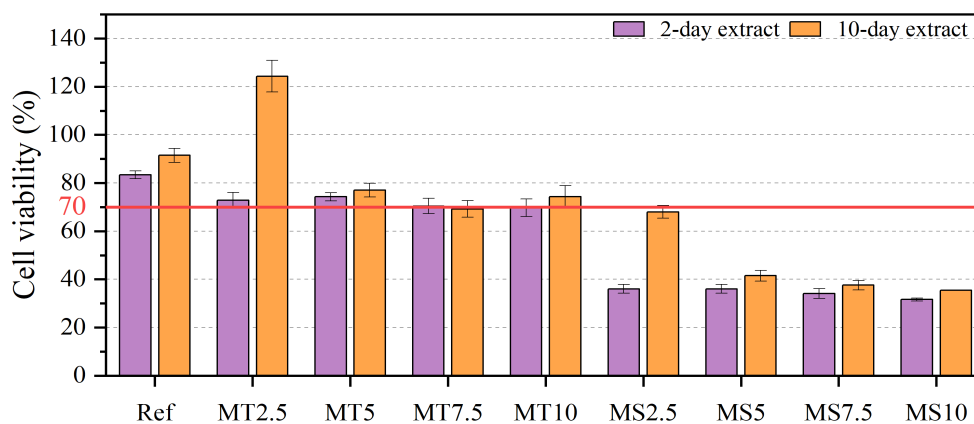


Figure 6.26. Cell viability results

As observed, the reference material demonstrates higher cell viability than the required minimum of 70%, per the safety data provided by the reference material producer. The impact of incorporating herbs into the PDMS matrix varies depending on the type and content of the herbs. All thyme-based composites exhibit the minimal required cell viability, or higher, for both 2-day and 10-day extracts. In contrast, while cell viability in sage-based composites increases after 10 days of incubation, these materials do not achieve sufficient cell viability, indicating limited cell proliferation in the wound bed [205]. Although the literature acknowledges the positive impact of sage on wound healing, it also highlights its antiproliferative and highly antimicrobial properties, as discussed in Section 6.5. It is possible that the bioactive compounds in sage, which inhibit bacterial cell proliferation and thereby accelerate wound healing, may also inhibit human cell proliferation. Similarly, an increase in cell viability is observed in thyme-based composites, with the highest increase noted for the lowest filler content. This increase can be attributed to the presence of *Thymus vulgaris*, which is rich in compounds known to enhance cytokine production, such as thymine and tannins, leading to higher cell proliferation [206]. However, when the filler content exceeds 2.5 wt.%, this effect is insignificant, resulting in lower cell viability, although still above the minimal required level. This may be due to the excessive concentration and diffusion of bioactive compounds at higher filler contents, which could limit proliferative activity.

## 7. Summary and conclusions

### 7.1. Summary

Materials must meet a range of stringent requirements in order to be utilized in the medical field, whether for internal or external applications such as wound dressings. Several key factors must be considered to address these demands, including the material selection, properties, modifications, and processing technologies, all of which must be tailored to the specific application. Particular attention must be paid to medical applications that involve direct contact with patients, with biocompatibility being the paramount criterion. However, the material often requires further modification to enhance certain desirable properties, such as antibacterial activity.

This study explores the development of biocomposites based on polydimethylsiloxane (PDMS), modified with thyme, sage, and rosemary, with the goal of enhancing the polymer's bioactivity, particularly its antibacterial properties. The approach combines the biocompatibility and unique characteristics of PDMS with the health-promoting properties of these herbs, which include anti-inflammatory, antibacterial, and other beneficial effects. To achieve this, a technology was developed to modify the herbal fillers and incorporate them into the PDMS matrix. This processing technology was designed to preserve the full potential of the herbs, particularly the polyphenolic compounds, which are the primary constituents and the focus of this work, as these compounds are sensitive to temperature. Subsequently, the modified materials were subjected to a series of physicochemical, mechanical, and biological tests to evaluate the impact of the herbal fillers on these properties. Initial tests revealed that modifications of the fillers were necessary, as the mechanical properties obtained were unsatisfactory. Furthermore, in the case of rosemary, the high content of terpenes and fatty acids (Table 5.7) impeded the cross-linking process, necessitating further refinement.

Three groups of biocomposites were developed: those based on unmodified and modified herbs, as well as their extracts. The incorporation of these additives into polydimethylsiloxane significantly influenced the mechanical properties of the resulting materials. For instance, biocomposites incorporating unmodified herbs exhibited a notable decrease in both stress at break and strain at break properties. This reduction

was primarily attributed to the presence of large particles within the unmodified herbs, which tended to detach under tensile stress, creating voids that acted as notches and consequently reduced tensile strength.

The modification of the herbs, as discussed in Section 5.1.2, proved beneficial in enhancing the tensile properties of the biocomposites. This improvement is due to the reduction in terpene and fatty acid content (Tables 5.5 through 5.7), as well as the elimination of larger particles (Table 5.3). However, the mechanical properties of the sage- and rosemary-based materials were still inferior to those of thyme-based composites. Microscopic analysis of the fracture surfaces revealed that this disparity was primarily due to the presence of agglomerates in the sage and rosemary composites. On the other hand, biocomposites based on herbal extracts demonstrated relatively diminished mechanical properties compared to those incorporating unmodified or modified herbs. This finding suggests that both fatty compounds and polyphenolic compounds play a significant role in determining the material properties. Although the stress at break values were lower for the obtained biocomposites, the strain at break for several of these materials, particularly the modified thyme composites, as well as MS10 and ER5, exceeded that of the reference. This increased strain at break is desirable for potential applications requiring flexibility to ensure patient comfort. The most significant impact was observed in biocomposites containing unmodified herbs, followed by those with modified sage and rosemary, while the extract-based composites generally exhibited comparable results. Similar trends were observed in hardness measurements, although the degree of change did not exceed 10%. It is noteworthy that the hardness of the fillers themselves plays a crucial role in shaping these results, as well as explaining the variability in measurements. The results represent an average hardness obtained from the sedimented and opposite sides of the material. Additionally, it was observed that higher filler content generally resulted in less variability in the measured properties due to higher filler concentration on the sedimented side, leading to a more uniform distribution, as seen in Figures 6.22 – 6.24. Several factors, including the methods used to prepare the fillers and incorporate them into the matrix, as well as issues such as sedimentation, agglomeration, and particle detachment, likely contributed to the observed scatter in the test results. These findings are consistent with the results of FTIR analysis, which showed a decrease in the peaks associated with the material's mechanical strength.

It was demonstrated that the addition of herbal fillers did not alter the hydrophobic nature of PDMS; the material remained hydrophobic regardless of the type or content of the fillers, with the biocomposites' results aligning with the range of values observed in the reference material. However, the minimal changes observed between the groups can be attributed to the presence of polyphenolic compounds, known for their high water solubility and hydrophilicity. Furthermore, the results confirmed the inhibition and limitation of *Staphylococcus aureus*, a primary contributor to wound infections. This was evidenced in the antibacterial activity assessment, where all tested materials, except for the reference, exhibited bacteriostatic or nearly bactericidal properties against *S. aureus*. However, it was found that the modifications performed on the fillers reduced the antibacterial activity, highlighting the significance of terpene and fatty acid compounds in limiting biofilm formation.

Given that the modified herb-based materials demonstrated more suitable properties for the intended application in wound dressings, only these materials, along with the reference, were subjected to further testing.

The in vitro absorption results clearly indicate the hygroscopic nature of the fillers and the influence of the plant's morphology. Specifically, among the biocomposites, rosemary, with its more waxy leaves, exhibited limited water retention, whereas sage and thyme, characterized by a dense network of trichomes on their leaves, showed enhanced moisture retention. It should be noted that the method of sample preparation, which involved cutting and exposing the fillers to an artificial plasma solution, contributed to significant variability in the results, with the scatter increasing as the incubation period lengthened. Nonetheless, the biocomposites with the lowest filler content (2.5 wt.%) demonstrated a stabilization of absorption after 72 hours. The presence of water from the incubation solution was further confirmed by FTIR analysis, where these materials displayed a broad peak corresponding to the hydroxyl group. In the context of wound dressing applications, absorption is a critical property, as it effectively manages excess exudate.

Another important set of properties includes rebound resilience and abrasion resistance, both of which are crucial for ensuring patient comfort in wound dressings. In terms of rebound resilience, all thyme-based composites, except those with the highest filler concentration, showed increased values, as did MS2.5 and MS5. The remaining

materials exhibited decreased resilience, with MR10 showing a reduction of nearly 80% compared to pure PDMS. The characteristics of the fillers significantly influence these results; for example, the higher stiffness of rosemary particles increases the material's overall stiffness, thereby reducing its ability to return to its original shape. Additionally, the small particle size of thyme and sage contributes to increased rebound resilience. However, in sage and rosemary cases, agglomerates' formation disrupted the even distribution of impacting energy, leading to decreased resilience at higher filler concentrations. Furthermore, it is noteworthy that the test was conducted on the sample's upper side, consisting of a thin layer of transparent PDMS opposite the sedimented side. This choice was based on the fact that the side with a higher concentration of fillers was intended to be in contact with the wound, while the opposite side would be exposed to external factors, such as clothing. On the other hand, all biocomposites exhibited decreased abrasion resistance as filler concentration increased, with MR10 experiencing nearly 70% greater volume loss compared to the reference material. Similar to rebound resilience, the formation of agglomerates influenced abrasion resistance, as did the presence of fatty compounds, where a higher concentration resulted in greater volume loss. Moreover, the results are influenced by the degree of crystallinity (Table 6.4), with lower values indicating a more amorphous structure and reduced rigidity and stiffness of the material. These findings also correlate with the hardness results, as reduced deformation resistance makes the material more susceptible to wear when in contact with a rigid surface. It is important to note that the testing conditions were significantly more severe than those typically encountered in actual use. As with other mechanical properties, these observations align with the findings from FTIR analysis.

An accelerated degradation test was performed using an artificial plasma solution to evaluate the material behavior under simulated use conditions. The resulting changes were assessed through tensile testing and FTIR analysis. The reference material initially exhibited a decrease in stress at break, which subsequently increased after 7 days of incubation, indicating enhanced cross-linking, as corroborated by higher peak intensities in the IR spectra. Thyme-based composites generally followed this trend, except for MT10, which consistently showed a decrease due to high filler content. Sage-based composites displayed variable behaviors, with higher filler concentrations often leading to reduced stress and strain at break. Rosemary-based composites exhibited the lowest stress and strain values, with increasing filler concentrations further diminishing tensile



performance. These changes were primarily influenced by filler content and distribution rather than chemical structure and aligned with IR spectra findings. Notably, for wound dressing applications, the material's flexibility remains a critical attribute, and this property was maintained at satisfactory levels even after exposure to accelerated degradation conditions, which are more severe than typical conditions.

Although the primary objective of this work was to develop bioactive materials with antibacterial properties for use in wound dressings, a supplementary cell viability assay was conducted to ensure their safety. Thyme-based composites consistently meet or exceed the 70% cell viability threshold, with lower filler concentrations yielding optimal results due to beneficial compounds such as thymine and tannins. Sage-based composites initially show improved viability but fall short after 10 days, likely due to sage's antimicrobial and antiproliferative effects resulting from its phytochemical compounds, such as salvianolic acid and luteolin. High filler content in thyme-based composites reduces cell viability, possibly due to excessive bioactive compounds limiting cell proliferation, though values remain above the minimum required level.

This work does not address all aspects related to this type of application, such as the long-term effectiveness of the materials, the duration of their antibacterial activity, or their efficacy against fungal strains, which are also critical for wound infections. However, the various approaches and findings presented in this study could significantly contribute to future research on bioactive dressings.

## 7.2. Conclusions

Based on the analysis and observations from the results, it can be conclusively stated that the primary aim of this work – to evaluate and confirm the following proposed thesis – has been accomplished:

**“The introduction of specially prepared organic fillers, derived from selected parts of bioactive herbs, into polydimethylsiloxane significantly enhances its antibacterial activity while maintaining the necessary functional properties for external medical applications, such as dressings, i.e., mechanical and physicochemical properties, while at the same time ensuring long-term functionality and reliability in medical contexts.”**

Furthermore, the research conducted on polydimethylsiloxane-based biocomposites modified with herbal fillers for external medical applications with enhanced antibacterial properties allowed the following conclusions to be drawn:

1. The composition of herbal fillers influenced the crosslinking process of polydimethylsiloxane and thereby impacts both its antibacterial and physicochemical properties. Increased levels of fatty acids and terpenes led to greater disruption of the cross-linking process. Composition analysis revealed that the critical threshold for fatty acids and terpenes is approximately  $24\pm 2\%$  (Tables 5.5 – 5.7). Specifically, in rosemary, along with the overall content of fatty acids and terpenes, rosmadial and rosmanol played a particularly significant role in cross-linking.
2. The density of the fillers and their total polyphenolic content are closely associated with the method of filler modification. The highest values were achieved by extracts, while the lowest by unmodified herbs. This suggests that the modifications performed have a beneficial effect on both density and TPC values.
3. The developed technology for modifying fillers using alcohol and water vapor treatment effectively reduced the terpenes and fatty acids levels in both sage and rosemary. This reduction enhanced the physicochemical properties, such as tensile strength and hardness, but led to a decrease in antibacterial activity. For unmodified fillers, the log reduction of *S. aureus* was 4.4, whereas for modified

fillers, it was above 2. The *E. coli* strain was not included in this evaluation. Moreover, the use of herbal extracts at concentrations equivalent to the amount of the polyphenol in the raw powder forms diminished their antibacterial effectiveness.

4. The mechanical properties are influenced by the filler's geometry and its ability to be wetted by the matrix, as extensively described in the literature. Due to their regular shape (Figure 5.5), extract particles exhibited better wetting by the matrix compared to particles from herbal powders. However, as shown in Figure 5.6, their size significantly impacted the tested properties.
5. The density of the composites with modified herbs was slightly higher than that of extract-based materials (by approximately 3%). However, the tensile strength of the biocomposites decreased compared to PDMS by up to over 75%. Nevertheless, modified herb- and extract-based materials exhibited higher values compared to unmodified herbal composites. The hardness of the materials remained similar for both unmodified and modified herbs as well as extract composites. In the case of rosemary, ER2.5 and ER5 exhibited comparable or higher hardness than the reference.
6. The incorporation of herbal fillers did not alter the hydrophobic characteristics of PDMS, which helps in preventing bacterial adherence and biofilm formation. However, it affected abrasion resistance and rebound resilience, with higher filler content generally leading to decreased properties, as indicated by the reduction in crystallinity degree.
7. The impact of accelerated degradation in artificial plasma solution varied among the materials tested, with thyme-based biocomposites exhibiting the highest stress and strain at break, while rosemary-based composites showed the lowest. For thyme and sage biocomposites, an initial decrease in these characteristics was observed after two days of incubation, followed by an increase in values. However, composites with higher filler content exhibited a decreasing trend, indicating that high filler content accelerated material degradation, leading to a deterioration of mechanical properties. In contrast, rosemary biocomposites, particularly MR10, showed increasing characteristics, suggesting further cross-linking. Despite these changes, the mechanical properties of all composites remained satisfactory after seven days of incubation at elevated temperatures ( $70\pm 2$  °C).

8. Thyme-based composites demonstrated non-toxicity, achieving over 70% cell viability. When incorporated at a 2.5 wt.% filler concentration, the biocomposite provided enhanced beneficial health properties over an extended period (10 days). In contrast, all sage biocomposites exhibited insufficient cell viability. Additionally, all materials showed increasing cytotoxicity with higher filler content, indicating that elevated herb content negatively impacts cell proliferation.
9. The methods used for preparing the fillers and incorporating them into the matrix, including sedimentation of fillers and formation of agglomerates, as seen in Figures 6.22 – 6.24, filler hardness and particle size, phytochemical composition, and the specific characteristics of the herbal plants, particularly their leaves, all played significant roles in shaping the properties, influencing test results, and contributing to variability.

### 7.3. Future research directions

The results of this work offer valuable insights into the development of polydimethylsiloxane-based biocomposites modified with selected herbal additives. The framework used allowed for the assessment of the impact of fillers on various physicochemical, mechanical, and biological properties. The primary goal of creating antibacterial materials for external applications was achieved. However, these materials may prove inadequate for internal applications requiring high stiffness and durability.

Future research will focus on enhancing these characteristics. Specifically, one approach will involve using lower concentrations of fillers. Preliminary findings suggest that sage and thyme exhibit higher antibacterial properties at lower concentrations, which decrease as filler content increases. Thus, exploring lower concentrations may yield materials with comparable or improved antibacterial activity while enhancing mechanical properties, given that higher filler concentrations generally reduce mechanical performance. Additionally, it is crucial to refine the method of incorporating fillers into the matrix, e.g., by using ultrasound. Improved dispersion of particles and the reduction or elimination of agglomerates will be essential for enhancing mechanical properties.

Another avenue for future research is to incorporate higher quantities of polyphenolic extracts, which may better leverage their substantial antibacterial potential. Additionally, the research could involve testing the materials as coatings, conducting clinical trials, and modifying the materials to exhibit antibacterial activity against Gram-negative bacteria.

## 8. References

- [1] Todros, S., Todesco, M., & Bagno, A. (2021). Biomaterials and Their Biomedical Applications: From Replacement to Regeneration. *Processes*, 9(11), 1949. <https://doi.org/10.3390/pr9111949>.
- [2] Rahimi, A., & Mashak, A. (2013). Review on Rubbers in Medicine: Natural, Silicone and Polyurethane Rubbers. *Plastics, Rubber and Composites*, 42(6), 223–230. <https://doi.org/10.1179/1743289811y.0000000063>.
- [3] Duran, M. M., Moro, G., Zhang, Y., & Islam, A. (2023). 3D Printing of Silicone and Polyurethane Elastomers for Medical Device Application: A Review. *Advances in Industrial and Manufacturing Engineering*, 7, 100125. <https://doi.org/10.1016/j.aime.2023.100125>.
- [4] Parameswaranpillai, J., Midhun Dominic, C. D., Mavinkere Rangappa, S., Siengchin, S., & Ozbakkaloglu, T. (2022). Introduction to Elastomers. In *Elastomer Blends and Composites*, Elsevier, 1–9. <https://doi.org/10.1016/b978-0-323-85832-8.00002-x>.
- [5] Guerra, N. B., Sant’Ana Pegorin, G., Boratto, M. H., De Barros, N. R., De Oliveira Graeff, C. F., & Herculano, R. D. (2021). Biomedical Applications of Natural Rubber Latex from the Rubber Tree *Hevea Brasiliensis*. *Materials Science and Engineering: C*, 126, 112126. <https://doi.org/10.1016/j.msec.2021.112126>.
- [6] Cherian, S., Ryu, S. B., & Cornish, K. (2019). Natural Rubber Biosynthesis in Plants, the Rubber Transferase Complex, and Metabolic Engineering Progress and Prospects. *Plant Biotechnology Journal*, 17(11), 2041–2061. <https://doi.org/10.1111/pbi.13181>.
- [7] Wei, X., Peng, P., Peng, F., & Dong, J. (2021). Natural Polymer *Eucommia Ulmoides* Rubber: A Novel Material. *Journal of Agricultural and Food Chemistry*, 69(13), 3797–3821. <https://doi.org/10.1021/acs.jafc.0c07560>.
- [8] Bîrcă, A., Gherasim, O., Grumezescu, V., & Grumezescu, A. M. (2019). Introduction in Thermoplastic and Thermosetting Polymers. In *Materials for Biomedical Engineering*, Elsevier, 1–28. <https://doi.org/10.1016/b978-0-12-816874-5.00001-3>.

- [9] Basak, S. (2021). Thermoplastic Elastomers in Biomedical Industry – Evolution and Current Trends. *Journal Of Macromolecular Science, Part A*, 58(9), 579–593. <https://doi.org/10.1080/10601325.2021.1922086>.
- [10] Holden, G. (2024). Thermoplastic Elastomers. In *Applied Plastics Engineering Handbook*, Elsevier, 97–113. <https://doi.org/10.1016/b978-0-323-88667-3.00020-5>.
- [11] Luo, J., Demchuk, Z., Zhao, X., Saito, T., Tian, M., Sokolov, A. P., & Cao, P.-F. (2022). Elastic Vitrimers: Beyond Thermoplastic and Thermoset Elastomers. *Matter*, 5(5), 1391–1422. <https://doi.org/10.1016/j.matt.2022.04.007>.
- [12] Ye, H., Zhang, K., Kai, D., Li, Z., & Loh, X. J. (2018). Polyester Elastomers for Soft Tissue Engineering. *Chemical Society Reviews*, 47(12), 4545–4580. <https://doi.org/10.1039/c8cs00161h>.
- [13] Siehr, A., Flory, C., Callaway, T., Schumacher, R. J., Siegel, R. A., & Shen, W. (2021). Implantable and Degradable Thermoplastic Elastomer. *ACS Biomaterials Science & Engineering*, 7(12), 5598–5610. <https://doi.org/10.1021/acsbiomaterials.1c01123>.
- [14] Wu, Y., Liu, C., Lapiere, M., Ciatti, J. L., Yang, D. S., Berkovich, J., Model, J. B., Banks, A., Ghaffari, R., Chang, J., Nuzzo, R. G., & Rogers, J. A. (2023). Thermoplastic Elastomers for Wireless, Skin-Interfaced Electronic, And Microfluidic Devices. *Advanced Materials Technologies*, 8(19). <https://doi.org/10.1002/admt.202300732>.
- [15] Sivaslioglu, A. A., Sun, X., Hodgson, R., & Riccetto, C. (2024). Wide-Bore Polyester Sutures May Create Sufficient Collagen for Cure of Prolapse/Incontinence: A Work In Progress. *Annals of Translational Medicine*, 12(2), 36–36. <https://doi.org/10.21037/atm-23-1774>.
- [16] Koutsamanis, I., Paudel, A., Alva Zúñiga, C. P., Wiltschko, L., & Spoerk, M. (2021). Novel Polyester-Based Thermoplastic Elastomers for 3D-Printed Long-Acting Drug Delivery Applications. *Journal of Controlled Release*, 335, 290–305. <https://doi.org/10.1016/j.jconrel.2021.05.030>.
- [17] Rezvova, M. A., Klyshnikov, K. Y., Gritskevich, A. A., & Ovcharenko, E. A. (2023). Polymeric Heart Valves Will Displace Mechanical and Tissue Heart Valves: A New Era for the Medical Devices. *International Journal of Molecular Sciences*, 24(4), 3963. <https://doi.org/10.3390/ijms24043963>.

- [18] Shin, E. J., & Choi, S. M. (2018). Advances in Waterborne Polyurethane-Based Biomaterials for Biomedical Applications, 251–283. [https://doi.org/10.1007/978-981-13-0947-2\\_14](https://doi.org/10.1007/978-981-13-0947-2_14).
- [19] Gorbunova, M. A., Shukhardin, D. M., Lesnichaya, V. A., Badamshina, E. R., & Anokhin, D. V. (2019). New Polyurethane Urea Thermoplastic Elastomers with Controlled Mechanical and Thermal Properties for Medical Applications. *Key Engineering Materials*, 816, 187–191. <https://doi.org/10.4028/www.scientific.net/kem.816.187>.
- [20] Jiang, C., Zhang, L., Yang, Q., Huang, S., Shi, H., Long, Q., Qian, B., Liu, Z., Guan, Q., Liu, M., Yang, R., Zhao, Q., You, Z., & Ye, X. (2021). Self-Healing Polyurethane-Elastomer with Mechanical Tunability for Multiple Biomedical Applications in Vivo. *Nature Communications*, 12(1), 4395. <https://doi.org/10.1038/s41467-021-24680-x>.
- [21] Guo, X., Liang, J., Wang, Z., Qin, J., Zhang, Q., Zhu, S., Zhang, K., & Zhu, H. (2023). Tough, Recyclable, and Degradable Elastomers for Potential Biomedical Applications. *Advanced Materials*, 35(20). <https://doi.org/10.1002/adma.202210092>.
- [22] Norman, T., Guenther, J., Asante, I., & Adler, B. L. (2024). Analysis of Contact Allergens in Polyvinyl Chloride Examination Gloves in the United States. *Dermatitis®*, 35(2), 160–166. <https://doi.org/10.1089/derm.2023.0150>,
- [23] Ovcharenko, E., Rezvova, M., Nikishau, P., Kostjuk, S., Glushkova, T., Antonova, L., Trebushat, D., Akentieva, T., Shishkova, D., Krivikina, E., Klyshnikov, K., Kudryavtseva, Y., & Barbarash, L. (2019). Polyisobutylene-Based Thermoplastic Elastomers for Manufacturing Polymeric Heart Valve Leaflets: In Vitro And In Vivo Results. *Applied Sciences*, 9(22), 4773. <https://doi.org/10.3390/app9224773>.
- [24] Mark, J. E. (2017). Thermoset Elastomers. In *Applied Plastics Engineering Handbook*, Elsevier, 109–125. <https://doi.org/10.1016/b978-0-323-39040-8.00006-7>.
- [25] Mojsiewicz-Pieńkowska, K., Jamrógiewicz, M., Szymkowska, K., & Krenczkowska, D. (2016). Direct Human Contact With Siloxanes (Silicones) – Safety Or Risk Part 1. Characteristics of Siloxanes (Silicones). *Frontiers in Pharmacology*, 7. <https://doi.org/10.3389/fphar.2016.00132>.



- [26] González Calderón, J. A., Contreras López, D., Pérez, E., & Vallejo Montesinos, J. (2020). Polysiloxanes as Polymer Matrices in Biomedical Engineering: Their Interesting Properties as the Reason for the Use in Medical Sciences. *Polymer Bulletin*, 77(5), 2749–2817. <https://doi.org/10.1007/s00289-019-02869-x>.
- [27] Colas, A., & Curtis, J. (2013). Silicones. In *Handbook of Polymer Applications in Medicine and Medical Devices*, Elsevier, 131–143. <https://doi.org/10.1016/b978-0-323-22805-3.00007-4>.
- [28] Blanco, I. (2018). Polysiloxanes in Theranostics and Drug Delivery: A Review. *Polymers*, 10(7), 755. <https://doi.org/10.3390/polym10070755>.
- [29] Riehle, N., Thude, S., Kandelbauer, A., Tovar, G. E. M., & Lorenz, G. (2019). Synthesis of Soft Polysiloxane-Urea Elastomers for Intraocular Lens Application. *Journal of Visualized Experiments*, 145. <https://doi.org/10.3791/58590>.
- [30] Lorenz, G., & Kandelbauer, A. (2014). Silicones. In *Handbook of Thermoset Plastics*, Elsevier, 555–575. <https://doi.org/10.1016/b978-1-4557-3107-7.00014-2>.
- [31] Bai, L., Yan, H., Bai, T., Feng, Y., Zhao, Y., Ji, Y., Feng, W., Lu, T., & Nie, Y. (2019). High Fluorescent Hyperbranched Polysiloxane Containing B-Cyclodextrin for Cell Imaging and Drug Delivery. *Biomacromolecules*, 20(11), 4230–4240. <https://doi.org/10.1021/acs.biomac.9b01217>.
- [32] Barman, A., Rashid, F., Farook, T. H., Jamayet, N. Bin, Dudley, J., Yhaya, M. F. Bin, & Alam, M. K. (2020). The Influence of Filler Particles on the Mechanical Properties of Maxillofacial Prosthetic Silicone Elastomers: A Systematic Review and Meta-Analysis. *Polymers*, 12(7), 1536. <https://doi.org/10.3390/polym12071536>.
- [33] Kurella, K. S., Thiyaneswaran, N., & Abhinav, R. P. (2020). Comparison of Accuracy/Dimensional Stability of High-Rigid Vinyl Polysiloxane, Polyvinyl Siloxane, and Polyether Impression Materials in Full Arch Implant-Supported Prosthesis: In Vitro Study. *Journal of Long-Term Effects of Medical Implants*, 30(3), 179–186. <https://doi.org/10.1615/jlongtermeffmedimplants.2020036008>.
- [34] Li, P., Zhang, A., & Zhou, S. (2020). One-Component Waterborne In Vivo Cross-Linkable Polysiloxane Coatings for Artificial Skin. *Journal of Biomedical Materials Research Part B: Applied Biomaterials*, 108(4), 1725–1737. <https://doi.org/10.1002/jbm.b.34517>.

- [35] Xia, S., Chen, Y., Fu, W., Tian, J., Zhou, Y., Sun, Y., Cao, R., Zou, H., & Liang, M. (2022). A Humidity-Resistant Bio-Inspired Microfibrillar Adhesive Fabricated Using A Phenyl-Rich Polysiloxane Elastomer For Reliable Skin Patches. *Journal of Materials Chemistry B*, 10(44), 9179–9187. <https://doi.org/10.1039/d2tb01955h>.
- [36] Cozma, V., Rosca, I., Radulescu, L., Martu, C., Nastasa, V., Varganici, C.-D., Ursu, E.-L., Doroftei, F., Pinteala, M., & Racles, C. (2021). Antibacterial Polysiloxane Polymers and Coatings for Cochlear Implants. *Molecules*, 26(16), 4892. <https://doi.org/10.3390/molecules26164892>.
- [37] Francis, A., Detsch, R., & Boccaccini, A. R. (2016). Fabrication and Cytotoxicity Assessment of Novel Polysiloxane/Bioactive Glass Films for Biomedical Applications. *Ceramics International*, 42(14), 15442–15448. <https://doi.org/10.1016/j.ceramint.2016.06.195>.
- [38] Jenney, C., Millson, P., Grainger, D. W., Grubbs, R., Gunatillake, P., Mccarthy, S. J., Runt, J., & Beith, J. (2021). Assessment Of A Siloxane Poly(Urethane-Urea) Elastomer Designed for Implantable Heart Valve Leaflets. *Advanced Nanobiomed Research*, 1(2). <https://doi.org/10.1002/anbr.202000032>.
- [39] Wolf, M. P., Salieb-Beugelaar, G. B., & Hunziker, P. (2018). PDMS with Designer Functionalities—Properties, Modifications Strategies, and Applications. *Progress in Polymer Science*, 83, 97–134. <https://doi.org/10.1016/j.progpolymsci.2018.06.001>.
- [40] Ariati, R., Sales, F., Souza, A., Lima, R. A., & Ribeiro, J. (2021). Polydimethylsiloxane Composites Characterization and Its Applications: A Review. *Polymers*, 13(23), 4258. <https://doi.org/10.3390/polym13234258>.
- [41] Ramli, M. R., Othman, M. B. H., Arifin, A., & Ahmad, Z. (2011). Cross-Link Network of Polydimethylsiloxane via Addition and Condensation (RTV) Mechanisms. Part I: Synthesis and Thermal Properties. *Polymer Degradation and Stability*, 96(12), 2064–2070. <https://doi.org/10.1016/j.polymdegradstab.2011.10.001>.
- [42] An, A. K., Guo, J., Lee, E.-J., Jeong, S., Zhao, Y., Wang, Z., & Leiknes, T. (2017). PDMS/PVDF Hybrid Electrospun Membrane with Superhydrophobic Property and Drop Impact Dynamics for Dyeing Wastewater Treatment Using Membrane Distillation. *Journal of Membrane Science*, 525, 57–67. <https://doi.org/10.1016/j.memsci.2016.10.028>.

- [43] Shi, Y., Hu, M., Xing, Y., & Li, Y. (2020). Temperature-Dependent Thermal and Mechanical Properties of Flexible Functional PDMS/Paraffin Composites. *Materials & Design*, 185, 108219. <https://doi.org/10.1016/j.matdes.2019.108219>.
- [44] Dalla Monta, A., Razan, F., Le Cam, J.-B., & Chagnon, G. (2018). Using Thickness-Shear Mode Quartz Resonator for Characterizing the Viscoelastic Properties Of PDMS During Cross-Linking, from the Liquid to the Solid State and at Different Temperatures. *Sensors and Actuators A: Physical*, 280, 107–113. <https://doi.org/10.1016/j.sna.2018.07.003>.
- [45] Yi, D., Huo, Z., Geng, Y., Li, X., & Hong, X. (2020). PDMS-Coated No-Core Fiber Interferometer with Enhanced Sensitivity for Temperature Monitoring Applications. *Optical Fiber Technology*, 57, 102185. <https://doi.org/10.1016/j.yofte.2020.102185>.
- [46] Victor, A., Ribeiro, J., & F. Araújo, F. (2019). Study of PDMS Characterization and Its Applications in Biomedicine: A Review. *Journal of Mechanical Engineering and Biomechanics*, 4(1), 1–9. <https://doi.org/10.24243/jmeb/4.1.163>.
- [47] Sun, W.-J., Kothari, S., & Sun, C. C. (2018). The Relationship among Tensile Strength, Young's Modulus, and Indentation Hardness of Pharmaceutical Compacts. *Powder Technology*, 331, 1–6. <https://doi.org/10.1016/j.powtec.2018.02.051>.
- [48] Zhang, G., Sun, Y., Qian, B., Gao, H., & Zuo, D. (2020). Experimental Study on Mechanical Performance of Polydimethylsiloxane (PDMS) At Various Temperatures. *Polymer Testing*, 90, 106670. <https://doi.org/10.1016/j.polymertesting.2020.106670>.
- [49] Mojsiewicz-Pieńkowska, K. (2015). Review of Current Pharmaceutical Applications of Polysiloxanes (Silicones). In *Handbook of Polymers for Pharmaceutical Technologies*, Wiley, 363–381. <https://doi.org/10.1002/9781119041412.ch13>.
- [50] Kim, S., Ye, S., Adamo, A., Orizondo, R. A., Jo, J., Cho, S. K., & Wagner, W. R. (2020). A Biostable, Anti-Fouling Zwitterionic Polyurethane-Urea Based on PDMS for Use in Blood-Contacting Medical Devices. *Journal of Materials Chemistry B*, 8(36), 8305–8314. <https://doi.org/10.1039/d0tb01220c>.

- [51] Dabaghi, M., Rochow, N., Saraei, N., Mahendran, R. K., Fusch, G., Chan, A. K. C., Brash, J. L., Fusch, C., & Selvaganapathy, P. R. (2020). Miniaturization of Artificial Lungs Toward Portability. *Advanced Materials Technologies*, 5(7). <https://doi.org/10.1002/admt.202000136>.
- [52] Khan, R. H. (2022). A Brief Review on Contact Lens, Complications and Improvements in Their Prolong Wear. 20, 505–522. <https://doi.org/10.14704/nq.2022.20.8.nq44058>.
- [53] Roostaei, N., & Hamidi, S. M. (2022). Two-Dimensional Biocompatible Plasmonic Contact Lenses for Color Blindness Correction. *Scientific Reports*, 12(1), 2037. <https://doi.org/10.1038/s41598-022-06089-8>.
- [54] Zhang, J., Kim, K., Kim, H. J., Meyer, D., Park, W., Lee, S. A., Dai, Y., Kim, B., Moon, H., Shah, J. V., Harris, K. E., Collar, B., Liu, K., Irazoqui, P., Lee, H., Park, S. A., Kollbaum, P. S., Boudouris, B. W., & Lee, C. H. (2022). Smart Soft Contact Lenses for Continuous 24-Hour Monitoring of Intraocular Pressure in Glaucoma Care. *Nature Communications*, 13(1), 5518. <https://doi.org/10.1038/s41467-022-33254-4>.
- [55] Paranjape, M., Garra, J., Brida, S., Schneider, T., White, R., & Currie, J. (2003). A PDMS Dermal Patch for Non-Intrusive Transdermal Glucose Sensing. *Sensors and Actuators A: Physical*, 104(3), 195–204. [https://doi.org/10.1016/s0924-4247\(03\)00049-9](https://doi.org/10.1016/s0924-4247(03)00049-9).
- [56] Bae, J., Hwang, Y., Park, S. J., Ha, J.-H., Kim, H. J., Jang, A., An, J., Lee, C.-S., & Park, S.-H. (2018). Study on the Sensing Signal Profiles for Determination Of Process Window of Flexible Sensors Based on Surface Treated PDMS/CNT Composite Patches. *Polymers*, 10(9), 951. <https://doi.org/10.3390/polym10090951>.
- [57] Mikolaszek, B., Kazlauske, J., Larsson, A., & Sznitowska, M. (2020). Controlled Drug Release by the Pore Structure in Polydimethylsiloxane Transdermal Patches. *Polymers*, 12(7), 1520. <https://doi.org/10.3390/polym12071520>.
- [58] Huang, J., & Huang, D. (2022). Graphene-Enhanced Polydimethylsiloxane Patch for Wearable Body Temperature Remote Monitoring Application. *Sensors*, 22(23), 9426. <https://doi.org/10.3390/s22239426>.

- [59] Nag, A., Feng, S., Mukhopadhyay, S. C., Kosel, J., & Inglis, D. (2018). 3D Printed Mould-Based Graphite/PDMS Sensor for Low-Force Applications. *Sensors and Actuators A: Physical*, 280, 525–534. <https://doi.org/10.1016/j.sna.2018.08.028>.
- [60] De Martino, A., Milano, A. D., Barbera, M. Della, Thiene, G., & Bortolotti, U. (2022). The Caged-Ball Prosthesis 60 Years Later: A Historical Review of a Cardiac Surgery Milestone. *Texas Heart Institute Journal*, 49(2). <https://doi.org/10.14503/thij-20-7267>.
- [61] Rozeik, M., Wheatley, D., & Gourlay, T. (2014). The Aortic Valve: Structure, Complications and Implications for Transcatheter Aortic Valve Replacement. *Perfusion*, 29(4), 285–300. <https://doi.org/10.1177/0267659114521650>.
- [62] Coulter, F. B., Schaffner, M., Faber, J. A., Rafsanjani, A., Smith, R., Appa, H., Zilla, P., Bezuidenhout, D., & Studart, A. R. (2019). Bioinspired Heart Valve Prosthesis Made by Silicone Additive Manufacturing. *Matter*, 1(1), 266–279. <https://doi.org/10.1016/j.matt.2019.05.013>.
- [63] Maaz Arif, M., Khan, S. M., Gull, N., Tabish, T. A., Zia, S., Ullah Khan, R., Awais, S. M., & Arif Butt, M. (2021). Polymer-Based Biomaterials for Chronic Wound Management: Promises and Challenges. *International Journal of Pharmaceutics*, 598, 120270. <https://doi.org/10.1016/j.ijpharm.2021.120270>.
- [64] Landén, N. X., Li, D., & Ståhle, M. (2016). Transition from Inflammation to Proliferation: A Critical Step During Wound Healing. *Cellular and Molecular Life Sciences*, 73(20), 3861–3885. <https://doi.org/10.1007/S00018-016-2268-0>.
- [65] Tottoli, E. M., Dorati, R., Genta, I., Chiesa, E., Pisani, S., & Conti, B. (2020). Skin Wound Healing Process and New Emerging Technologies for Skin Wound Care and Regeneration. *Pharmaceutics*, 12(8), 735. <https://doi.org/10.3390/pharmaceutics12080735>.
- [66] Singh, S., Young, A., & Mcnaught, C.-E. (2017). The Physiology of Wound Healing. *Surgery (Oxford)*, 35(9), 473–477. <https://doi.org/10.1016/j.mpsur.2017.06.004>.
- [67] Moreira, H. R., & Marques, A. P. (2022). Vascularization in Skin Wound Healing: Where Do We Stand And Where Do We Go? *Current Opinion in Biotechnology*, 73, 253–262. <https://doi.org/10.1016/j.copbio.2021.08.019>.
- [68] Mathew-Steiner, S. S., Roy, S., & Sen, C. K. (2021). Collagen in Wound Healing. *Bioengineering*, 8(5), 63. <https://doi.org/10.3390/bioengineering8050063>.

- [69] Rodrigues, M., Kosaric, N., Bonham, C. A., & Gurtner, G. C. (2019). Wound Healing: A Cellular Perspective. *Physiological Reviews*, 99(1), 665–706. <https://doi.org/10.1152/physrev.00067.2017>.
- [70] Gemeinder, J. L. P., Barros, N. R. De, Pegorin, G. S., Singulani, J. De L., Borges, F. A., Arco, M. C. G. Del, Giannini, M. J. S. M., Almeida, A. M. F., Salvador, S. L. De S., & Herculano, R. D. (2021). Gentamicin Encapsulated Within a Biopolymer for the Treatment of Staphylococcus Aureus And Escherichia Coli Infected Skin Ulcers. *Journal of Biomaterials Science, Polymer Edition*, 32(1), 93–111. <https://doi.org/10.1080/09205063.2020.1817667>.
- [71] Nobel, F. A., Islam, S., Babu, G., Akter, S., Jebin, R. A., Sarker, T. C., Islam, A., & Islam, M. J. (2022). Isolation of Multidrug Resistance Bacteria from the Patients with Wound Infection and Their Antibiotics Susceptibility Patterns: A Cross-Sectional Study. *Annals of Medicine & Surgery*, 84. <https://doi.org/10.1016/j.amsu.2022.104895>.
- [72] Puca, V., Marulli, R. Z., Grande, R., Vitale, I., Niro, A., Molinaro, G., Prezioso, S., Muraro, R., & Di Giovanni, P. (2021). Microbial Species Isolated From Infected Wounds and Antimicrobial Resistance Analysis: Data Emerging From a Three-Years Retrospective Study. *Antibiotics*, 10(10), 1162. <https://doi.org/10.3390/antibiotics10101162>.
- [73] Li, S., Renick, P., Senkowsky, J., Nair, A., & Tang, L. (2021). Diagnostics for Wound Infections. *Advances in Wound Care*, 10(6), 317–327. <https://doi.org/10.1089/wound.2019.1103>.
- [74] Siddiqui, A. R., & Bernstein, J. M. (2010). Chronic Wound Infection: Facts and Controversies. *Clinics in Dermatology*, 28(5), 519–526. <https://doi.org/10.1016/j.clindermatol.2010.03.009>.
- [75] Aderibigbe, B., & Buyana, B. (2018). Alginate in Wound Dressings. *Pharmaceutics*, 10(2), 42. <https://doi.org/10.3390/pharmaceutics10020042>.
- [76] Tabriz, A. G., & Douroumis, D. (2022). Recent Advances in 3D Printing for Wound Healing: A Systematic Review. *Journal of Drug Delivery Science and Technology*, 74, 103564. <https://doi.org/10.1016/j.jddst.2022.103564>.

- [77] Duan, W., Wang, H., Wang, Z., Ren, Z., Li, X., He, F., Li, S., Guan, Y., Liu, F., Chen, L., Yan, P., & Hou, X. (2024). Multi-Functional Composite Dressings with Sustained Release of MSC-SLP and Anti-Adhesion Property for Accelerating Wound Healing. *Materials Today Bio*, 25, 100979. <https://doi.org/10.1016/j.mtbio.2024.100979>.
- [78] Varshney, N., Sahi, A. K., Vajanthri, K. Y., Poddar, S., Balavigneswaran, C. K., Prabhakar, A., Rao, V., & Mahto, S. K. (2019). Culturing Melanocytes and Fibroblasts Within Three-Dimensional Macroporous PDMS Scaffolds: Towards Skin Dressing Material. *Cytotechnology*, 71(1), 287–303. <https://doi.org/10.1007/s10616-018-0285-6>.
- [79] Li, M., Wang, H., Chen, X., Jin, S., Chen, W., Meng, Y., Liu, Y., Guo, Y., Jiang, W., Xu, X., & Wang, B. (2020). Chemical Grafting of Antibiotics into Multilayer Films through Schiff Base Reaction for Self-Defensive Response to Bacterial Infections. *Chemical Engineering Journal*, 382, 122973. <https://doi.org/10.1016/j.cej.2019.122973>.
- [80] Montemezzo, M., Ferrari, M. D., Kerstner, E., Santos, V. Dos, Victorazzi Lain, V., Wollheim, C., Frozza, C. O. Da S., Roesch-Ely, M., Baldo, G., & Brandalise, R. N. (2021). PHMB-Loaded PDMS and Its Antimicrobial Properties for Biomedical Applications. *Journal of Biomaterials Applications*, 36(2), 252–263. <https://doi.org/10.1177/08853282211011921>.
- [81] Cambiaso-Daniel, J., Boukovalas, S., Bitz, G. H., Branski, L. K., Herndon, D. N., & Culnan, D. M. (2018). Topical Antimicrobials in Burn Care. *Annals of Plastic Surgery*, Publish Ah. <https://doi.org/10.1097/sap.0000000000001297>.
- [82] Qian, W., Hu, X., He, W., Zhan, R., Liu, M., Zhou, D., Huang, Y., Hu, X., Wang, Z., Fei, G., Wu, J., Xing, M., Xia, H., & Luo, G. (2018). Polydimethylsiloxane Incorporated With Reduced Graphene Oxide (RGO) Sheets For Wound Dressing Application: Preparation And Characterization. *Colloids and Surfaces B: Biointerfaces*, 166, 61–71. <https://doi.org/10.1016/j.colsurfb.2018.03.008>.
- [83] Hu, X., Qian, W., Li, X., Fei, G., Luo, G., Wang, Z., & Xia, H. (2019). A Novel Method to Prepare Homogeneous Biocompatible Graphene-Based PDMS Composites with Enhanced Mechanical, Thermal and Antibacterial Properties. *Polymer Composites*, 40(S2). <https://doi.org/10.1002/pc.25019>.

- [84] Wang, H., Duan, W., Ren, Z., Li, X., Ma, W., Guan, Y., Liu, F., Chen, L., Yan, P., & Hou, X. (2023). Engineered Sandwich-Structured Composite Wound Dressings with Unidirectional Drainage and Anti-Adhesion Supporting Accelerated Wound Healing. *Advanced Healthcare Materials*, 12(8). <https://doi.org/10.1002/adhm.202202685>.
- [85] Li, F., Han, X., Cao, D., Yin, J., Chen, L., Li, D., Cui, L., Liu, Z., & Guo, X. (2023). Heat Preservation, Antifouling, Hemostatic and Antibacterial Aerogel Wound Dressings for Emergency Treatment. *Frontiers of Materials Science*, 17(2), 230641. <https://doi.org/10.1007/s11706-023-0641-0>.
- [86] Kou, S. (Gabriel), Peters, L. M., & Mucalo, M. R. (2021). Chitosan: A Review of Sources and Preparation Methods. *International Journal of Biological Macromolecules*, 169, 85–94. <https://doi.org/10.1016/j.ijbiomac.2020.12.005>.
- [87] Huang, H., Liao, D., Zou, Y., & Chi, H. (2020). The Effects of Chitosan Supplementation on Body Weight and Body Composition: A Systematic Review and Meta-Analysis of Randomized Controlled Trials. *Critical Reviews in Food Science and Nutrition*, 60(11), 1815–1825. <https://doi.org/10.1080/10408398.2019.1602822>.
- [88] Wang, W., Xue, C., & Mao, X. (2020). Chitosan: Structural Modification, Biological Activity and Application. *International Journal of Biological Macromolecules*, 164, 4532–4546. <https://doi.org/10.1016/j.ijbiomac.2020.09.042>.
- [89] Kou, S. (Gabriel), Peters, L., & Mucalo, M. (2022). Chitosan: A Review of Molecular Structure, Bioactivities and Interactions with the Human Body and Micro-Organisms. *Carbohydrate Polymers*, 282, 119132. <https://doi.org/10.1016/j.carbpol.2022.119132>.
- [90] Tanaka, C. B., Lopes, D. P., Kikuchi, L. N. T., Moreira, M. S., Catalani, L. H., Braga, R. R., Kruzic, J. J., & Gonçalves, F. (2020). Development of Novel Dental Restorative Composites with Dibasic Calcium Phosphate Loaded Chitosan Fillers. *Dental Materials*, 36(4), 551–559. <https://doi.org/10.1016/j.dental.2020.02.004>.
- [91] Felician, F. F., Xia, C., Qi, W., & Xu, H. (2018). Collagen from Marine Biological Sources and Medical Applications. *Chemistry & Biodiversity*, 15(5). <https://doi.org/10.1002/cbdv.201700557>.



- [92] Rezvani Ghomi, E., Nourbakhsh, N., Akbari Kenari, M., Zare, M., & Ramakrishna, S. (2021). Collagen-Based Biomaterials for Biomedical Applications. *Journal of Biomedical Materials Research Part B: Applied Biomaterials*, 109(12), 1986–1999. <https://doi.org/10.1002/jbm.b.34881>.
- [93] Mcgrath, M., Zimkowska, K., Genoud, K. J., Maughan, J., Gutierrez Gonzalez, J., Browne, S., & O'Brien, F. J. (2023). A Biomimetic, Bilayered Antimicrobial Collagen-Based Scaffold for Enhanced Healing of Complex Wound Conditions. *ACS Applied Materials & Interfaces*, 15(14), 17444–17458. <https://doi.org/10.1021/acsami.2c18837>.
- [94] Della Sala, F., Longobardo, G., Fabozzi, A., Di Gennaro, M., & Borzacchiello, A. (2022). Hyaluronic Acid-Based Wound Dressing with Antimicrobial Properties for Wound Healing Application. *Applied Sciences*, 12(6), 3091. <https://doi.org/10.3390/app12063091>.
- [95] Falbo, F., Spizzirri, U. G., Restuccia, D., & Aiello, F. (2023). Natural Compounds and Biopolymers-Based Hydrogels Join Forces to Promote Wound Healing. *Pharmaceutics*, 15(1), 271. <https://doi.org/10.3390/pharmaceutics15010271>.
- [96] Zamboni, F., Wong, C. K., & Collins, M. N. (2023). Hyaluronic Acid Association With Bacterial, Fungal and Viral Infections: Can Hyaluronic Acid Be Used as An Antimicrobial Polymer for Biomedical and Pharmaceutical Applications? *Bioactive Materials*, 19, 458–473. <https://doi.org/10.1016/j.bioactmat.2022.04.023>.
- [97] Zhang, Z., Suner, S. S., Blake, D. A., Ayyala, R. S., & Sahiner, N. (2020). Antimicrobial Activity and Biocompatibility of Slow-Release Hyaluronic Acid-Antibiotic Conjugated Particles. *International Journal of Pharmaceutics*, 576, 119024. <https://doi.org/10.1016/j.ijpharm.2020.119024>.
- [98] Michalska-Sionkowska, M., Kaczmarek, B., Walczak, M., & Sionkowska, A. (2018). Antimicrobial Activity of New Materials Based on the Blends of Collagen/Chitosan/Hyaluronic Acid with Gentamicin Sulfate Addition. *Materials Science and Engineering: C*, 86, 103–108. <https://doi.org/10.1016/j.msec.2018.01.005>.

- [99] Álvarez-Martínez, F. J., Barrajon-Catalán, E., Herranz-López, M., & Micol, V. (2021). Antibacterial Plant Compounds, Extracts and Essential Oils: An Updated Review on Their Effects and Putative Mechanisms of Action. *Phytomedicine*, 90, 153626. <https://doi.org/10.1016/j.phymed.2021.153626>.
- [100] Abbas, M., Saeed, F., Anjum, F. M., Afzaal, M., Tufail, T., Bashir, M. S., Ishtiaq, A., Hussain, S., & Suleria, H. A. R. (2017). Natural Polyphenols: An Overview. *International Journal of Food Properties*, 20(8), 1689–1699. <https://doi.org/10.1080/10942912.2016.1220393>.
- [101] Belščak-Cvitanović, A., Durgo, K., Huđek, A., Bačun-Družina, V., & Komes, D. (2018). Overview of Polyphenols and Their Properties. In *Polyphenols: Properties, Recovery, And Applications*, Elsevier, 3–44. <https://doi.org/10.1016/b978-0-12-813572-3.00001-4>.
- [102] Yang, W., Chen, X., Li, Y., Guo, S., Wang, Z., & Yu, X. (2020). Advances in Pharmacological Activities of Terpenoids. *Natural Product Communications*, 15(3), 1934578X2090355. <https://doi.org/10.1177/1934578x20903555>.
- [103] Zeng, T., Liu, Z., Liu, H., He, W., Tang, X., Xie, L., & Wu, R. (2019). Exploring Chemical and Biological Space of Terpenoids. *Journal of Chemical Information and Modeling*, 59(9), 3667–3678. <https://doi.org/10.1021/acs.jcim.9b00443>.
- [104] Abookleesh, F. L., Al-Anzi, B. S., & Ullah, A. (2022). Potential Antiviral Action of Alkaloids. *Molecules*, 27(3), 903. <https://doi.org/10.3390/molecules27030903>.
- [105] Gutiérrez-Grijalva, E. P., López-Martínez, L. X., Contreras-Angulo, L. A., Elizalde-Romero, C. A., & Heredia, J. B. (2020). Plant Alkaloids: Structures and Bioactive Properties. In *Plant-Derived Bioactives*, Springer Singapore, 85–117. [https://doi.org/10.1007/978-981-15-2361-8\\_5](https://doi.org/10.1007/978-981-15-2361-8_5).
- [106] Hamzat, T. A., Louis, H., & Apebende, G. (2019). A Review on Classes, Extraction, Purification and Pharmaceutical Importance of Plants Alkaloid. <https://doi.org/10.13140/rg.2.2.12867.96809>.
- [107] Taghouti, M., Martins-Gomes, C., Félix, L. M., Schäfer, J., Santos, J. A., Bunzel, M., Nunes, F. M., & Silva, A. M. (2020). Polyphenol Composition and Biological Activity of *Thymus Citriodorus* and *Thymus Vulgaris*: Comparison with Endemic Iberian *Thymus* Species. *Food Chemistry*, 331, 127362. <https://doi.org/10.1016/j.foodchem.2020.127362>.

- [108] Mancini, E., Senatore, F., Del Monte, D., De Martino, L., Grulova, D., Scognamiglio, M., Snoussi, M., & De Feo, V. (2015). Studies on Chemical Composition, Antimicrobial and Antioxidant Activities of Five *Thymus Vulgaris* L. Essential Oils. *Molecules*, 20(7), 12016–12028. <https://doi.org/10.3390/molecules200712016>.
- [109] Jabri-Karoui, I., Bettaieb, I., Msaada, K., Hammami, M., & Marzouk, B. (2012). Research on the Phenolic Compounds and Antioxidant Activities of Tunisian *Thymus Capitatus*. *Journal of Functional Foods*, 4(3), 661–669. <https://doi.org/10.1016/j.jff.2012.04.007>.
- [110] Sh, Sharafzadeh, M., Khosh-Khui, K., Javidnia, O., Alizadeh, O., & Ordoorkhani. (2010). Identification and Comparison of Essential Oil Components in Leaf and Stem of Garden Thyme Grown Under Greenhouse Conditions. *Advances in Environmental Biology*, 4, 520–523.
- [111] Jafari, B., Jafari-Sales, Abolfazl, Khaneshpour, Homeira, Fatemi, S., Pashazadeh, M., Al-Snafi, A. E., & Shariat, A. (2020). Antibacterial Effects of *Thymus Vulgaris*, *Mentha Pulegium*, *Crocus Sativus* and *Salvia Officinalis* on Pathogenic Bacteria: A Brief Review Study Based on Gram-Positive and Gram-Negative Bacteria. *Jorjani-Biomedicine-Journal*, 8(3), 58–74. <https://doi.org/10.52547/jorjanibiomedj.8.3.58>.
- [112] Vivcharenko, V., & Przekora, A. (2021). Modifications of Wound Dressings with Bioactive Agents to Achieve Improved Pro-Healing Properties. *Applied Sciences*, 11(9), 4114. <https://doi.org/10.3390/app11094114>.
- [113] Mohammed, R., Musa, F., Mehdi, B. Yasein, & Al-Rawe, A. (2020). Impacts of the Alcoholic Extract and Essential Oil of *Thymus Vulgaris* L. Against the Causative Agent Of Acne Formation (*Staphylococcus Aureus*). *Systematic Reviews in Pharmacy*, 11, 498. <https://doi.org/10.5530/srp.2020.2.75>.
- [114] Jakovljević, M., Jokić, S., Molnar, M., Jašić, M., Babić, J., Jukić, H., & Banjari, I. (2019). Bioactive Profile of Various *Salvia Officinalis* L. Preparations. *Plants*, 8(3), 55. <https://doi.org/10.3390/plants8030055>.
- [115] Ghorbani, A., & Esmaeilzadeh, M. (2017). Pharmacological Properties of *Salvia Officinalis* and Its Components. *Journal of Traditional and Complementary Medicine*, 7(4), 433–440. <https://doi.org/10.1016/j.jtcme.2016.12.014>.

- [116] Duletic-Lausevic, S., Alimpic-Aradski, A., Zivkovic, J., Gligorijevec, N., Savikin, K., Radulovic, S., Cocic, D., & Marin, P. (2019). Evaluation of Bioactivities and Phenolic Composition of Extracts of *Salvia Officinalis* L. (Lamiaceae) Collected in Montenegro. *Botanica Serbica*, 43(1), 47–58. <https://doi.org/10.2298/botserb1901047d>.
- [117] Jazo, Z., Glumac, M., Paštar, V., Bektić, S., Radan, M., & Carev, I. (2023). Chemical Composition and Biological Activity of *Salvia Officinalis* L. Essential Oil. *Plants*, 12(9), 1794. <https://doi.org/10.3390/plants12091794>.
- [118] Wojtunik-Kulesza, K. A. (2022). Toxicity of Selected Monoterpenes and Essential Oils Rich in These Compounds. *Molecules*, 27(5), 1716. <https://doi.org/10.3390/molecules27051716>.
- [119] Boufadi, M. Y., Keddari, S., Moulaiyacene, F., & Chaa, S. (2020). Chemical Composition, Antioxidant and Anti-Inflammatory Properties of *Salvia Officinalis* Extract from Algeria. *Pharmacognosy Journal*, 13(2), 506–515. <https://doi.org/10.5530/pj.2021.13.64>.
- [120] Sadowska, U., Kopeć, A., Kourimska, L., Zarubova, L., & Kloucek, P. (2017). The Effect of Drying Methods on the Concentration of Compounds in Sage and Thyme. *Journal of Food Processing and Preservation*, 41(6), E13286. <https://doi.org/10.1111/jfpp.13286>.
- [121] Choukairi, Z., Hazzaz, T., José, M. F., & Fechtali, T. (2021). The Cytotoxic Activity of *Salvia Officinalis* L. and *Rosmarinus Officinalis* L. Leaves Extracts on Human Glioblastoma Cell Line and Their Antioxidant Effect. *Journal of Complementary and Integrative Medicine*, 17(4). <https://doi.org/10.1515/jcim-2018-0189>.
- [122] Farahpour, M. R., Pirkhezr, E., Ashrafian, A., & Sonboli, A. (2020). Accelerated Healing by Topical Administration of *Salvia Officinalis* Essential Oil on *Pseudomonas Aeruginosa* and *Staphylococcus Aureus* Infected Wound Model. *Biomedicine & Pharmacotherapy*, 128, 110120. <https://doi.org/10.1016/j.biopha.2020.110120>.
- [123] Kontogianni, V. G., Tomic, G., Nikolic, I., Nerantzaki, A. A., Sayyad, N., Stosic-Grujicic, S., Stojanovic, I., Gerothanassis, I. P., & Tzakos, A. G. (2013). Phytochemical Profile of *Rosmarinus Officinalis* and *Salvia Officinalis* Extracts and Correlation to Their Antioxidant and Anti-Proliferative Activity. *Food Chemistry*, 136(1), 120–129. <https://doi.org/10.1016/j.foodchem.2012.07.091>.

- [124] De Macedo, L. M., Santos, É. M. Dos, Militão, L., Tundisi, L. L., Ataíde, J. A., Souto, E. B., & Mazzola, P. G. (2020). Rosemary (*Rosmarinus Officinalis* L., *Salvia Rosmarinus*) and Its Topical Applications: A Review. *Plants*, 9(5), 651. <https://doi.org/10.3390/plants9050651>.
- [125] Labib, R. M., Ayoub, I. M., Michel, H. E., Mehanny, M., Kamil, V., Hany, M., Magdy, M., Moataz, A., Maged, B., & Mohamed, A. (2019). Appraisal on the Wound Healing Potential of *Melaleuca Alternifolia* and *Rosmarinus Officinalis* L. Essential Oil-Loaded Chitosan Topical Preparations. *Plos One*, 14(9), E0219561. <https://doi.org/10.1371/journal.pone.0219561>.
- [126] Oualdi, I., Brahmi, F., Mokhtari, O., Abdellaoui, S., Tahani, A., & Oussaid, A. (2021). *Rosmarinus Officinalis* from Morocco, Italy and France: Insight into Chemical Compositions and Biological Properties. *Materials Today: Proceedings*, 45, 7706–7710. <https://doi.org/10.1016/j.matpr.2021.03.333>.
- [127] Jafari-Sales, A., & Pashazadeh, M. (2020). Study of Chemical Composition and Antimicrobial Properties of Rosemary (*Rosmarinus Officinalis*) Essential Oil on *Staphylococcus Aureus* and *Escherichia Coli* in Vitro. *International Journal of Life Sciences and Biotechnology*, 3(1), 62–69. <https://doi.org/10.38001/ijlsb.693371>.
- [128] Muhammad, A.-A., Suleman, L., & Salisu, A. (2019). Phytochemical Screening and Elemental Analysis of Crude Extract of *Mentha Piperita* (Peppermint) Leaves. *Chemistry Research Journal*, 4(4), 35–40.
- [129] Almatroodi, S. A., Alsahli, M. A., Almatroudi, A., Khan, A. A., & Rahmani, A. H. (2021). Peppermint, (*Mentha × Piperita*): Role in Management of Diseases Through Modulating Various Biological Activities. *Pharmacognosy Journal*, 13(3), 822–827. <https://doi.org/10.5530/pj.2021.13.104>.
- [130] Kürekci, C., & Beyazit, N. (2022). Chemical Composition and Antibacterial Activity of *Mentha Piperita* Var. *Citrata* Extracts Obtained by Different Extraction Solvents. *Gıda*, 47(3), 531–538. <https://doi.org/10.15237/gida.gd21156>.
- [131] Dorman, H. J. D., Koşar, M., Başer, K. H. C., & Hiltunen, R. (2009). Phenolic Profile and Antioxidant Evaluation of *Mentha X Piperita* L. (Peppermint) Extracts. *Natural Product Communications*, 4(4), 1934578X0900400. <https://doi.org/10.1177/1934578x0900400419>.

- [132] Camele, I., Gruľová, D., & Elshafie, H. S. (2021). Chemical Composition and Antimicrobial Properties of *Mentha* × *Piperita* Cv. 'Kristinka' Essential Oil. *Plants*, 10(8), 1567. <https://doi.org/10.3390/plants10081567>.
- [133] Chraibi, M., Fadil, M., Farah, A., Lebrazi, S., & Fikri-Benbrahim, K. (2021). Antimicrobial Combined Action of *Mentha Pulegium*, *Ormenis Mixta* and *Mentha Piperita* Essential Oils Against *S. Aureus*, *E. Coli* And *C. Tropicalis*: Application of Mixture Design Methodology. *LWT*, 145, 111352. <https://doi.org/10.1016/j.lwt.2021.111352>.
- [134] Silva, W. M. F., Bona, N. P., Pedra, N. S., Cunha, K. F. Da, Fiorentini, A. M., Stefanello, F. M., Zavareze, E. R., & Dias, A. R. G. (2022). Risk Assessment of in Vitro Cytotoxicity, Antioxidant and Antimicrobial Activities of *Mentha Piperita* L. Essential Oil. *Journal of Toxicology And Environmental Health, Part A*, 85(6), 230–242. <https://doi.org/10.1080/15287394.2021.1999875>.
- [135] Świder, K., Startek, K., & Wijaya, C. H. (2019). The Therapeutic Properties of Lemon Balm (*Melissa Officinalis* L.): Reviewing Novel Findings and Medical Indications. *Journal of Applied Botany and Food Quality*, 92, 327–335. <https://doi.org/10.5073/jabfq.2019.092.044>.
- [136] Ghazizadeh, J., Sadigh-Eteghad, S., Marx, W., Fakhari, A., Hamedeyazdan, S., Torbati, M., Taheri-Tarighi, S., Araj-Khodaei, M., & Mirghafourvand, M. (2021). The Effects of Lemon Balm (*Melissa Officinalis* L.) on Depression and Anxiety in Clinical Trials: A Systematic Review and Meta-Analysis. *Phytotherapy Research*, 35(12), 6690–6705. <https://doi.org/10.1002/ptr.7252>.
- [137] Abdel-Naime, W. A., Fahim, J. R., Abdelmohsen, U. R., Fouad, M. A., Al-Footy, K. O., Abdel-Lateff, A. A., & Kamel, M. S. (2019). New Antimicrobial Triterpene Glycosides from Lemon Balm (*Melissa Officinalis*). *South African Journal of Botany*, 125, 161–167. <https://doi.org/10.1016/j.sajb.2019.07.004>.
- [138] Caleja, C., Barros, L., Barreira, J. C. M., Ciric, A., Sokovic, M., Calhelha, R. C., Beatriz, M., Oliveira, P. P., & Ferreira, I. C. F. R. (2018). Suitability of Lemon Balm (*Melissa Officinalis* L.) Extract Rich in Rosmarinic Acid as A Potential Enhancer of Functional Properties in Cupcakes. *Food Chemistry*, 250, 67–74. <https://doi.org/10.1016/j.foodchem.2018.01.034>.

- [139] Arceusz, A., Wesolowski, M., & Ulewicz-Magulska, B. (2015). Flavonoids and Phenolic Acids in Methanolic Extracts, Infusions and Tinctures from Commercial Samples of Lemon Balm. *Natural Product Communications*, 10(6), 1934578X1501000. <https://doi.org/10.1177/1934578x1501000645>.
- [140] Šic Žlabur, J., Voća, S., Dobričević, N., Pliestić, S., Galić, A., Boričević, A., & Borić, N. (2016). Ultrasound-Assisted Extraction of Bioactive Compounds from Lemon Balm and Peppermint Leaves. *International Agrophysics*, 30(1), 95–104. <https://doi.org/10.1515/intag-2015-0077>.
- [141] Heidarian, S., Ataie Kachoe, M., Mousavi-Fard, S., & Moattar, F. (2022). Antimicrobial Effects Oflemon Balm (*Melissa Officinalisl.*) Essential Oil Against Pathogenic Bacteria. *Journal of Positive School Psychology*, 6(7), 2033–2038.
- [142] Bouloumpasi, E., Hatzikamari, M., Christaki, S., Lazaridou, A., Chatzopoulou, P., Biliaderis, C. G., & Irakli, M. (2024). Assessment of Antioxidant and Antibacterial Potential of Phenolic Extracts from Post-Distillation Solid Residues of Oregano, Rosemary, Sage, Lemon Balm, and Spearmint. *Processes*, 12(1), 140. <https://doi.org/10.3390/pr12010140>.
- [143] Sipos, S., Moacă, E.-A., Pavel, I. Z., Avram, Ș., Crețu, O. M., Coricovac, D., Racoviceanu, R.-M., Ghiulai, R., Pană, R. D., Șoica, C. M., Borcan, F., Dehelean, C. A., & Crăiniceanu, Z. (2021). *Melissa Officinalis L.* Aqueous Extract Exerts Antioxidant and Antiangiogenic Effects and Improves Physiological Skin Parameters. *Molecules*, 26(8), 2369. <https://doi.org/10.3390/molecules26082369>.
- [144] Sanghvi, K., Chandrasheker, K. S., Pai, V., & N. Aswatha, R. H. (2020). Review on *Curcuma Longa*: Ethnomedicinal Uses, Pharmacological Activity and Phytochemical Constituents. *Research Journal of Pharmacy and Technology*, 13(8), 3983. <https://doi.org/10.5958/0974-360x.2020.00704.0>.
- [145] Fuloria, S., Mehta, J., Chandel, A., Sekar, M., Rani, N. N. I. M., Begum, M. Y., Subramaniyan, V., Chidambaram, K., Thangavelu, L., Nordin, R., Wu, Y. S., Sathasivam, K. V., Lum, P. T., Meenakshi, D. U., Kumarasamy, V., Azad, A. K., & Fuloria, N. K. (2022). A Comprehensive Review on the Therapeutic Potential of *Curcuma Longa* Linn. in Relation to Its Major Active Constituent Curcumin. *Frontiers in Pharmacology*, 13. <https://doi.org/10.3389/fphar.2022.820806>.

- [146] Vo, T. S., Vo, T. T. B. C., Vo, T. T. T. N., & Lai, T. N. H. (2021). Turmeric (*Curcuma Longa L.*): Chemical Components and Their Effective Clinical Applications. *Journal of the Turkish Chemical Society Section A: Chemistry*, 8(3), 883–898. <https://doi.org/10.18596/jotcsa.913136>.
- [147] De Oliveira Filho, J. G., De Almeida, M. J., Sousa, T. L., Dos Santos, D. C., & Egea, M. B. (2021). Bioactive Compounds of Turmeric (*Curcuma Longa L.*) 297–318. [https://doi.org/10.1007/978-3-030-57415-4\\_37](https://doi.org/10.1007/978-3-030-57415-4_37).
- [148] Tonin, L. T. D., De Oliveira, T. F. V., De Marco, I. G., Palioto, G. F., & Düsman, E. (2021). Bioactive Compounds and Antioxidant, Antimicrobial and Cytotoxic Activities of Extracts of *Curcuma Longa*. *Journal of Food Measurement and Characterization*, 15(4), 3752–3760. <https://doi.org/10.1007/s11694-021-00950-6>.
- [149] Liu, Y., Liu, J., & Zhang, Y. (2019). Research Progress on Chemical Constituents of *Zingiber Officinale Roscoe*. *Biomed Research International*, 2019, 1–21. <https://doi.org/10.1155/2019/5370823>.
- [150] Mao, Q.-Q., Xu, X.-Y., Cao, S.-Y., Gan, R.-Y., Corke, H., Beta, T., & Li, H.-B. (2019). Bioactive Compounds and Bioactivities of Ginger (*Zingiber Officinale Roscoe*). *Foods*, 8(6), 185. <https://doi.org/10.3390/foods8060185>.
- [151] Gao, Y., Lu, Y., Zhang, N., Udenigwe, C. C., Zhang, Y., & Fu, Y. (2024). Preparation, Pungency and Bioactivity of Gingerols from Ginger (*Zingiber Officinale Roscoe*): A Review. *Critical Reviews in Food Science and Nutrition*, 64(9), 2708–2733. <https://doi.org/10.1080/10408398.2022.2124951>.
- [152] Jayasundara, N. D. B., & Arampath, P. (2021). Effect of Variety, Location & Maturity Stage at Harvesting, on Essential Oil Chemical Composition, and Weight Yield of *Zingiber Officinale Roscoe* Grown in Sri Lanka. *Heliyon*, 7(3), E06560. <https://doi.org/10.1016/j.heliyon.2021.e06560>.
- [153] Zhang, M., Zhao, R., Wang, D., Wang, L., Zhang, Q., Wei, S., Lu, F., Peng, W., & Wu, C. (2021). Ginger (*Zingiber Officinale Rosc.*) and Its Bioactive Components Are Potential Resources for Health Beneficial Agents. *Phytotherapy Research*, 35(2), 711–742. <https://doi.org/10.1002/ptr.6858>.
- [154] Ahkam, A. H., Hermanto, F. E., Alamsyah, A., Aliyyah, I. H., & Fatchiyah, F. (2020). Virtual Prediction of Antiviral Potential of Ginger (*Zingiber Officinale*) Bioactive Compounds Against Spike And Mpro of SARS-Cov2 Protein. *Berkala Penelitian Hayati Journal of Biological Researches*, 25(2). <https://doi.org/10.23869/50>.



- [155] Bouchama, C., Zinedine, A., Rocha, J. M., Chadli, N., El Ghadraoui, L., Chabir, R., Raoui, S. M., & Errachidi, F. (2023). Effect of Phenolic Compounds Extracted from Turmeric (*Curcuma Longa L.*) and Ginger (*Zingiber Officinale*) on Cutaneous Wound Healing in Wistar Rats. *Cosmetics*, 10(5), 137. <https://doi.org/10.3390/cosmetics10050137>.
- [156] Sampath, T., Thamizharasan, S., Saravanan, M., & Timiri Shanmugam, P. S. (2020). Materials Testing. In *Trends in Development of Medical Devices*, Elsevier, 77–96. <https://doi.org/10.1016/b978-0-12-820960-8.00006-x>.
- [157] Peters, K., Unger, R. E., & Kirkpatrick, C. J. (2021). Biocompatibility Testing. In *Biomedical Materials*, Springer International Publishing, 423–453. [https://doi.org/10.1007/978-3-030-49206-9\\_13](https://doi.org/10.1007/978-3-030-49206-9_13).
- [158] Najdanović, J., Rajković, J., & Najman, S. (2018). Bioactive Biomaterials: Potential for Application in Bone Regenerative Medicine. In *Biomaterials in Clinical Practice*, Springer International Publishing, 333–360. [https://doi.org/10.1007/978-3-319-68025-5\\_12](https://doi.org/10.1007/978-3-319-68025-5_12).
- [159] Amalraj, A., Raj, K. K. J., Haponiuk, J. T., Thomas, S., & Gopi, S. (2020). Preparation, Characterization, and Antimicrobial Activity of Chitosan/Gum Arabic/Polyethylene Glycol Composite Films Incorporated with Black Pepper Essential Oil and Ginger Essential Oil as Potential Packaging and Wound Dressing Materials. *Advanced Composites and Hybrid Materials*, 3(4), 485–497. <https://doi.org/10.1007/s42114-020-00178-w>.
- [160] Amalraj, A., Haponiuk, J. T., Thomas, S., & Gopi, S. (2020). Preparation, Characterization and Antimicrobial Activity of Polyvinyl Alcohol/Gum Arabic/Chitosan Composite Films Incorporated with Black Pepper Essential Oil And Ginger Essential Oil. *International Journal of Biological Macromolecules*, 151, 366–375. <https://doi.org/10.1016/j.ijbiomac.2020.02.176>.
- [161] Altaf, F., Niazi, M. B. K., Jahan, Z., Ahmad, T., Akram, M. A., Safdar, A., Butt, M. S., Noor, T., & Sher, F. (2021). Synthesis and Characterization Of PVA/Starch Hydrogel Membranes Incorporating Essential Oils Aimed to Be Used in Wound Dressing Applications. *Journal of Polymers and the Environment*, 29(1), 156–174. <https://doi.org/10.1007/s10924-020-01866-w>.

- [162] Liu, J.-X., Dong, W.-H., Mou, X.-J., Liu, G.-S., Huang, X.-W., Yan, X., Zhou, C.-F., Jiang, S., & Long, Y.-Z. (2020). In Situ Electrospun Zein/Thyme Essential Oil-Based Membranes as An Effective Antibacterial Wound Dressing. *ACS Applied Bio Materials*, 3(1), 302–307. <https://doi.org/10.1021/acsabm.9b00823>.
- [163] Alsakhawy, S. A., Baghdadi, H. H., El-Shenawy, M. A., Sabra, S. A., & El-Hosseiny, L. S. (2022). Encapsulation of Thymus Vulgaris Essential Oil in Caseinate/Gelatin Nanocomposite Hydrogel: In Vitro Antibacterial Activity and In Vivo Wound Healing Potential. *International Journal of Pharmaceutics*, 628, 122280. <https://doi.org/10.1016/j.ijpharm.2022.122280>.
- [164] Gheorghita, D., Grosu, E., Robu, A., Ditu, L., Deleanu, I., Gradisteanu Pircalabioru, G., Raiciu, A.-D., Bitu, A.-I., Antoniac, A., & Antoniac, V. (2022). Essential Oils as Antimicrobial Active Substances in Wound Dressings. *Materials*, 15(19), 6923. <https://doi.org/10.3390/ma15196923>.
- [165] Berechet, M. D., Gaidau, C., Miletic, A., Pilic, B., Râpă, M., Stanca, M., Ditu, L.-M., Constantinescu, R., & Lazea-Stoyanova, A. (2020). Bioactive Properties of Nanofibres Based on Concentrated Collagen Hydrolysate Loaded with Thyme and Oregano Essential Oils. *Materials*, 13(7), 1618. <https://doi.org/10.3390/ma13071618>.
- [166] Gherman, T., Popescu, V., Carpa, R., Gavril, G. L., Rapa, M., & Oprescu, E. E. (2018). Salvia Officinalis Essential Oil Loaded Gelatin Hydrogel as Potential Antibacterial Wound Dressing Materials. *Revista De Chimie*, 69(2), 410–414. <https://doi.org/10.37358/rc.18.2.6118>.
- [167] Rather, A. H., Khan, R. S., Wani, T. U., Rafiq, M., Jadhav, A. H., Srinivasappa, P. M., Abdal-Hay, A., Sultan, P., Rather, S., Macossay, J., & Sheikh, F. A. (2023). Polyurethane and Cellulose Acetate Micro-Nanofibers Containing Rosemary Essential Oil, and Decorated with Silver Nanoparticles for Wound Healing Application. *International Journal of Biological Macromolecules*, 226, 690–705. <https://doi.org/10.1016/j.ijbiomac.2022.12.048>.
- [168] Chin, C.-Y., Jalil, J., Ng, P. Y., & Ng, S.-F. (2018). Development and Formulation of Moringa Oleifera Standardised Leaf Extract Film Dressing for Wound Healing Application. *Journal of Ethnopharmacology*, 212, 188–199. <https://doi.org/10.1016/j.jep.2017.10.016>.

- [169] Sabando, C., Ide, W., Rodríguez-Díaz, M., Cabrera-Barjas, G., Castaño, J., Bouza, R., Müller, N., Gutiérrez, C., Barral, L., Rojas, J., Martínez, F., & Rodríguez-Llamazares, S. (2020). A Novel Hydrocolloid Film Based on Pectin, Starch and *Gunnera Tinctoria* and *Ugni Molinae* Plant Extracts for Wound Dressing Applications. *Current Topics in Medicinal Chemistry*, 20(4), 280–292. <https://doi.org/10.2174/1568026620666200124100631>.
- [170] Suryamathi, M., Ruba, C., Viswanathamurthi, P., Balasubramanian, V., & Perumal, P. (2019). Tridax Procumbens Extract Loaded Electrospun PCL Nanofibers: A Novel Wound Dressing Material. *Macromolecular Research*, 27(1), 55–60. <https://doi.org/10.1007/s13233-019-7022-7>.
- [171] Li, Y., Yan, X., Zhang, L., & Diao, L. (2022). Thyme-Loaded Nanofibrous Dressing For Skin Wound Healing: A Combination Of Chinese Traditional Medicine with Cutting-Edge Technology. *Journal of Biomedical Nanotechnology*, 18(8), 1930–1937. <https://doi.org/10.1166/jbn.2022.3440>.
- [172] Maleki, H., Doostan, M., Khoshnevisan, K., Baharifar, H., Maleki, S. A., & Fatahi, M. A. (2024). Zingiber Officinale and Thymus Vulgaris Extracts Co-Loaded Polyvinyl Alcohol and Chitosan Electrospun Nanofibers for Tackling Infection and Wound Healing Promotion. *Heliyon*, 10(1), E23719. <https://doi.org/10.1016/j.heliyon.2023.e23719>.
- [173] Koushki, P., Bahrami, S. H., & Ranjbar-Mohammadi, M. (2018). Coaxial Nanofibers From Poly(Caprolactone)/ Poly(Vinyl Alcohol)/Thyme And Their Antibacterial Properties. *Journal of Industrial Textiles*, 47(5), 834–852. <https://doi.org/10.1177/1528083716674906>.
- [174] Vasile, C., Stoleru, E., Darie-Nița, R. N., Dumitriu, R. P., Pamfil, D., & Tarțau, L. (2019). Biocompatible Materials Based on Plasticized Poly(Lactic Acid), Chitosan and Rosemary Ethanolic Extract I. Effect of Chitosan on the Properties of Plasticized Poly(Lactic Acid) Materials. *Polymers*, 11(6), 941. <https://doi.org/10.3390/polym11060941>.
- [175] Gavan, A., Colobatiu, L., Hanganu, D., Bogdan, C., Olah, N., Achim, M., & Mirel, S. (2022). Development and Evaluation of Hydrogel Wound Dressings Loaded with Herbal Extracts. *Processes*, 10(2), 242. <https://doi.org/10.3390/pr10020242>.

- [176] Kumar, T. S. M., Chandrasekar, M., Senthilkumar, K., Ilyas, R. A., Sapuan, S. M., Hariram, N., Rajulu, A. V., Rajini, N., & Siengchin, S. (2021). Characterization, Thermal and Antimicrobial Properties of Hybrid Cellulose Nanocomposite Films with In-Situ Generated Copper Nanoparticles in Tamarindus Indica Nut Powder. *Journal of Polymers and The Environment*, 29(4), 1134–1142. <https://doi.org/10.1007/s10924-020-01939-w>.
- [177] Bazan, P., Mazur, K. E., Rybicka, K., & Kuciel, S. (2023). The Influence of Organic and Inorganic Antibacterial Additives on the Strength and Biocidal Properties of Thermoplastic Elastomers (TPO). *Industrial Crops and Products*, 198, 116682. <https://doi.org/10.1016/j.indcrop.2023.116682>.
- [178] Rusin-Żurek, K., & Kuciel, S. (2024). Strength Properties and Ability to Dissipate Mechanical Energy of Biopolypropylene Basalt/Cellulose Composites with the Addition of Antibacterial Turmeric. *Scientific Reports*, 14(1), 820. <https://doi.org/10.1038/s41598-023-51145-6>.
- [179] Chaaben, R., Taktak, R., Mnif, B., Guermazi, N., & Elleuch, K. (2022). Innovative Biocomposite Development Based on the Incorporation of *Salvadora Persica* in Acrylic Resin for Dental Material. *Journal of Thermoplastic Composite Materials*, 35(11), 1815–1831. <https://doi.org/10.1177/0892705720939167>.
- [180] Kartal, F., & Kaptan, A. (2023). Mechanical Performance Of *Salvadora Persical* (Miswak) Reinforced Polylactic Acid Matrix Composites for Three Dimensional Printing. *Black Sea Journal of Engineering and Science*, 6(4), 458–468. <https://doi.org/10.34248/bsengineering.1327903>.
- [181] Ahmed Ismail, K., El Askary, A., Farea, M. O., Awwad, N. S., Ibrahim, H. A., Eid Moustapha, M., & Menazea, A. A. (2022). Perspectives on Composite Films of Chitosan-Based Natural Products (Ginger, Curcumin, and Cinnamon) as Biomaterials for Wound Dressing. *Arabian Journal of Chemistry*, 15(4), 103716. <https://doi.org/10.1016/j.arabjc.2022.103716>.
- [182] Moopayak, W., & Tangboriboon, N. (2020). Mangosteen Peel and Seed as Antimicrobial and Drug Delivery in Rubber Products. *Journal of Applied Polymer Science*, 137(37). <https://doi.org/10.1002/app.49119>.

- [183] Dragon Skin 30. Available Online: <https://www.smooth-on.com/products/dragon-skin-30/> (Accessed on April 7th, 2024).
- [184] Moučka, R., Sedlačík, M., Osička, J., & Pata, V. (2021). Mechanical Properties of Bulk Sylgard 184 and Its Extension with Silicone Oil. *Scientific Reports*, 11(1), 19090. <https://doi.org/10.1038/s41598-021-98694-2>.
- [185] Rezvani Ghomi, E., Khalili, S., Nouri Khorasani, S., Esmaeely Neisiany, R., & Ramakrishna, S. (2019). Wound Dressings: Current Advances and Future Directions. *Journal of Applied Polymer Science*, 136(27). <https://doi.org/10.1002/app.47738>.
- [186] Gao, Y., Elhadad, A., & Choi, S. (2024). Janus Paper-Based Wound Dressings for Effective Exudate Absorption and Antibiotic Delivery. *Advanced Engineering Materials*, 26(5). <https://doi.org/10.1002/adem.202301422>.
- [187] Yu, Y., Xu, G., Zhao, P., & Zhang, J. (2024). Biocompatible, Robust, Waterproof and Breathable PDMS-Based PU Fibrous Membranes for Potential Application in Wound Dressing. *Materials Today Communications*, 38, 107870. <https://doi.org/10.1016/j.mtcomm.2023.107870>.
- [188] Kavooosi, G., Dadfar, S. M. M., & Purfard, A. M. (2013). Mechanical, Physical, Antioxidant, and Antimicrobial Properties of Gelatin Films Incorporated with Thymol for Potential Use as Nano Wound Dressing. *Journal of Food Science*, 78(2). <https://doi.org/10.1111/1750-3841.12015>.
- [189] Bialik-Wąs, K., Pluta, K., Malina, D., Barczewski, M., Malarz, K., & Mrozek-Wilczkiewicz, A. (2021). Advanced SA/PVA-Based Hydrogel Matrices with Prolonged Release of Aloe Vera As Promising Wound Dressings. *Materials Science and Engineering: C*, 120, 111667. <https://doi.org/10.1016/j.msec.2020.111667>.
- [190] Paydayesh, A., Heleil, L., & Sh Dadkhah, A. (2022). Preparation and Application of Poly (Hydroxyl Ethyl Methacrylate) Nanocomposite Hydrogels Containing Iron Oxide Nanoparticles as Wound Dressing. *Polymers and Polymer Composites*, 30, 096739112110631. <https://doi.org/10.1177/09673911211063106>.
- [191] De-La-Pinta, I., Cobos, M., Ibarretxe, J., Montoya, E., Eraso, E., Guraya, T., & Quindós, G. (2019). Effect of Biomaterials Hydrophobicity and Roughness on Biofilm Development. *Journal of Materials Science: Materials in Medicine*, 30(7), 77. <https://doi.org/10.1007/s10856-019-6281-3>.

- [192] Yang, K., Shi, J., Wang, L., Chen, Y., Liang, C., Yang, L., & Wang, L.-N. (2022). Bacterial Anti-Adhesion Surface Design: Surface Patterning, Roughness and Wettability: A Review. *Journal of Materials Science & Technology*, 99, 82–100. <https://doi.org/10.1016/j.jmst.2021.05.028>.
- [193] Cunliffe, A. J., Askew, P. D., Stephan, I., Iredale, G., Cosemans, P., Simmons, L. M., Verran, J., & Redfern, J. (2021). How Do We Determine the Efficacy of An Antibacterial Surface? A Review of Standardised Antibacterial Material Testing Methods. *Antibiotics*, 10(9), 1069. <https://doi.org/10.3390/antibiotics10091069>.
- [194] Drauch, V., Ibesich, C., Vogl, C., Hess, M., & Hess, C. (2020). In-Vitro Testing of Bacteriostatic and Bactericidal Efficacy of Commercial Disinfectants Against *Salmonella Infantis* Reveals Substantial Differences Between Products and Bacterial Strains. *International Journal of Food Microbiology*, 328, 108660. <https://doi.org/10.1016/j.ijfoodmicro.2020.108660>.
- [195] Zadrazilova, I., Pospisilova, S., Pauk, K., Imramovsky, A., Vinsova, J., Cizek, A., & Jampilek, J. (2015). In Vitro Bactericidal Activity Of 4- And 5-Chloro-2-Hydroxy- N -[1-Oxo-1-(Phenylamino)Alkan-2-Yl]Benzamides Against MRSA. *Biomed Research International*, 2015, 1–8. <https://doi.org/10.1155/2015/349534>.
- [196] Liu, B., Furevi, A., Perepelov, A. V, Guo, X., Cao, H., Wang, Q., Reeves, P. R., Knirel, Y. A., Wang, L., & Widmalm, G. (2020). Structure and Genetics of *Escherichia Coli* O Antigens. *FEMS Microbiology Reviews*, 44(6), 655–683. <https://doi.org/10.1093/femsre/fuz028>.
- [197] Jindal, S., Anand, S., Huang, K., Goddard, J., Metzger, L., & Amamcharla, J. (2016). Evaluation of Modified Stainless Steel Surfaces Targeted to Reduce Biofilm Formation by Common Milk Sporeformers. *Journal of Dairy Science*, 99(12), 9502–9513. <https://doi.org/10.3168/jds.2016-11395>.
- [198] Zaugg, L. K., Astasov-Frauenhoffer, M., Braissant, O., Hauser-Gerspach, I., Waltimo, T., & Zitzmann, N. U. (2017). Determinants of Biofilm Formation and Cleanability of Titanium Surfaces. *Clinical Oral Implants Research*, 28(4), 469–475. <https://doi.org/10.1111/clr.12821>.
- [199] Obagi, Z., Damiani, G., Grada, A., & Falanga, V. (2019). Principles of Wound Dressings: A Review. *Surgical Technology International*, 35.

- [200] Riyajan, S.-A., & Sukhlaaied, W. (2019). Fabrication and Properties of A Novel Porous Material from Biopolymer and Natural Rubber for Organic Compound Absorption. *Journal of Polymers and the Environment*, 27(9), 1918–1936. <https://doi.org/10.1007/s10924-019-01474-3>.
- [201] Huang, J., Cai, P., Li, M., Wu, Q., Li, Q., & Wang, S. (2020). Preparation of CNF/PDMS Superhydrophobic Coatings with Good Abrasion Resistance Using A One-Step Spray Method. *Materials*, 13(23), 5380. <https://doi.org/10.3390/ma13235380>.
- [202] Brogly, M., Bistac, S., Delaite, C., & Alzina, C. (2020). Influence Of Semi-Crystalline Poly( E -Caprolactone) and Non-Crystalline Polylactide Blocks on the Thermal Properties of Polydimethylsiloxane-Based Block Copolymers. *Polymer International*, 69(11), 1105–1112. <https://doi.org/10.1002/pi.5964>.
- [203] Gupta, N. S., Lee, K.-S., & Labouriau, A. (2021). Tuning Thermal and Mechanical Properties of Polydimethylsiloxane with Carbon Fibers. *Polymers*, 13(7), 1141. <https://doi.org/10.3390/polym13071141>.
- [204] Klonos, P., Sulym, I. Y., Sternik, D., Konstantinou, P., Goncharuk, O. V., Deryło–Marczewska, A., Gun’ko, V. M., Kyritsis, A., & Pissis, P. (2018). Morphology, Crystallization and Rigid Amorphous Fraction in PDMS Adsorbed onto Carbon Nanotubes And Graphite. *Polymer*, 139, 130–144. <https://doi.org/10.1016/j.polymer.2018.02.020>.
- [205] Güzel, S., Özay, Y., Kumaş, M., Uzun, C., Özkorkmaz, E. G., Yıldırım, Z., Ülger, M., Güler, G., Çelik, A., Çamlıca, Y., & Kahraman, A. (2019). Wound Healing Properties, Antimicrobial and Antioxidant Activities of *Salvia Kronenburgii* Rech. F. and *Salvia Euphratica* Montbret, Aucher & Rech. F. Var. *Euphratica* on Excision and Incision Wound Models in Diabetic Rats. *Biomedicine & Pharmacotherapy*, 111, 1260–1276. <https://doi.org/10.1016/j.biopha.2019.01.038>.
- [206] Hamed Al-Dahbi, A., Fadhel, A., & Ali, S. (2019). Histological And Immunological Study of Daily Supplement of Aqueous Extract of *Thymus Vulgaris* Leaf in Mice Challenged with *Vibrio Alginolyticus*. *Journal of Global Pharma Technology*, 11, 262–271.

## 9. Standards references

- [S1] EN ISO 1183-1: 2006; Plastics—Methods for Determining the Density of Non-Cellular Plastics—Part 1: Immersion Method, Liquid Pycnometer Method and Titration Method. International Organization of Standardization: Geneva, Switzerland, 2006.
- [S2] EN 828:2013; Adhesives. Wettability. Determination by Measurement of Contact Angle and Surface Free Energy of Solid Surface. European Standard: Pilsen, Czech Republic, 2013.
- [S3] EN ISO 10993-15:2019; Biological Evaluation of Medical Devices—Part 15: Identification and Quantification of Degradation Products from Metals and Alloys; International Organization for Standardization: Geneva, Switzerland, 2019.
- [S4] ISO 62:2008; Plastics—Determination of Water Absorption. International Organization for Standardization: Geneva, Switzerland, 2008.
- [S5] EN ISO 4662:2017; Rubber, Vulcanized or Thermoplastic—Determination of Rebound Resilience. International Organization of Standardization: Geneva, Switzerland, 2017.
- [S6] ISO 7619-1:2010; Rubber, Vulcanized or Thermoplastic-Determination of Indentation Hardness—Part 1: Durometer Method (Shore Hardness). International Organization of Standardization: Geneva, Switzerland, 2010.
- [S7] ISO 4649:2010; Rubber, Vulcanized or Thermoplastic — Determination of Abrasion Resistance Using a Rotating Cylindrical Drum Device. International Organization of Standardization: Geneva, Switzerland, 2010.
- [S8] EN ISO 527-1:2012; Plastics—Determination of Tensile Properties—Part 1: General Principles. International Organization of Standardization: Geneva, Switzerland, 2012.
- [S9] EN ISO 10993-13:2010; Biological Evaluation of Medical Devices—Part 13: Identification and Quantification of Degradation Products from Polymeric Medical Devices. International Organization of Standardization: Geneva, Switzerland, 2010.



- [S10] EN ISO 11357-1:2016; Plastics—Differential Scanning Calorimetry (DSC)—  
Part 1: General Principles. International Organization of Standardization:  
Geneva, Switzerland, 2016.
- [S11] ISO 22196:2011; Measurement of Antibacterial Activity on Plastics and Other  
Non-Porous Surfaces. International Organization of Standardization: Geneva,  
Switzerland, 2011.
- [S12] ISO 10993-5:2009; Biological Evaluation of Medical Devices—Part 5: Tests for  
In Vitro Cytotoxicity. International Organization of Standardization: Geneva,  
Switzerland, 2011.

## List of figures

Figure 1.1. The compounded annual growth rate of medical elastomers .....	14
Figure 2.1. PDMS chemical structure formula .....	21
Figure 2.2. PDMS-based contact lens: fabrication process – a), the obtained PDMS lenses – b), and incubation of lenses in gold solution – c) [53] .....	24
Figure 2.3. Starr-Edwards heart valve [60].....	25
Figure 2.4. Bioinspired 3D-printed heart valve [62] .....	25
Figure 2.5. Wound dressings classification [75].....	27
Figure 2.6. Classification of polyphenols [100] .....	34
Figure 5.1. Research methodology .....	58
Figure 5.2. IR spectrum of the matrix.....	59
Figure 5.3. Modifying fillers: thyme – a), sage – b), rosemary – c).....	60
Figure 5.4. The selected fillers: raw material – a), d), g), modified material – b), e), h), polyphenolic extract – c), f), i) .....	61
Figure 5.5. SEM micrographs of the tested fillers: raw material – a), d), g), modified material – b). e), h), polyphenolic extract – c), f), i).....	64
Figure 5.6. Fillers' particle size.....	65
Figure 5.7. Fillers' density .....	66
Figure 5.8. Phytochemical composition of rosemary: unmodified – a), modified – b), extract – c) .....	68
Figure 5.9. The algorithm employed for acquiring the biocomposites.....	71
Figure 5.10. Making of biocomposites: rotary mixing – a), gravity casted material – b) .....	72
Figure 5.11. The obtained materials in the shape adapted for tensile testing.....	74
Figure 5.12. Density measurements apparatus .....	75
Figure 5.13. The post-test drops of reference – a) and MT2.5 – b).....	76
Figure 5.14. The setting of the in vitro absorption experiment: tested sample – a) and incubator – b).....	77
Figure 5.15. MT2.5 test sample for rebound resilience .....	78
Figure 5.16. MT2.5 samples for the abrasion test .....	79
Figure 5.17. Tensile testing sample .....	80

Figure 5.18. Tensile testing of MT2.5 sample: before – a) and during testing – b) .....	80
Figure 5.19. Stress-strain curve of MT2.5 .....	80
Figure 5.20. Incubated MT2.5 samples for accelerated degradation test .....	81
Figure 5.21. EDS analysis of MT2.5 performed after 7 days of incubation in artificial saliva under accelerated degradation conditions .....	83
Figure 5.22. Inoculated samples for antibacterial activity assessment .....	85
Figure 6.1. Density results .....	87
Figure 6.2. Stress at break results .....	88
Figure 6.3. Strain at break results .....	91
Figure 6.4. Hardness measurements results .....	93
Figure 6.5. Water contact angle measurements results .....	95
Figure 6.6. Kirby-Bauer test results for <i>S. aureus</i> : thyme – a), sage – b), rosemary – c) and <i>E. coli</i> : thyme – d), sage – e), rosemary – f) .....	97
Figure 6.7. Absorption results .....	101
Figure 6.8. Rebound resilience measurements results .....	103
Figure 6.9. Abrasion resistance results .....	104
Figure 6.10. FTIR analysis results .....	105
Figure 6.11. DSC analysis results .....	106
Figure 6.12. FTIR spectra of aged reference samples .....	108
Figure 6.13. FTIR spectra of aged thyme-based composite samples .....	109
Figure 6.14. FTIR spectra of aged sage-based composite samples .....	110
Figure 6.15. FTIR spectra of aged rosemary-based composite samples .....	111
Figure 6.16. Stress at break results for aged thyme samples .....	112
Figure 6.17. Strain at break results for aged thyme samples .....	112
Figure 6.18. Stress at break results for aged sage samples .....	113
Figure 6.19. Strain at break results for aged sage samples .....	114
Figure 6.20. Stress at break results for aged rosemary samples .....	115
Figure 6.21. Strain at break results for aged rosemary samples .....	115
Figure 6.22. Fracture surface micrographs of modified thyme composites: MT2.5 – a), MT5 – b), MT7.5 – c), MT10 – d) .....	118
Figure 6.23. Fracture surface micrographs of modified sage composites: MS2.5 – a), MS5 – b), MS7.5 – c), MS10 – d) .....	119
Figure 6.24. Fracture surface micrographs of modified rosemary composites: MR2.5 – a), MR5 – b), MR7.5 – c), MR10 – d), reference – e) .....	120

Figure 6.25. Fracture surface micrographs of selected 7-day aged samples: MT5 – a), MT10 – b), MS7.5 – c), MS10 – d), MR10 – e).....	121
Figure 6.26. Cell viability results .....	124

## List of tables

Table 2.1. Polysiloxane units [30] .....	19
Table 2.2. A summary of selected plants.....	41
Table 5.1. Selected properties of PDMS [183].....	59
Table 5.2. Fillers codes .....	63
Table 5.3. The average size of the fillers' particles .....	65
Table 5.4. Total phenolic content of the tested fillers .....	67
Table 5.5. Selected detected compounds in thyme, expressed as percentages (%).....	69
Table 5.6. Selected detected compounds in sage, expressed as percentages (%).....	69
Table 5.7. Selected detected compounds in rosemary, expressed as percentages (%)...	70
Table 5.8. Obtained materials abbreviations and fillers' mass concentration .....	73
Table 5.9. Artificial plasma composition [S3].....	77
Table 6.1. Antibacterial activity assessment results – part I.....	96
Table 6.2. Antibacterial activity assessment results – part II .....	98
Table 6.3. I multicriteria analysis results .....	100
Table 6.4. Crystallinity degree calculated based on the DSC thermograms.....	107
Table 6.5. II multicriteria analysis results.....	123